Effect of Termination of Long-term Free Air CO_2 Enrichment

on Physiology and Carbon Allocation in a Loblolly Pine Dominated Forest

by

Do Hyoung Kim

Environment
Duke University

Date:_____
Approved:

_____
Ram Oren, Supervisor

_____
Gabriel G. Katul

_____
James S. Clark

_____
Sari Palmroth

_____
Jean-Christophe Domec

Dissertation submitted in partial fulfillment of
the requirements for the degree of Doctor of Philosophy in
Environment in the Graduate School of
Duke University

2016

ABSTRACT

Effect of Termination of Long-term Free Air CO_2 Enrichment

on Physiology and Carbon Allocation in a Loblolly Pine Dominated Forest

by

Do Hyoung Kim

Environment
Duke University

Date:_____

Approved:

_____
Ram Oren, Supervisor

_____
Gabriel G. Katul

_____
James S. Clark

_____
Sari Palmroth

_____
Jean-Christophe Domec

An abstract of a dissertation submitted in partial fulfillment of
the requirements for the degree of Doctor of Philosophy in
Environment in the Graduate School of
Duke University

2016

Abstract

The work described here focuses on the last period of enrichment at the Duke FACE site, as well as the following two years post-enrichment, as the forest acclimates to the decreased availability of CO_2. The first chapter, **Response to CO_2 enrichment of understory vegetation in the shade of forests** (Kim *et al.* 2016) states that "Responses of forest ecosystems to increased atmospheric CO_2 concentration have been studied in few free-air CO_2 enrichment (FACE) experiments during last two decades. Most studies focused principally on the overstory trees with little attention given to understory vegetation. Despite its small contribution to total productivity of an ecosystem, understory vegetation plays an important role in predicting successional dynamics and future plant community composition. Thus, the response of understory vegetation in *Pinus taeda* plantation at the Duke Forest FACE site after 15-17 years of exposure to elevated CO_2, 6-13 of which with nitrogen (N) amendment, were examined." Previous work at the Duke FACE site concluded that *Toxicodendron radicans* (poison ivy) will thrive in a future with CO_2-enriched atmosphere (Mohan *et al.* 2006) and that among the subcanopy species, shade-tolerant species will be able to take advantage of eCO_2, thus perform better than shade intolerant species (Kerstiens 2001; Ellsworth *et al.* 2012). From Kim *et al*. (2016) "aboveground biomass and density of the understory decreased across all treatments with increasing overstory leaf area index (*L*). However, the CO_2 and N treatments had no effect on aboveground biomass, tree density, community composition and the fraction of shade-tolerant species." Indeed, none of the vine species, including

poison ivy, showed a treatment-induced enhancement of biomass or density. "The increases of overstory *L* (~28%) under elevated CO_2 resulted in a reduction of light available to the understory (~18%) sufficient to nullify the expected growth-enhancing effect of elevated CO_2 on understory vegetation." Alternatively, *L* of the untreated stand was already so high, that the increase of overstory *L* with CO_2 caused only a small change in light availability below the overstory canopy. Under such deep shade, it is possible that light was too limiting for any species to respond to CO_2, with or without N addition.

The discrepancy between earlier results (Mohan *et al.* 2007) and these may reflect the difference in the size of the sample plots. Previous studies investigated relatively small plots (1.44 m^2), small enough to be affected by local variation in *L* and, thus, light. The small sample size, may have biased the results, especially because these studies were done over the period of time before the canopy recovered from the damage it endured during the December 2002 ice storm (McCarthy *et al.* 2006). The current study used data from harvest of 40% of the area in each plot, representing >100 m^2 for each CO_2 × N treatment combination, and the stand canopy completely recovered following eight years without disturbance. In conclusion, there is no indication that elevated atmospheric CO_2, in forests on N-poor or rich soils, will affect the understory density, biomass or composition under intact canopy.

The following investigation, on the effect of eCO_2 termination on belowground C allocation, required to first assess what impact it had on C uptake in

photosynthesis. To do so, it is possible to use the tested assumption that c_i/c_a is unaffected by eCO_2 (Ellsworth *et al.* 2012) and, because c_a following termination was as in aCO2 plots, differences in photosynthesis would be proportional to difference in mean canopy stomatal conductance multiplied by *L* (i.e., total canopy conductance). Mean canopy conductance of each species is calculated from scaled sap-flux, and the simplest approach to the calculation is to assume that leaves are well coupled to the atmosphere, an assumption that was verified for *P. taeda*, but not for the broadleaved species in the stand. A more complete data set from an adjacent stand was used to test the assumption, as captured in Kim *et al*. (2014) **Sensitivity of stand transpiration to wind velocity in a mixed broadleaved deciduous forest.** "Wind velocity (*U*) within and above forest canopies can alter the coupling between the vapor-saturated sub-stomatal airspace and the drier atmosphere aloft, thereby influencing transpiration rates. In practice, however, the actual increase in transpiration with increasing *U* depends on the aerodynamic resistance (R_A) to vapor transfer compared to canopy resistance to water vapor flux out of leaves (R_C, dominated by stomatal resistance, R_{stom}), and the rate at which R_A decreases with increasing *U*. We investigated the effect of *U* on transpiration at the canopy scale using filtered meteorological data and sap flux measurements gathered from six diverse species of a mature broadleaved deciduous forest. Only under high light conditions, stand transpiration (E_C) increased slightly (6.5%) with increasing *U* ranging from ~0.7 to ~4.7 m s^{-1}. Under other conditions, sap flux density (J_s) and E_C responded weakly or did not change with *U*. R_A, estimated from Monin-Obukhov similarity theory, decreased with

increasing U, but this decline was offset by increasing R_C, estimated from a rearranged Penman-Monteith equation, due to a concurrent increase in vapor pressure deficit (D). The increase of R_C with D over the observed range of U was consistent with increased R_{stom} by ~40% based on hydraulic theory. Except for very rare half-hourly values, the proportion of R_A to total resistance (R_T) remained < 15% over the observed range of conditions. These results suggest that in similar forests and conditions, the direct effect of U reducing R_A and thus increasing transpiration is negligible. However, the observed U-D relationship and its effect on R_{stom} must be considered when modeling canopy photosynthesis." Because, in the FACE site, D was measured within the canopy, and was not affected by CO_2, one can proceed to calculate mean canopy stomatal conductance from sap flux, L and D.

Before termination of eCO_2, mean canopy stomatal conductance was lower under eCO_2 than aCO_2. Indeed, canopy conductance was occasionally lower, even accounting for the higher L under eCO_2 (Chapter III. **Response of stomatal conductance to termination of long-term CO_2 enrichment**). Following termination of enrichment, the increase in mean canopy stomatal conductance more than compensated for the reduction in L, resulting in occasionally higher total canopy conductance in plots previously subjected to eCO_2. Given the likely similarity of c_i/c_a, it seems safe to assume that canopy photosynthesis was higher in these plots than plots subjected to aCO_2 all along, or at least that canopy photosynthesis is not different. Thus, changes in soil CO_2 efflux (F_{CO2}) must

reflect changes in C allocation belowground, and the consequences to belowground constituents.

Armed with this information, it is possible to interpret the effect of termination of eCO_2, as presented in Chapter IV (**Dynamics of soil CO_2 efflux under varying atmospheric CO_2 concentrations reveal dominance of slow processes).** In this chapter, we evaluated the effect on soil respiration (R_S) of sudden changes of photosynthetic rates by altering CO_2 enrichment in plots subjected to +200 ppmv for 15 years. Five-day intervals ranging 1.0 - 1.8 × ambient did not affect F_{CO2}. Only ~160 days following eCO_2 termination did F_{CO2} decrease, longer than the 10 days observed for experimental blocking of C flow to belowground, but shorter than >400 days it took for increase of F_{CO2} following initiation of CO_2 enrichment. The reduction of F_{CO2} upon termination of enrichment (~35% in native and N-fertilized soils) cannot be explain by the reduction in leaf area (~15%) and associated carbohydrate production and allocation, suggesting a disproportional contraction of the belowground ecosystem components; this was consistent with the reductions in base respiration and F_{CO2}-temperature sensitivity. These asymmetric responses pose a tractable challenge to process based models attempting to isolate the effect of individual processes on R_S.

Contents

List of Tables

List of Figures

1. Introduction

Knowing how rising atmospheric CO_2 is affecting forests now, and will affect forests in the future, is essential for predicting the composition, structure and function of future forests, and assessing their role in providing services such as cellulose for various products, diverse ecosystems, water, carbon (C) sequestration, and surface cooling. Rising CO_2 concentration is accompanied by changes in additional atmospheric (e.g., temperature, vapor pressure deficit) and soil (e.g., temperature, moisture) conditions, as well as in the severity of climate events (e.g., ice storms; da Silva *et al.* 2006), all of which interact with atmospheric CO_2 in affecting forest productivity (McCarthy *et al.* 2006). Very few elevated CO_2 (eCO_2) studies were performed worldwide, and results from these studies cannot be directly applied, even to like ecosystems. The primary goal of these studies was to help evaluate how well the response of forests to eCO_2 can be predicted with commonly used models (Thornton *et al.* 2007; Medvigy *et al.* 2009; Parton *et al.* 2010; Zaehle & Friend 2010; Wang *et al.* 2011). As several data-modeling activities show, for various reasons none of these models performed particularly well (Walker *et al.* 2014).

The results discussed in this dissertation, focus on the effect of elevating only atmospheric CO_2 and soil N supply in otherwise unaltered forest, considers neither interactions with other climate change variables and events, nor the responses described in ~300 papers during the 15 – 17 years of the Duke Free-Air CO_2 Enrichment (FACE) study. Instead, the results are based on the last two years of eCO_2, and a two-year long "relaxation" period following termination of eCO_2 at the end of 2010. Conducting a study

focused on data from the end of such a long study, the implicit assumption made is that the forest reached equilibrium with the CO_2 × N treatments, and that discontinuing the treatment would help separate adjustments in quickly responding processes (e.g., stomatal conductance, carbohydrate production), moderately slow responses (e.g., leaf area index, *L*), and very slow response (xylem hydraulic properties, amount of roots and soil C). Although not all of these variables were available, or used in this study, the response of some of the variables studied can help identify the responsible processes, thus providing information useful for improved model specification and testing.

The first objective of the study was to assess whether eCO_2 alters the composition and biomass of the subcanopy plants. Relatively few studies were published on the subcanopy. Based on these, vines and woody vegetation were more responsive to elevated CO_2 than ground cover plants (Ainsworth & Long 2005; Schnitzer & Bongers 2011). However, the scale of the subcanopy measurements were always much smaller than the scale of variation in canopy *L*, and thus light and radiation penetration, potentially confounding the results. In this work, 40% of the area of each plot, half representing native soil N and half representing high soil N, were entirely harvested and used to test the hypotheses (see Kim *et al.* 2016; Chapter I) that, "…mirroring the effect of elevated CO_2 on overstory vegetation, (**H1**) total understory biomass and density will be greater in elevated CO_2. However, N deficiency in the soil had hindered the direct effect of elevated CO_2 at this site (Oren *et al.* 2001). Thus, (**H2**) the effect of elevated CO_2 on understory biomass will be more obvious with N fertilization. Conversely, elevated CO_2 increased leaf area of the *Pinus taeda* and entire canopy at this site

(McCarthy *et al.* 2007), and increase in leaf area of *P. taeda* is likely to make overstory *L* in elevated CO_2 higher than in ambient CO_2. Overstory *L* corresponds to all foliage above understory vegetation. Because increases in overstory *L* may reduce light availability in the understory, and the daily photosynthesis of understory vegetation in moderate shade depends on light-saturated photosynthesis (Naumburg *et al.* 2001), understory biomass and density may be lower in higher overstory *L* plots (i.e. negative indirect effect of elevated CO_2). Thus, the alternative hypothesis (**H3**) was that the increase of *L* may diminish, or even reverse, the expected responses of understory vegetation to CO_2 and N enrichment." Another expectation based on published results was that "…the different sensitivities among functional groups and species to eCO_2 may cause a difference in the community composition between plots in ambient and elevated CO_2" (Nowak *et al.* 2004). This gave rise to the hypothesis "…(**H4**) that the prevalence of shade-tolerant species would increase both due to direct effect of CO_2 on their photosynthesis and the indirect effect of decreasing light on shade-intolerant species, thus reducing species richness."

A second objective was to isolate the processes most likely influencing the amount of CO_2 returning to the atmosphere from the forest floor-soil system (F_{CO2}). This investigation relied on data sets representing changes in eCO_2 at intervals ranging from five days, just before the CO_2 was terminated, to changes following the onset of enrichment at the commencement of the study and termination of enrichment two years before the conclusion of the study. A critical uncertainty in tackling this objective was the likely effect of changes in atmospheric CO_2 on carbohydrate production. If changes in

eCO_2 produce proportional changes in canopy scale photosynthesis, meaning stomatal conductance and the ratio of leaf-internal to external CO_2 concentration (c_i/c_a) remain unaffected, than changes in F_{CO2} (reflecting soil respiration, R_S) represent changes in the amount of carbohydrates allocated to belowground, and the consequences of these changes (e.g., mycorrhizae and root mortality and decomposition). Recent work utilizing the five-day step-changes of eCO_2 demonstrated that, although mean canopy stomatal conductance under eCO_2 was lower than under ambient CO_2 concentration (aCO_2) for *P. taeda* and its major competitor, *Liquidambar styraciflua* (sweetgum), and thus for the entire canopy, the conductance did not respond to the short-term changes in eCO_2 anywhere between ambient and 1.8 × ambient. Because c_i/c_a was unresponsive to eCO_2 (Ellsworth 1999), suggesting that carbohydrate production changed proportionally with eCO_2. This allows interpreting the both short-term and long-term changes in eCO_2 on F_{CO2}, and identifying the processes most likely contributing to these processes – the subject of Chapter IV.

However, prior to tackling this objective, it was necessary to quantify the effect of eCO_2 on mean canopy stomatal conductance during the last two years of enrichment, and two years following termination. During the latter period, a large reduction of *L* was observed under eCO_2, decreasing from ~17% above aCO_2 plots while under enrichment, becoming similar to that under aCO_2 within the two years post-enrichment (Chapter III). Lower mean canopy stomatal conductance on eCO_2 was attributed to both higher *L* (and thus lower mean light intensity on leaf surface; Tor-ngern *et al.* 2015) and lower hydraulic conductance (Domec *et al.* 2009). Thus, it was unclear whether mean canopy

stomatal conductance will increase as *L* decreases (while also increasing the hydraulic variable A_S/A_L), thus simply compensating and keeping total conductance similar in aCO_2 plots and those formerly under eCO_2, or whether lower tissue-specific hydraulic conductivity would keep eCO_2 below that of aCO_2, thus reducing carbohydrate production, and complicating interpretation of F_{CO2} because, in this case, both production and allocation might have changed. Mean canopy stomatal conductance was computed from sap flux density measurements, *L* and vapor pressure deficit (*D*), thus assuming strong coupling between leaves and the atmosphere. This assumption has been found acceptable for *P. taeda* (Ewers & Oren 2000), but was not tested for the broadleaved species at the site. Because only *P. teada* and *L. styraciflua* were measured long-term at the site, a nearby broadleaved deciduous forest of similar *L* but more complete data set, including accompanying stand-scale eddy covariance measurements, provided a better setting to evaluate the assumption for *L. styraciflua*. Because most species studied at that stand had greater characteristics leaf dimensions than that of *L. styraciflua*, the conclusions from that analyses (Kim *et al.* 2014; Chapter II) represent a conservative assessment of the assumption.

Armed with these answers, the hypotheses of the final chapter (IV) could be addressed. As stated in Chapter IV: "(**H1**) the effect of five-day CO_2 changes during the end of the growing season will be reflected in corresponding changes of F_{CO2}. [Further]…if eCO_2 confers some protection from drought effects, the effect of **H1** will be relatively greater during low soil moisture, high vapor pressure (*D*) conditions. The reduction of F_{CO2} has been explained not only by a decrease in sugar flow to

belowground, but also in terms of rapidly decreasing biomass of mycorrhizae and fine roots (Högberg *et al.* 2001; Drake *et al.* 2012; Jing *et al.* 2015; Hasselquist *et al.* 2016). Reductions of mycorrhizae may occur within a week (Högberg *et al.* 2001), and those of fine roots are observed after three months (Jing *et al.* 2015). Thus, …(**H2**) following the termination of eCO_2 at the Duke FACE, F_{CO2} (reflecting R_S) will decline to that of the reference within approximately three months, remaining at that level for the following two years of monitoring. Alternatively, a larger pool of carbohydrate reserves in roots may buffer against short-term variation in photosynthesis, and a pulse of dying roots may provide for greater microbial activity, maintaining greater F_{CO2} in plots previously subjected to eCO_2."

2. Response to CO_2 enrichment of understory vegetation in the shade of forests

2.1 Introduction

Forests cover approximately 31% of the land surface and store more carbon than other terrestrial ecosystem (FAO & JRC, 2012). Because of biosphere-atmosphere feedbacks, observations of the response of terrestrial ecosystem to changing atmospheric condition are essential for reducing uncertainties in predictions from models coupling terrestrial biosphere behavior to future atmospheric CO_2 concentration and climate (Gregory *et al.*, 2009, Huntingford *et al.*, 2009, Medvigy *et al.*, 2012, Medvigy & Moorcroft, 2012, Niu *et al.*, 2014). To investigate the responses of forest ecosystem to future increases of atmospheric CO_2, including tree growth, carbon sequestration, and hydrologic and energy balance, long-term free-air CO_2 enrichment (FACE) experiments have been conducted for about two decades in different forest settings (Hendrey *et al.*, 1999, Karnosky *et al.*, 1999, Körner *et al.*, 2005, Miglietta *et al.*, 2001, Norby *et al.*, 2001). Most studies in forest FACE experiments focused on responses of the overstory tree components (Asshoff *et al.*, 2006, Dawes *et al.*, 2013, Ellsworth *et al.*, 2012, Liberloo *et al.*, 2009, McCarthy *et al.*, 2010, Talhelm *et al.*, 2014). However, long-term plant biodiversity and forest composition, and thus ecosystem structure and function, may depend on the responses to elevated CO_2 of the sub-canopy or understory vegetation.

Despite the small contribution of understory vegetation to the total productivity of a forest ecosystem, understory vegetation contribute increased structural and compositional variation with positive effects on wildlife (Oliver & Larson, 1996), and

potential negative effect on fire as it can produce a continuous fire ladder to the canopy (Perry, 2008). Furthermore, some of the understory represent regeneration (from seedling to advanced stage) of species that in the absence of large scale and intensive disturbance will ultimately replace the canopy species (Oliver, 1981, Oliver & Larson, 1996, Runkle & Yetter, 1987). Thus, information on the survival and growth of species in the understory of FACE experiments is critical for properly modeling the successional dynamics and future plant community composition in ecosystem models, with consequences ranging from predictions of biodiversity to carbon sequestration and biosphere-atmosphere interactions (Dietze, 2014, Oliver & Larson, 1996, Royo & Carson, 2006).

Few studies examined herbaceous and woody understory vegetation at FACE sites, but the results were not consistent (see Table A1 in Supporting Information for the previous studies of the response of understory vegetation to CO_2 enrichment). To summarize, light-saturated net photosynthetic rate of saplings of six broadleaved species ranging in shade-tolerance (*Acer rubrum*, *Carya glabra*, *Cercis canadensis*, *Cornus florida*, *Liquidambar styraciflua* and *Liriodendron tulipifera*) in the understory of a loblolly pine (*Pinus taeda*) forest increased under elevated CO_2 at the Duke FACE experiment (DeLucia & Thomas, 2000, Naumburg & Ellsworth, 2000), with smaller to no enhancement of apparent quantum yield (DeLucia & Thomas, 2000, Ellsworth *et al.*, 2012, Singsaas *et al.*, 2000, Springer & Thomas, 2007). Moving from photosynthesis to survival and growth, the relative growth rate and survivorship probabilities of seedlings of 14 tree species (12 broadleaved species) germinating in enclosures was investigated

over six years of CO_2 enrichment (1998-2003; Mohan *et al.*, 2007); although growth rates of most species did not respond to elevated CO_2, when combined with survivorship, overall understory biomass in elevated CO_2 was estimated to be 26% greater than that in ambient CO_2. Similarly, consistent with higher photosynthesis, elevated CO_2 in a *L. styraciflua* plantation increased aboveground biomass of understory vegetation by 25% (60% for woody saplings only) after 10 years of CO_2 enrichment, with the contribution of woody species increasing over time (Souza *et al.*, 2010). However, such CO_2-induced response was not detected in stands of aspen (*Populus tremuloides*) and mixed aspen-birch (*Betula papyrifera*) overstory (Aspen FACE; Bandeff *et al.*, 2006). At that site, both above- and belowground biomass of red clover (*Trifolium pratense*) decreased due to lower light levels under elevated CO_2 (Awmack *et al.*, 2007).

The inconsistent responses of understory vegetation to elevated CO_2 may have resulted from a combinations of direct growth-enhancing effect of CO_2 and indirect alteration of biotic (e.g. feeding behavior of herbivores) or abiotic (e.g. light, water and soil nutrients) conditions to which understory vegetation was subjected under elevated CO_2 (Awmack *et al.*, 2007, Bandeff *et al.*, 2006, Belote *et al.*, 2004, Kubiske *et al.*, 2002). For example, at the Aspen FACE site, a positive correlation was observed between biomass and photosynthetically active radiation (PAR) in the understory, which decreased under elevated CO_2 (Awmack *et al.*, 2007, Bandeff *et al.*, 2006). Furthermore, the effect of elevated CO_2 on understory vegetation may depend on root-zone soil water availability. For example, aboveground net primary productivity (NPP) of Japanese honeysuckle (*Lonicera japonica*) increased with CO_2 regardless of growing season

precipitation, but that of another understory-dominant Nepal grass (*Microstegium vimineum*) decreased in a wet but not in a dry year (Belote *et al.*, 2004).

Differences in sensitivity to elevated CO_2 by plant functional group (e.g. trees, shrubs, legumes, forbs, grasses and crops) or by species may also contribute to inconsistent responses of understory vegetation to elevated CO_2 (Ainsworth & Long, 2005, Ainsworth & Rogers, 2007, Hättenschwiler, 2001, Poorter & Navas, 2003, Sefcik *et al.*, 2006). In terms of light-saturated CO_2 uptake, trees were more responsive to elevated CO_2 than herbaceous plants and shrubs (Ainsworth & Long, 2005, Ainsworth & Rogers, 2007). Shade-tolerant tree species (e.g. *A. barbatum*, *C. florida* and *Ulmus alata*) showed greater response to elevated CO_2 than shade-intolerant species (Ellsworth et al., 2012). A meta-analysis of pre-FACE experiments also observed a greater biomass response ratio to CO_2 of shade-tolerant species than shade-intolerant species; the difference disappeared when available light was too low (Kerstiens, 2001). Responses of hydraulic pathway to elevated CO_2 differed among species; some species (e.g. *L. styraciflua* and *C. florida*) reduced stomatal conductance by altering liquid phase transport through the hydraulic pathway, and might not show growth enhancement in elevated CO_2 (Domec *et al.*, 2010, Schäfer *et al.*, 2002). Overall, trees were expected to have a greater capacity to respond to elevated CO_2 because they can accumulate the effects of increased leaf area and biomass from CO_2 enrichment (Ainsworth & Long, 2005, Souza *et al.*, 2010), but this generality may not hold in the light-limited sub-canopy environment.

Vines may respond more than trees to elevated CO_2 because they invest less carbon in structural support, allowing a greater partitioning of extra carbon to leaf production with potential positive feedback to plant photosynthesis and growth (Schnitzer & Bongers, 2011). The aboveground NPP of a vine species (*L. japonica*) in elevated CO_2 was 2.5-4 folds greater than that in ambient CO_2 at ORNL FACE site (Belote *et al.*, 2004, Sanders *et al.*, 2004). In an irrigated and fertilized vineyard, the biomass (excluding fruit) of a twenty-year-old *Vitis vinifera* increased 28-42% during two years of CO_2 enrichment (550 ppm; Bindi *et al.*, 2001). At Duke FACE site, percent increase in plant biomass of poison ivy (*Toxicodendron radicans*) growing under elevated CO_2 concentration for six years (~62%; Mohan *et al.*, 2006) was greater than mean response of 59 woody species to elevated CO_2 (28.8 ± 2.4%; Curtis & Wang, 1998). Not only the responses differed among plant functional types, but contrasting responses can also be found between species of one genera; while the population of one common understory clover species (*T. pratense*) at Aspen FACE site was larger under elevated CO_2, the population of another common clover species (*T. repens*) did not change, perhaps reflecting differential ability to take advantage of increased supply of CO_2 where nutrients were limiting (Awmack *et al.*, 2007).

Here, we investigated the effects of elevated atmospheric CO_2 concentration on understory vegetation in a *P. taeda* plantation at Duke FACE site. Aboveground biomass and densities of three plant functional groups, ground cover plants (combining grasses, forbs and seedlings less than one year old), vines and advanced broadleaved regeneration in ambient and elevated CO_2 under native soil and nitrogen (N)-fertilized conditions were

assessed. Due to generally high canopy leaf area index (LAI) at the site, including that contributed by vines and regenerating broadleaved trees, these two groups accounted for most of the understory biomass. Based on this, and the above summary of scant information on understory indicating that vines and woody vegetation were more responsive to elevated CO_2 than ground cover plants, we hypothesized that mirroring the effect of elevated CO_2 on overstory vegetation, (**H1**) total understory biomass and density will be greater in elevated CO_2. However, N deficiency in the soil had hindered the direct effect of elevated CO_2 at this site (Oren *et al.*, 2001). Thus, (**H2**) the effect of elevated CO_2 on understory biomass will be more obvious with N fertilization. Conversely, elevated CO_2 increased leaf area of the *P. taeda* and entire canopy at this site (McCarthy *et al.*, 2007), and increase in leaf area of *P. taeda* is likely to make overstory LAI in elevated CO_2 higher than in ambient CO_2. Overstory LAI corresponds to all foliage above understory vegetation. Because increases in overstory LAI may reduce light availability in the understory, and the daily photosynthesis of understory vegetation in moderate shade depends on light-saturated photosynthesis (Naumburg *et al.*, 2001), understory biomass and density may be lower in higher overstory LAI plots (i.e. negative indirect effect of elevated CO_2). Thus, the alternative hypothesis (**H3**) was that the increase of LAI may diminish, or even reverse, the expected responses of understory vegetation to CO_2 and N enrichment. We also expected that the different sensitivities among functional groups and species to CO_2 enrichment may cause a difference in the community composition between plots in ambient and elevated CO_2. Specifically we hypothesized (**H4**) that the prevalence of shade-tolerant species would increase both due to direct effect

of CO_2 on their photosynthesis and the indirect effect of decreasing light on shade-intolerant species, thus reducing species richness.

2.2 Materials and Methods

2.2.1 Site description

The study was conducted at the Duke Forest FACE site, North Carolina, USA (36° 58´ N, 79° 06´ W). The annual mean air temperature and precipitation of the site are 15.5 °C and 1145 mm, respectively. Precipitation is generally evenly distributed throughout the year. The *P. taeda* seedlings were planted after clear-cut and burn at the site in 1983 at 2 × 2.4 m spacing (McCarthy *et al.*, 2007), and the mean and maximum heights in 2010 reached 21.5 and 26 m, respectively. Under the planted and naturally seeded pine canopy, broadleaved species such as *L. styraciflua*, *U. alata*, *A. rubrum*, and *Fraxinus americana* were established naturally. Most broadleaved individuals were present only in the mid- to lower-canopy, but some extended to the upper canopy (McCarthy *et al.*, 2007). LAI of broadleaved species at the site accounted for 40.8 ± 8.6% of total LAI during growing season in 2009.

A total of eight, 30 m diameter circular plots were established, beginning with the FACE prototype and its reference (plots 7 and 8) in 1993, and concluding with six additional plots in 1996. Four plots had received CO_2 enrichment, targeted at 200 ppm above ambient, according to the FACE protocol, beginning in 1994 (plot 7) or 1996 (plots 2, 3 and 4; Hendrey *et al.*, 1999); the enrichment terminated on October 31, 2010. In 1998, the prototype and its reference plot were divided in half by inserting an

impermeable barrier to 70 cm from the soil surface, the depth of the fine root system (Matamala & Schlesinger, 2000), and a complete fertilization was applied annually (1998-2004), depending on the nutrient requirements for that year. After similarly splitting the remaining plots in early 2005, a common protocol of annual N-only application (ammonium-nitrate pellets, 11.2 g N m^{-2} yr^{-1}) was employed on one half (two sectors) of each plot.

2.2.2 Data

The aboveground biomass of ground cover plants (grasses, forbs and seedlings), vines and small (DBH < 8 cm) broadleaved regeneration in one native soil and one N-fertilized sector (105.6 ± 13.3 m^2) in each plot were harvested in October and November 2010. Trees dominating in the upper canopy (*P. taeda* and larger broadleaved regeneration) were harvested from February through April 2011. Some vine species, grapevine (*Vitis* spp.) and poison ivy (*T. radicans*), extended into the upper canopy, entwining the tree branches. We were able to harvest these vines during the harvest of the canopy trees and added their contribution to the vine biomass. The average height of *P. taeda* in elevated CO_2 (22.3 ± 2.1 and 22.6 ± 2.2 m under native soil and N-fertilized conditions, respectively) were greater than those in ambient CO_2 (20.5 ± 2.4 and 20.7 ± 2.4 m), yet the 90% of the crown bases of *P. taeda* were located at similar heights across treatments (11.8, 12.8, 11.7 and 12.6 m; the heights were not different by treatment). Thus, all vegetation reaching less than the average of all plots across treatments (~12 m) were classified as understory vegetation (Fig. 2.1; see Fig. A1 for the distribution of log transformed aboveground biomass across individuals). Approximately 0.8% (ranging 0 to

18%) of understory broadleaved regeneration biomass was *Juniperus virginiana*, exceeding 1% in only 2 half-plots and founded in only 4 half-plots. Therefore, we included *J. virginiana* as part of broadleaved regeneration. Individuals harvested in each quarter plot were identified and counted by species. All samples were oven-dried at 65 ºC for one week and weighed.

To account for understory light condition, five-year (2005-2009) average growing season overstory LAI was estimated by multiplying total LAI and the proportion of leaf area found above 12 m. The proportion of overstory leaf area was calculated with LAI profiles of each plot which were measured at 12-13 heights using an optical plant canopy analyzer, LAI-2000 (Li-Cor, Lincoln, NE) in August 2010 (Fig. 2.1b). The total LAI was estimated based on leaf litterfall measurements, which were collected once or twice (October to January due to high volume of leaf litter) per month from 12 (three per sector) 0.16 m^2 litter baskets in each plot. Collected leaf litter were sub-sampled to determine specific leaf area (SLA), oven-dried at 45 ºC for four days, separated by species (*P. taeda*, *L. styraciflua* and other broadleaved species), and weighed. LAI of *P. taeda* and broadleaved species were estimated separately because their timing of leaf production and loss are different. LAI of *P. taeda* was calculated using the annual leaf area production, leaf area loss and relative leaf area expansion from needle elongation measurement. Because the average *P. taeda* needle longevity is 19 months (Zhang & Allen, 1996), the annual leaf area production was calculated by multiplying SLA and mass of leaf litter, based on litter collected beginning May of the following year to May the year after. LAI of broadleaved species was calculated with SLA, leaf litter mass,

relative leaf area expansion and leaf area loss in each year. Details on LAI estimation are given in McCarthy *et al.* (2007).

To investigate the relationship between understory light condition and the overstory LAI, diffuse and direct radiation reaching the understory were estimated using diffuse non-interceptance (DIFN) and gap fraction values from LAI-2000 measurements. In August, about the midpoint of the annual amplitude of LAI, LAI-2000 measurements were made from the central tower of each plot, 12 m aboveground, in four cardinal directions; only two of the four measurements, those taken radially from the plot-center towards the middle of the outer arc representing a fertilization treatment half-plot, were used to estimate five-year average (2005-2009) DIFN and gap fraction for direct radiation. Among the gap fractions at five mid-point zenith angles (7, 23, 38, 53 and 68°) of LAI-2000, values from the lowest angle (68°) were always zero and not used. Values from the other four angles over five years were used to derive a relationship of gap fraction as a function of solar zenith angle. The mean daytime growing season solar zenith angle at the site was then used to estimate the gap fraction for direct radiation. Because DIFN and the gap fractions for direct radiation was highly correlated ($r = 0.992$), DIFN was used as a representative factor of understory light condition.

2.2.3 Statistical analysis

Assessing treatment effects using multiple comparisons emphasizes what would happen if the null of no difference is true. This approach often results in a reduced significance level (much smaller than 0.05), and thus a much reduced statistical power. Furthermore, concerns of multiple comparisons are real for some problems.

Mathematically, such concerns stem from a simple mathematical theorem stating that sample averages are often more extreme than the real population means (Efron, 1978). When there are multiple variables x_{ij} (ith data point from variable j) and $x_{ij} \sim N(\theta_j, \sigma)$, where θ_j are the true means, this mathematical theorem indicates:

$$\Pr\left(\sum_j (\bar{x}_j - \mu)^2 > \sum_j (\bar{\theta}_j - \mu)^2\right) > 0.5$$

The result suggests that when estimating multiple means, the estimation can be improved by shrinking the sample averages towards the overall mean, thereby avoid the use of multiple comparisons (Gelman *et al.*, 2012). Thus the overall accuracy can be increased by using the Bayesian hierarchical model (BHM), which uses shrinkage estimators, facilitating estimating treatment effects.

We used BHM implemented in Stan and R (RStan package in R 3.0.3; Stan Development Team, 2014), which can be more informative and detect smaller treatment effects than ANOVA (Gelman & Hill, 2007, Qian *et al.*, 2009). Because there were two treatments (CO_2 enrichment and N fertilization) with two levels each, we combined them into a treatment of 4 levels (native soil / ambient CO_2; native soil / elevated CO_2; N-fertilized soil / ambient CO_2; N-fertilized soil / elevated CO_2) to improve numerical stability:

$$y_{ij} = \beta_0 + \beta_i + \varepsilon_{ij} \quad (1)$$

$$\beta_i \sim N(0, \sigma_\beta^2) \quad (2)$$

$$\varepsilon_{ij} \sim N(0, \sigma^2) \quad (3)$$

where y_{ij} is *j*th observation of aboveground biomass or density in *i*th treatment, β_0 is the overall mean, β_i is the effect of *i*th treatment, ε_{ij} is the error term, σ_β^2 is the between group variance and σ^2 is the within group variance. There were four observations in each of the four treatments (N = 16). BHM approach in the linear regression setting was used to investigate the effect of understory light environment with overstory LAI or DIFN:

$$y_{ij} = \alpha_{0i} + \alpha_{1i}x_{ij} + \varepsilon_{ij} \quad (4)$$

$$\begin{pmatrix}\alpha_{0i}\\ \alpha_{1i}\end{pmatrix} \sim MVN\begin{bmatrix}\theta_0\\ \theta_1\end{bmatrix}, \Sigma \quad (5)$$

$$\varepsilon_{ij} \sim N(0, \sigma^2) \quad (6)$$

where y_{ij} is *j*th observation of aboveground biomass (log-transformed) or density in *i*th treatment, α_{0i} and α_{1i} are the regression coefficients with a multivariate normal distribution and x_{ij} is the five-year average growing season overstory LAI or DIFN for observation *j* in treatment *i*.

Our analysis accepted the no-change (or null) hypothesis. Although accepting the null was considered to be less rigorous as the probability of type II error is unknown (e.g., Steidl *et al.*, 1997), we used the BHM approach (as discussed in Gelman & Tuerlinckx, 2000) for our inference, thereby avoiding the problems associated with the classical hypothesis testing method.

Species diversity and community similarity in ambient and elevated CO_2 under native soil and N-fertilized conditions were compared using the Gini-Simpson index and (Gini, 1912, Simpson, 1949) the Morisita-Horn index (Horn, 1966) both based on Simpson index (Simpson, 1949). Simpson index was preferred because it is unbiased and

is linked to other diversity indices with a generalized formulation of entropy (Keylock, 2005). The indices were calculated separately for each sector.

2.3 Results

The total aboveground biomass of understory vegetation in ambient and elevated CO_2 were 1696.70 ± 418.12 and 1509.85 ± 592.82 g m^{-2} under native soil condition, and 1772.32 ± 664.63 and 1240.83 ± 395.82 g m^{-2} under N-fertilized condition (see Table A2 for the aboveground biomass of each functional group and species; we carried two decimal places because some aboveground biomass were less than 1 g), representing ~6% of total plot aboveground (stem + branch) biomass (calculated from McCarthy *et al.*, 2010). Approximately 92% of the total aboveground biomass of the understory vegetation was composed of broadleaved regeneration; the other 8% was from vines. Although large amount of *Parthenocissus quinquefolia* and *L. japonica* were found in four of the 16 quarter plots, *Vitis* was the dominant vine genus across all treatments, accounting on average for 67.2 ± 36.7% of the total vine biomass (see Table A2). The aboveground biomass of ground cover plants was 0.11 ± 0.26 g m^{-2} on average (1.06 g m^{-2} at most), which comprised only 0.01% of the total understory biomass.

There were 1.32 ± 0.74 and 1.05 ± 0.08 understory individuals per unit ground area (m^2) in ambient and elevated CO_2 under native soil condition, and 0.74 ± 0.15 and 0.58 ± 0.25 understory vegetation under N-fertilized condition (see Table A2 for the density of each functional group and species). Ground cover plants, broadleaved

regeneration and vines accounted for 12.6 ± 9.8%, 64.1 ± 13.6% and 23.2 ± 15.3% of the total number of understory individuals, respectively.

Figure 2.2 showed posterior distributions of aboveground biomass and densities (number of individuals per 1 m^2 of ground area) of ground cover plants, broadleaved regeneration and vines. Because BHM approach presented the posterior distributions of each parameter as MCMC samples, we used a Monte Carlo simulation to compare the differences between CO_2 treatments. When the 95% credible interval of the difference did not include zero, we concluded that the difference is statistically significant; we determined that there was a close to significant difference when more than 90% of the posterior samples of the difference estimate were present below or above zero. Posterior distribution of differences in aboveground biomass and densities between ambient and elevated CO_2 treatments indicated no significant effect of elevated CO_2 in any of the three components of understory vegetation, regardless of soil fertility conditions (see insets of Fig. 2.2). Excluding large (DBH > 8cm) broadleaved regeneration, which was suspected to have greater influence on the biomass of each plot than smaller ones, did not change the results (see Fig. A3a and A3b). We reanalyzed the data partitioned to different plant groups, including ground cover, consisting of vegetation below 1 m, tree seedlings and saplings <2 cm in DBH reaching a height of 4 m, and tree saplings 2-8 cm in DBH, 99.1% of which below 12 m in height with a maximum height of <13 m. Consistent with the analysis of the combined data, neither aboveground biomass nor density of any class of vegetation was affected by CO_2 in either soil fertility condition (see Fig. A3). The

aboveground biomass and density of vines excluding the two species extending into the upper canopy (*Vitis* spp. and *T. radicans*) were not affected by CO_2 treatment (see Table A2 for aboveground biomass and density of each vine species).

Across treatments, a total of 30 broadleaved species were found in the understory of this site; *A. rubrum, C. Ovata, C. tomentosa, F. Americana, L. styraciflua* and *U. alata* were the most abundant species. Eighteen species were classified as shade tolerant (see Table A3 for the classification of shade tolerance of broadleaved trees in this study). Shade tolerant broadleaved individuals represented ~44 and ~46% of all broadleaved individuals in ambient and elevated CO_2 under native soil condition and ~49 and ~44% under N-fertilized condition (Fig. 2.3a), showing also no significant treatment effect on biomass (compare Tables A2 and A3). Posterior distributions of paired differences in the proportion of shade tolerant species between ambient and elevated CO_2 were not significant under both conditions.

The Gini-Simpson index and Morisita-Horn index were calculated to compare the community composition in ambient and elevated CO_2. Ground cover plants were excluded due to their small contribution to the total understory biomass. The mean Gini-Simpson indices were 0.84 ± 0.06 and 0.85 ± 0.03 in ambient and elevated CO_2 under native soil condition and 0.84 ± 0.04 and 0.85 ± 0.03 under N-fertilized condition; the indices were not significantly affected by CO_2 enrichment (Fig. 2.3b). The community similarities among all sectors were calculated using Morisita-Horn index. The indices of community similarity within sectors in the same CO_2 levels (i.e. between two sectors in

ambient CO_2 or between two sectors in elevated CO_2; 0.35 ± 0.24 and 0.44 ± 0.19) were not different from those between sectors in different CO_2 levels (0.27 ± 0.17 and 0.47 ± 0.22) under both native soil and N-fertilized conditions (Fig. 2.3c). We also examined the effect of CO_2 enrichment on community composition (including ground cover plants) by using redundancy analysis (vegan package in R 3.0.3; Oksanen *et al.*, 2015). CO_2 enrichment explained only 10 and 7% ($p = 0.792$ and 0.845 with 999 permutations) of the total variation of community composition under both native soil and N-fertilized conditions, respectively.

Total aboveground biomass and total density of understory vegetation showed a significant decrease and a tendency to decrease with increase in five-year average growing season overstory LAI (Fig. 2.4a and 2.4b). The decrease in total aboveground biomass and total density were due to the responses of broadleaved regeneration; responses of the aboveground biomass and densities of ground cover plants and vines were not significant (see Fig. A4). Posterior distributions of differences in slopes by CO_2 enrichment showed that slopes were similar in both CO_2 levels regardless of soil fertility (see inset of Fig. 2.4a). The differences of slopes from the relationship between overstory LAI and total densities of understory vegetation were also not different from zero (inset of Fig. 2.4b).

Among all regenerating broadleaved species found in this understory, there were 12 regenerating canopy species (e.g., *F. americana* and *L. styraciflua*) and 18 subcanopy species (e.g., *C. canadensis* and *U. alata*). Treatment effects on aboveground biomass

and density were not observed for both regenerating canopy species and subcanopy species (see Table A2). Increase in overstory LAI significantly reduced density (advanced generation only) of regenerating canopy species and close to significantly reduced aboveground biomass (Fig. 2.4c and 2.4d). For subcanopy species, the relation between overstory LAI and density of advanced generation and aboveground biomass were not significant (Fig. 2.4e and 2.4f).

When N fertilization effect was ignored, five-year average overstory LAI in elevated CO_2 (3.37 ± 0.48) was significantly greater than that in ambient CO_2 (2.70 ± 0.59; Fig. 2.5a). Figure 2.5b and 5c showed total aboveground biomass and total density of understory vegetation in ambient and elevated CO_2, ignoring the effect of fertility treatment. The difference in aboveground biomass and density were not significant.

Higher overstory LAI may reduce both light and moisture availability to the understory vegetation. A significant relationship between total LAI and relative extractable water in the root zone were not observed at this site (Fig. A2). Increase in overstory LAI significantly reduced DIFN (Fig. 2.6a); difference in mean DIFN between ambient CO_2 (0.14 ± 0.01) and elevated CO_2 (0.11 ± 0.01) was not significant, but observable (Fig. 2.6b). The total aboveground biomass of understory vegetation increased with the increase in DIFN significantly in elevated CO_2; the positive response in ambient CO_2 and the effect of CO_2 treatment on the sensitivity of the response (i.e. steeper slope in elevated CO_2) were visible, but not statistically significant (Fig. 2.6c and 2.6d). A classical split-plot (N nested within CO_2 treatment) analysis of covariance (DIFN) had a

similar outcome of no CO_2 effect on the slopes of the relationships of aboveground biomass ($p = 0.659$) and density ($p = 0.106$) *versus* DIFN (Table A4). The aboveground biomass of regenerating canopy species increased close to significantly with the increase in DIFN; the slopes in ambient and elevated CO_2 were not different (see Fig. A5a). Common subcanopy species did not show such tendency of increasing aboveground biomass with the increase in understory light availability (see Fig. A5b). We also reanalyzed the data partitioned three understory cover types based on the DIFN calculated at their maximum height (1 m for ground cover, 4 m for broadleaved regeneration with <2 cm DBH, and 12 m for broadleaved regeneration with 2-8 cm DBH); the aboveground biomass of broadleaved regeneration with 2-8 cm DBH showed a significant increase with DIFN, while the other two did not respond to changes in DIFN (Fig. A6).

2.4 Discussion

Increase in atmospheric CO_2 concentration generally enhanced carbon uptake and growth of plants (Ainsworth & Long, 2005, Norby & Zak, 2011). Given previous findings of the positive photosynthetic responses to CO_2 enrichment of understory vegetation in this site (DeLucia & Thomas, 2000, Ellsworth *et al.*, 2012, Springer & Thomas, 2007), increase in biomass and densities of understory vegetation after long-term CO_2 enrichment were expected. However, contrary to the hypothesized response (**H1** and **H2**), we did not observed enhancement of biomass or density in elevated CO_2 for any understory plant functional groups under native soil or N-fertilized conditions.

In fact, despite demonstration of nitrogen limitation to growth of canopy trees under elevated CO_2 in this site (Finzi *et al.* 2002, McCarthy et al. 2010) – a limitation resolved through N-fertilization (Finzi *et al.*, 2002, Oren *et al.*, 2001) – understory vegetation did not grow faster nor responded more to high CO_2 concentration under non-limiting nitrogen conditions. The results suggested that nitrogen was not a resource limiting the physiological performance of understory vegetation at the site, at least when compared to other factors such as light.

The contribution of ground cover to total understory biomass in this site (0.01%) was much smaller than that of Aspen (> 90%; Bandeff *et al.*, 2006) or ORNL (50-93%; Souza *et al.*, 2010) FACE sites. High LAI of the canopy trees, vines and advanced regeneration in the subcanopy might have retarded the growth of herbaceous and grass species so much that it would be unlikely to discern treatment effects, even if present, on the background of the high spatial variation typically observed in ground cover under forests. As anecdotal support from Duke FACE, a few patches of higher density ground cover were found only where the canopy did not fully recover from ice storm damage in 2002, allowing more light to forest floor. Not only this anecdote suggested strong light limitation to ground cover species, but would also increase the random variance within treatments. Indeed, high variability of aboveground biomass in the understory of Aspen FACE hampered attempts to distinguish elevated CO_2 effects on grasses and herbaceous species groups (Bandeff *et al.* 2006).

Vines represented 8% of the total biomass of understory vegetation and 0.5% of the stand aboveground biomass. The contribution of vines at this site was not very

different from that observed in temperate North America (0.9%; Kush et al., 1999) and much smaller than in tropical forest (<5%; Hegarty & Caballe, 1991). Few studies have investigated the responses to elevated CO_2 of vine species (*L. japonica*, *T. radicans* and *V. vinifera*) at FACE sites, generally showing increased growth (Belote *et al.*, 2004, Bindi *et al.*, 2001, Mohan *et al.*, 2006, Sanders *et al.*, 2004). However, none of these three vine species accumulated more biomass over 15-17 years of elevated CO_2 based on our larger sample. Furthermore, neither *L. japonica* nor *T. radicans* was found consistently in large quantity. The conditions of our forest were far from the optimal dominating in vineyards, yet the foliage of *Vitis* species was intermingled with that of the upper canopy trees (thus not likely light-limited), and in half of each plot the vines should not be nitrogen limited. Nevertheless, we observed no CO_2-induced increase in *Vitis* species.

Several studies observed greater aboveground biomass of understory broadleaved species in elevated CO_2 (Mohan *et al.*, 2007, Souza *et al.*, 2010). However, such positive responses were not observed in broadleaved species that naturally regenerated in the understory, a community exposed to elevated CO_2 for 15-17 years and to N-amendment for 6-13 years (the longer periods in the Duke FACE prototype). Thus, in this moist-warm climate, where water limitation was infrequent and N limitation was alleviated, the results pointed to light as the factor limiting the response of broadleaved regeneration to elevated CO_2.

While elevated CO_2 may allow shade intolerant species grow under low light (Hättenschwiler & Körner, 1997), those species at Duke FACE did not survive better in elevated CO_2 (Mohan *et al.*, 2007). Instead, previous studies observed greater biomass

production of shade tolerant than shade intolerant species with CO_2 enrichment, and suggested that elevated CO_2 may render shade tolerant species more competitive in future understory communities (Ellsworth *et al.*, 2012, Kerstiens, 2001, Mohan *et al.*, 2007). In this study, however, we detected no CO_2 effect on the proportion of shade tolerant broadleaved regeneration regardless of soil fertility. Given the equally diverse and similar broadleaved regeneration and vine communities, we were forced to reject the hypothesis (**H4**) that elevated CO_2 will result in shifts in community composition and diversity in the future.

The responses of the overstory trees to CO_2 enrichment can indirectly influence understory vegetation by altering environmental conditions below the main canopy. In this site, soil temperature and moisture did not change significantly by CO_2 enrichment (Oishi *et al.*, 2014). However, elevated CO_2 enhanced NPP and LAI of the dominant overstory species (*P. taeda*) and canopy broadleaved species by 28% and 14%, which generated a more shady understory environment than in ambient CO_2 (McCarthy *et al.*, 2007, McCarthy *et al.*, 2010), perhaps nullifying the direct effects on photosynthesis (according to **H3**). Given the closed canopy condition, the CO_2-induced 28 ± 22% increase in growing season overstory LAI reduced the mean DIFN by 18 ± 12% in the understory (Fig. 2.6a and 2.6b). The decrease of understory light availability with increasing overstory LAI seemed to have caused a corresponding decline of aboveground biomass and densities of the understory vegetation across treatments (Fig. 2.4, Fig. 2.6c and 2.6d). This was consistent with smaller biomass of potted *T. tretense* placed on the

forest floor in elevated than ambient CO_2 at the Aspen FACE site, attributed to decreased light reaching the understory (Awmack *et al.*, 2007). Likely due to their differences in shade tolerance, it was the responses of regenerating canopy species to increase of overstory LAI, as opposed to the non-responding subcanopy species, which underlie the negative effect of decreased light availability on the understory at this site.

In conclusion, aboveground biomass and densities of broadleaved regeneration were smaller, albeit not significantly, under elevated than ambient CO_2 in both native soil and N-fertilized conditions. This might have been the effect of reduced light availability due to higher overstory LAI in elevated CO_2. On the background of within-treatment variation, the light reduction with CO_2 enrichment was not be sufficient to generate a significant effect on the total aboveground biomass or density, or the characteristics of this understory community. Alternatively, it may be just enough to compensate for the direct growth-enhancing effect of elevated CO_2 (Hättenschwiler & Körner, 2000), an effect impelled by a rather modest increase of actual photosynthetic rates of understory individuals (Ellsworth *et al*. 2012). Regardless of the mechanism, 15-17 years of CO_2 enrichment and 6-13 years of CO_2×N fertilization failed to affect the understory community at this site in any and all measures. Differences among FACE experiments in the responses of overstory LAI to elevated CO_2 (Norby & Zak, 2011) may have been the dominant factor determining the response of the understory vegetation. However, intensive forest management, such as prescribed burning, thinning, and various intensities of harvests, as well as disturbances from climate events, diseases and insects, alter the

amount and composition of understory vegetation directly or by changing the availability of light and other growth resources (Harrington & Edwards, 1999, Horsley et al., 2002, Lieffers et al., 1999, McCarthy et al., 2007, McCarthy et al., 2006, Morin et al., 2007). As has been shown recently for the overwhelming effects of legacy on eastern US forest composition relative to effects of climate change (Nowacki & Abrams, 2015), such prescribed and natural events may allow a response to elevated atmospheric CO_2 not observed at the Duke FACE experiment, where forest management was limited to establishment. We note, however, that overstory LAI has been set back several times over the experiment duration due to hurricanes, droughts and ice storm, bringing LAI under elevated CO_2 closer to that of the ambient treatment (McCarthy et al., 2007, McCarthy et al., 2006), with no observed effects on the understory. Thus, the study provides information necessary for assessing the skills of terrestrial ecosystem models in predicting understory response to elevated CO_2 for a range of soil fertility conditions and LAI response, and sets expectations that can be tested in the new FACE experiments (Norby et al., 2015).

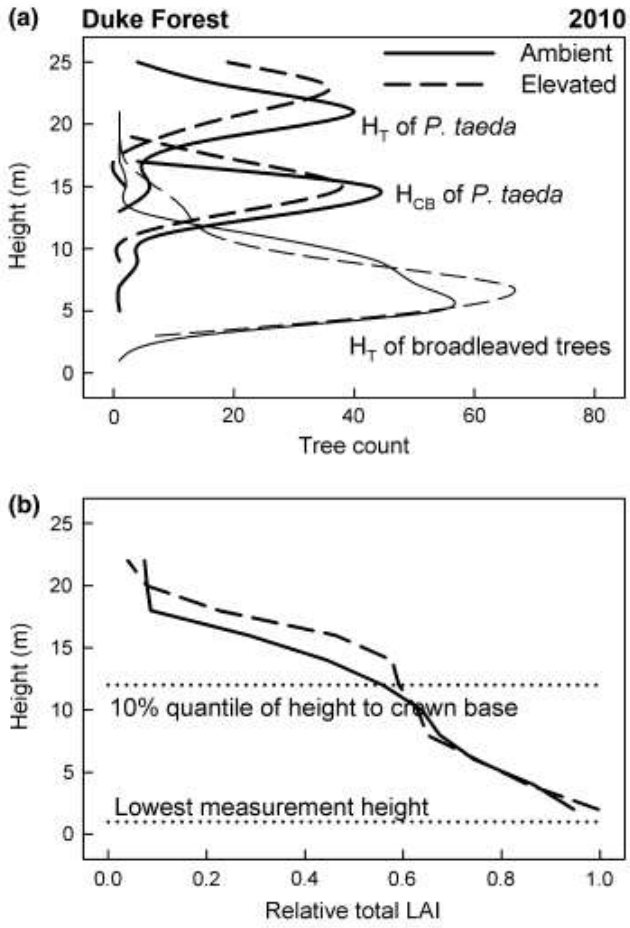

Figure 2.1. (a) Total height (H_T) of *Pinus taeda*, height to crown base (H_{CB}) of *P. taeda* and H_T of broadleaved trees in ambient and elevated CO_2. Thicker lines are for *P. taeda* and thinner lines are for the combined broadleaved species. (b) Cumulative relative total leaf area index (LAI) by height in ambient and elevated CO_2. Dotted lines are the lower 10 percent quantile of H_{CB} of *P. taeda* and the lowest LAI measurement height (1 m from the ground). In both (a) and (b), solid and dashed lines are values from ambient and elevated CO_2, respectively.

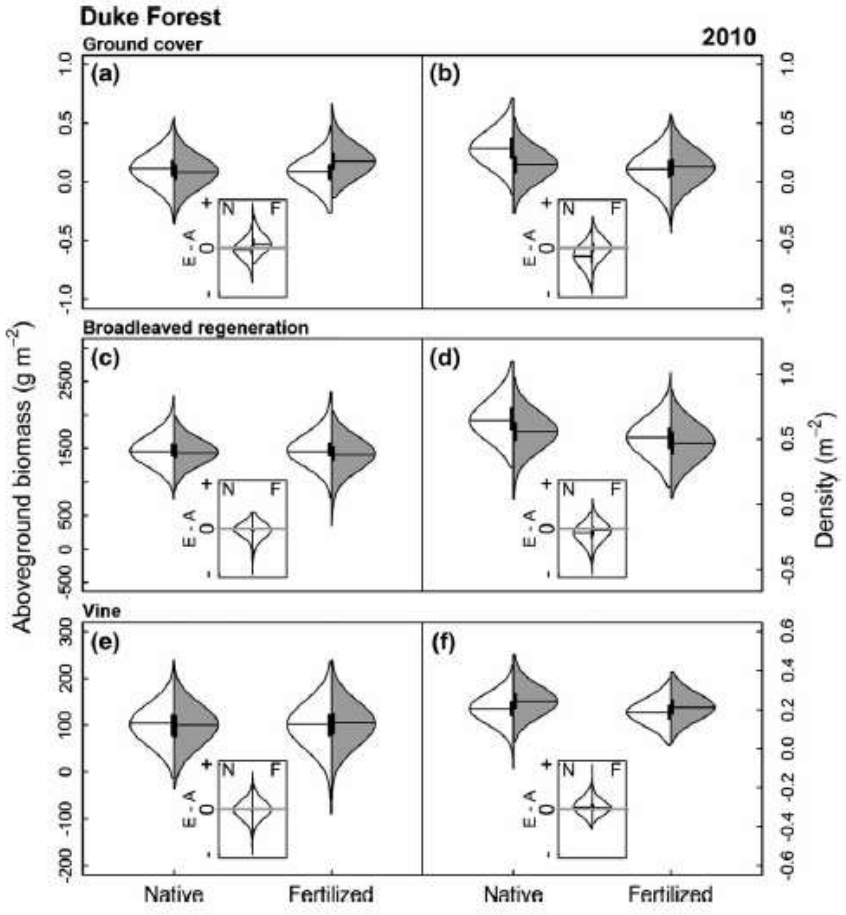

Figure 2.2. Aboveground biomass and density of ground cover plants (a, b), broadleaved regeneration (c, d) and vines (e, f) in ambient (white, left) and elevated (grey, right) CO_2 under native soil and N-fertilized conditions. Means (horizontal solid lines) and 50% posterior credible intervals (boxes) are presented. Inset figures are posterior distributions of differences (elevated – ambient CO_2). The horizontal grey lines in the inset figures are the zero difference lines.

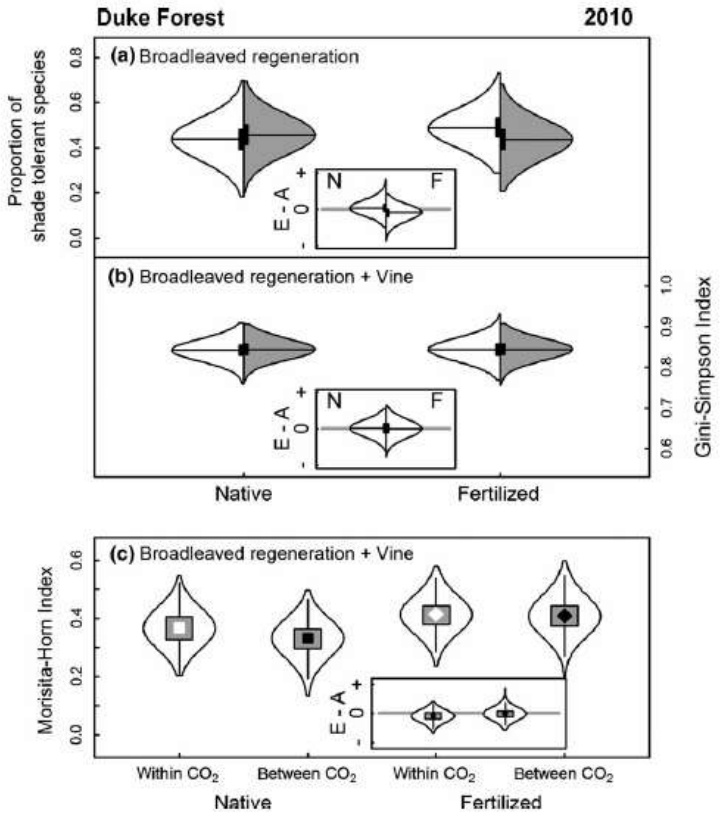

Figure 2.3. The proportion of shade tolerant broadleaved regeneration (a) and Gini-Simpson index for broadleaved regeneration and vines (b) in ambient (white, left) and elevated (grey, right) CO_2 under native soil and N-fertilized conditions. Morisita-Horn index (c) within sectors in the same CO_2 levels (open symbols) and between sectors in different CO_2 levels (closed symbols) under native soil (squares) and N-fertilized (diamonds) conditions. In (a), (b) and (c), boxes represent 50% posterior credible intervals. Inset figures are posterior distributions of differences (elevated – ambient CO_2). The horizontal grey lines in the inset figures are the zero difference lines.

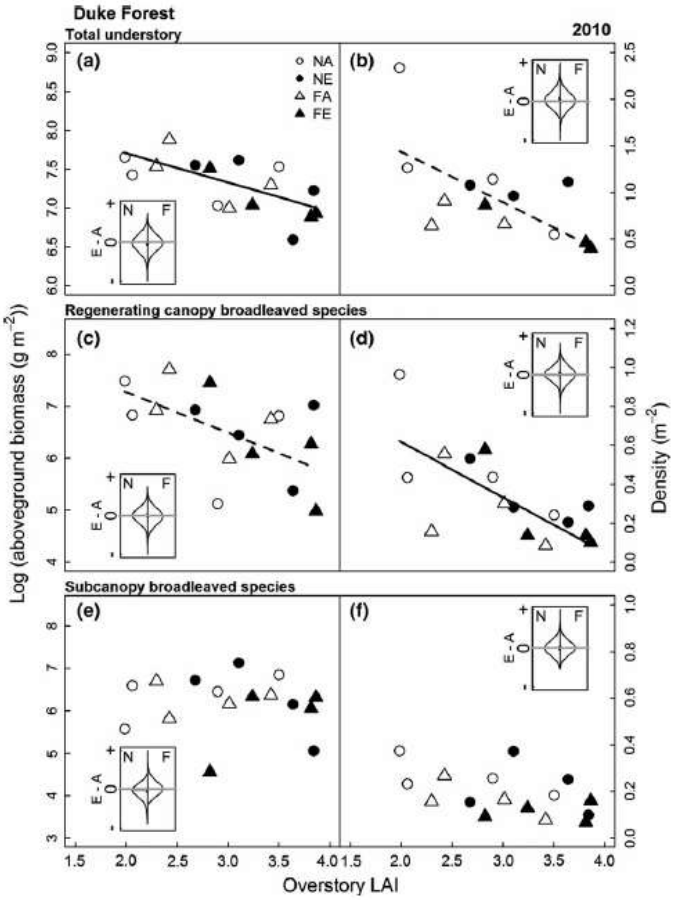

Figure 2.4. Responses of aboveground biomass (log transformed) and density of total understory vegetation (a, b), regenerating canopy broadleaved species (RCBS; c, d) and subcanopy broadleaved species (SBS; e, f) in ambient (open symbols) and elevated (closed symbols) CO_2 under native soil (circles) and N-fertilized (triangles) conditions to five-year average growing season overstory leaf area index (LAI). Solid and dashed lines represent significant and close to significant relationships. Inset figures show posterior distributions of difference (elevated – ambient CO_2) of slope. The horizontal grey lines are the zero lines. In (d) and (f), densities of seedlings were excluded.

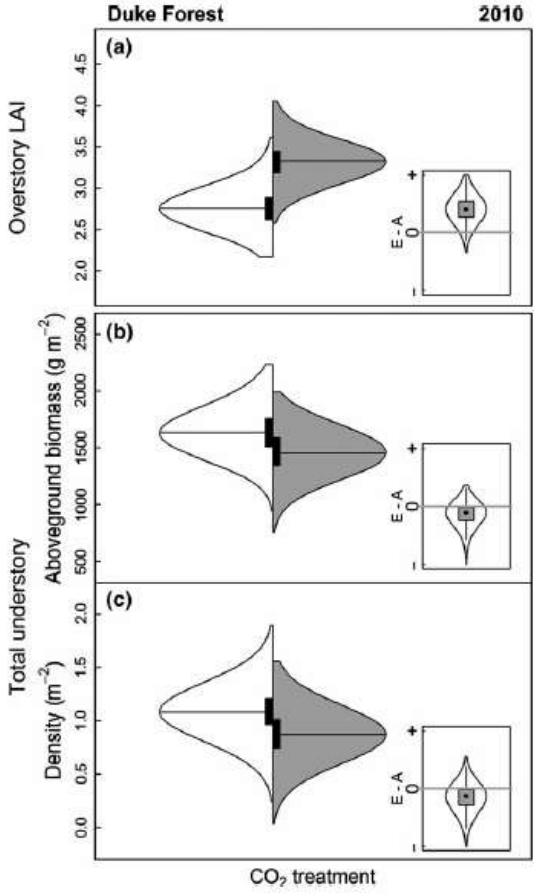

Figure 2.5. Overstory leaf area index (LAI; a), aboveground biomass (b) and tree density (c) in ambient (white, left) and elevated CO_2 (grey, right) ignoring nitrogen fertilization. Means (horizontal solid line) and 50% (boxes) posterior credible intervals are presented. Inset figures are posterior distributions of differences (elevated – ambient CO_2). The horizontal grey lines in the inset figures are the zero difference lines.

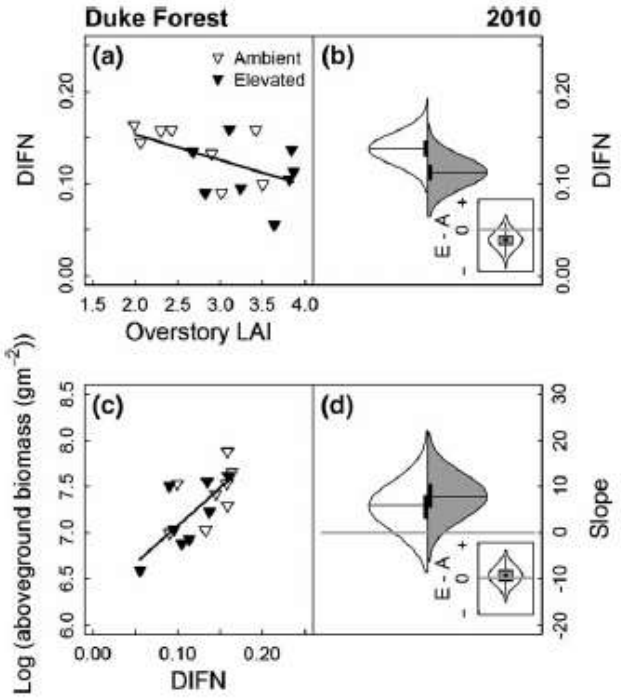

Figure 2.6. Response of diffuse non-interceptance (DIFN) at 12 m to overstory leaf area index (LAI) during five growing seasons (2005-2009; a, b) and response of total aboveground biomass (log transformed) of understory vegetation to DIFN at 12 m (c, d). In (b) and (d), posterior distributions of DIFN and slopes were presented. Inset figures show differences between ambient and elevated CO_2. The horizontal grey lines are the zero lines.

3. Sensitivity of stand transpiration to wind velocity in a mixed broadleaved deciduous forest

3.1 Introduction

Because of their expanse, forests greatly impact the exchange of mass and energy between the biosphere and atmosphere with consequences ranging from effects on local weather conditions (Juang et al., 2007; Konings et al., 2011) to influences on global atmospheric circulation (Avissar and Werth, 2005; Bauerle and Bowden, 2011). Forests also play an important role in the provision of ecosystem services, including water yield, biomass production and carbon sequestration. Improved understanding of these exchanges and benefits involves a combination of observations and models. Estimates of mass (including carbon and water) and energy exchange between the biosphere and atmosphere commonly rely on modeled and measurement-based estimates of a series of resistances to these exchanges, each affected by biological and physical factors.

The flux of water vapor through stomata (i.e. transpiration) is an important flux since it represents the major component of water returned to the atmosphere from forests. Transpiration is also tightly coupled to CO_2 exchange (i.e. canopy photosynthesis or gross primary production) because stomata serve as the common port for the fluxes of these gases. Thus, tree and ecosystem physiologists often investigate the sources of variation of resistances to water vapor flux in lieu of the variation of resistances to CO_2 flux (Kim et al., 2008; Schäfer et al., 2003), and models often computationally link canopy CO_2 uptake to transpiration via the carbon-based water-use efficiency (Running and Hunt, 1993). Transpiration is convenient flux to use in such analysis because, unlike

CO_2 flux, the dynamics of its exchange is straightforward to measure (Granier, 1987; Oishi et al., 2008; Oren et al., 1998; Schäfer et al., 2000).

Resistance to transpiration (R_T) can be partitioned into two serial components, bulk surface resistance (R_{sur}) and aerodynamic resistance (R_A),

$$R_T = R_{sur} + R_A \tag{1}$$

both of which depend on leaf physiology, canopy architecture and the atmospheric conditions above and within the canopy (Jones, 1992; Kumagai et al., 2004). R_{sur} is generally attributed to canopy resistance (R_C) and soil (or forest floor) resistance (R_{soil}) acting in parallel (Allen, 2005).

$$R_{sur} = \frac{R_C R_{soil}}{R_C + R_{soil}} \tag{2}$$

Soil evaporation is minor under high canopy leaf area, making R_C effectively equivalent to R_{sur} when leaf area index (LAI) is greater than 3 (Kelliher et al., 1995; Waring, 2007). R_C can be expressed as a combination of stomatal resistance (R_{stom}) and leaf boundary layer resistance (R_{bl}) in series (Aphalo and Jarvis, 1993):

$$R_C = R_{stom} + R_{bl} \tag{3}$$

R_{stom} reflects complex physiological responses of stomata to variation in atmospheric conditions, such as light availability, air temperature (T_a), humidity, CO_2 concentration (Jarvis, 1976). R_{bl} is the resistance to vapor transfer within the air layer near leaf surface, and can be affected by wind velocity (U), leaf shape, leaf size, edge characteristics, and

surface structure (Schuepp, 1993; Stokes et al., 2006). R_{bl} is generally much smaller than R_{stom} unless leaf size is large or U is low (Aphalo and Jarvis, 1993; Schuepp, 1993).

Over time scales in which soil moisture and plant hydraulic properties (e.g., soil-to-leaf path-length, sapwood-to-leaf area ratio, hydraulic conductivity) can be considered invariable, R_C is largely determined by R_{stom}. Jarvis (1976) described stomatal conductance (the inverse of R_{stom}) as a form of multiplicative function with photon flux density, vapor pressure deficit (D), T_a, ambient CO_2 concentration, and leaf water potential. Many formulations for R_{stom}, ranging from empirical to theoretically-based functions have been proposed and used (Holmgren et al., 1996; Jonard et al., 2011; Launiainen et al., 2011; Pataki and Oren, 2003; Stewart, 1988), but except for allowing interactions among the controlling variables (Ward et al., 2008), this approach remained fundamentally unaltered. The other primary component of R_T, R_A, is determined by the physical conditions above and within the canopy, such as U, atmospheric stability, and canopy structure (Kumagai et al., 2004; Lindroth, 1993; Morris et al., 1998). Although estimates of R_A in forests are usually small relative to R_C, reflected in that R_A is neglected in some biosphere-atmosphere exchange models (Granier et al., 2000; Kelliher et al., 1993; Köstner et al., 1992), few studies have actually quantified the effect of U on R_A and, in-turn, on transpiration (Table 3.1). The results of these studies are inconclusive: Some studies observed increased transpiration with U (Chu et al., 2009; Grace and Russel, 1982; Kitaya et al., 2004); others observed a decline (Caldwell, 1970; Campbell-Clause, 1998; Dixon and Grace, 1984; Gutiérrez et al., 1994), or found transpiration to be insensitive to U (Komatsu et al., 2006).

Here we analyze the effect of U on transpiration through measurements and by quantifying the response to U of estimated resistances in the water vapor pathway, focusing on the reduced expression:

$$R_T = R_A + R_{bl} + R_{stom} \quad (4)$$

Many of the studies on transpiration response to U were performed in wind tunnels (Caldwell, 1970; Chu et al., 2009; Dixon and Grace, 1984; Grace and Russel, 1982; Kitaya et al., 2004). However, results of wind tunnel experiments may differ from those of field experiments because they do not account for the effect of neighboring crowns (shelter effect) on the coupling between stomata and atmosphere in forest stands. In-situ experiments were performed to overcome the limits of wind tunnels, but most have focused on crops and other small statured canopies; eight of the ten in-situ studies we found were made on such canopies (Table 3.1). The response of these canopies to U may differ from that of forests canopies which tend to be rougher, and thus better coupled to the atmosphere (Jones, 1992). Furthermore, the aerodynamic roughness of forest canopies depends on tree height, stand density, tree size distribution, and LAI, all of which change with stand age (Chapin, 2002; Perry, 2008). Thus, if R_A is actually large, it would require quantification for each combination of stand characteristics before estimating biosphere-atmosphere exchanges.

As LAI increases, R_C decreases, improving the canopy-atmosphere coupling (Granier and Bréda, 1996; Granier et al., 2000; Katsoulas et al., 2007), yet the increase in canopy leaf area may impede air movement, increasing R_A while decreasing D within the canopy. At a given canopy LAI, as U increases, the accompanying decrease of R_A allows

for frequent replacement of moist canopy air with dry air from aloft, potentially driving more transpiration, yet the drier air may force stomatal closure and increase R_{stom} (Fig. 3.1). Thus, the effect of U on tree and canopy transpiration represents a balance among interacting processes and may not be simple to predict. Transpiration could therefore decrease with increasing U if R_C increases as a result of stomatal response to D, overwhelming both the decrease of R_A as well as the increase of D, the driving force for transpiration.

The goals of this study were to improve understanding of the effect of U on transpiration. We assessed the response to U of sap flux density (J_S), a proxy of transpiration, of six co-occurring species, ranging in shade tolerance, leaf dimensions and leaf clumping, in a mature broadleaved deciduous forest, testing the following hypotheses: (**H1**) transpiration will increase with U as a result of the combination of direct and indirect effects on resistances and forces above and within the canopy; (**H2**) R_A has a small effect on R_T meaning that R_T is dominated by the components of R_{sur} (mostly R_C, in-turn dominated by R_{stom}); thus (**H3**) the response of E_C to U will be determined by the effects of increases in D with U on R_{stom} and the increase in the driving force, rather than by the direct effect of U on R_A and R_{bl}.

3.2 Materials and Methods

3.2.1 Site description and data collection

The study was conducted at the Duke Forest hardwood site, North Carolina (36° 58´ N, 79° 05´ W) from 2002 to 2005. The maximum tree age of the hardwood stand is

~100 years. Mean and maximum canopy heights of the stand are 25 m and 35 m, respectively (Pataki and Oren, 2003). A total of 40 trees of the six dominant species, yellow (tulip) poplar (*Liriodendron tulipifera*), sweetgum (*Liquidambar styraciflua*), hickory (*Carya tomentosa*), white oak (*Quercus alba*), swamp chestnut oak (*Q. michauxii*), and willow oak (*Q. phellos*), were selected for sap flux measurement (Table 3.2). J_S was measured with 20 mm long Granier-type heat dissipation sensors (Granier, 1987). The Granier-type technique has a potential to produce bias of J_S due to its sensitivity to physical factors including thermal conductivity of sapwood, temperature gradients within sapwood, and variation in J_S with sapwood depth (Tatarinov et al., 2005; Wullschleger et al., 2011). However, using the same data, Oishi et al. (2010) showed that J_S produced similar estimates of latent heat flux when properly scaled to the site's eddy-covariance footprint. The measurement depths varied from 0-20 to 0-60 mm based on the expected depth of sapwood; sensors generating values at least two standard deviations apart from values collected by others in the same species and measurement depth were excluded to avoid potential underestimation caused by excessive penetration into heartwood (Lu et al., 2004).

T_a and relative humidity were measured at two-thirds of the mean canopy height with a temperature/RH probe (HMP35C, Campbell Scientific, Logan, UT, USA), and used to calculate *D* (Campbell and Norman, 1998). Photosynthetically active radiation (PAR) was measured above the canopy using a quantum sensor (LI-190SA, LI-COR, Lincoln, NE, USA). Volumetric soil moisture (θ) was measured in 12 locations, at 5-10 cm and 20-25 cm in each location, using ThetaProbe sensors (ML2x, Delta-T Devices,

Cambridge, UK). *U* was measured with a tri-axial sonic anemometer installed above the canopy at 39.8 m (CSAT3, Campbell Scientific, Logan, UT, USA). More details on the site and measurements are given in previous publications on the stand (Oishi et al., 2008; Pataki and Oren, 2003; Stoy et al., 2006). Thirty-minute averages of all the measurements were stored on data loggers (CR23X, Campbell Scientific, Logan, UT, USA).

3.2.2 Data preparation

To minimize the effects of meteorological variables other than *U*, we selected data during times in which leaf area index is reasonably stable (DOY 120-275, excluding the short period of fast leaf expansion and the long period of leaf abscission and shedding) and conditions where transpiration is not likely limited by T_a ($\geq$ 25 °C) and θ ($\geq$ 0.2 m^3 m^{-3}). Data under these conditions were further partitioned to four ranges of light (PAR, at 500 μmol m^{-2} s^{-1} up to 1500 μmol m^{-2} s^{-1}, and one class for data under PAR $\geq$ 1500 μmol m^{-2} s^{-1}, on which we concentrated most of the analyses for reasons that will become clear later).

J_S varies greatly among sensors (Granier, 1987). Typically, before estimating species or stand scale transpiration, missing data is gap-filled to avoid the effect on the average J_S of single sensors dropping in and out of the data set. However, we chose a conservative approach, relying on only operating sensors, selecting the largest number of sensors for each species resulting in at least 3000 half-hourly, species level averages over the study period, all produced by the same three to five sensors. The 2003 J_S data of *Q. michauxii* were excluded from analysis because the values were unstable. When calculating stand-scale E_C, missing average J_S of any species (~54% of potential values)

resulted in missing half-hourly stand-scale E_C. To gap-fill the missing average J_S, a power function ($y = a + bx^n$) was fitted among species when average J_S of at least three species were available (~64% of the time under the selected conditions). If the data of more than three species at a given half-hour were missing, the data were neither gap-filled nor used for E_C calculation; otherwise, missing data of a species were gap-filled using data of another species with the best fit in terms of R^2 value. Approximately 50% of the missing data were gap-filled. The performance of the gap-filling procedure was evaluated by comparing the data unused in developing the gap-filling functions (~36% of the time, when data for only one or two species were available) and estimates based on the function developed for each species. The estimated values were well fitted with observed ones ($R^2 > 0.89$; slope ranged from 0.88 to 1.10).

R_A in the air layer above the canopy surface was estimated by Monin-Obukhov similarity theory (Campbell and Norman, 1998):

$$R_A = \frac{\left[\ln\left(\frac{z-d}{z_{om}}\right)+\Psi_M\right]\left[\ln\left(\frac{z-d}{z_{oh}}\right)+\Psi_H\right]}{k^2\hat{\rho}U} \quad (\mathrm{m^2\ s\ mmol^{-1}}) \quad (5)$$

$$\Psi_H = \begin{cases} 6\ln(1+\zeta), & \text{for stable flow} \\ -2\ln\left[\frac{1+(1-16\zeta)^{\frac{1}{2}}}{2}\right], & \text{for unstable flow} \end{cases} \quad (6)$$

$$\Psi_M = \begin{cases} \Psi_H, & \text{for stable flow} \\ 0.6\Psi_H, & \text{for unstable flow} \end{cases} \quad (7)$$

where $\hat{\rho}$ is the molar density of air (mmol m^{-3}), k (=0.4) is the von Karman constant, U is the wind velocity (m s^{-1}), z is the height of measured wind velocity (m), d is the zero plane displacement (m), z_{om} is the momentum roughness length (m), z_{oh} is the scalar roughness length for heat transfer (m), Ψ_M and Ψ_H are the profile diabatic correction factors for buoyant instability, ζ is the atmospheric stability. The parameters d, z_{om}, and z_{oh} were taken as fixed values, 0.67, 0.1, and 0.02 of the canopy height in this study, making the effect of the surface roughness length constant during the growing season. A 10% variation of each of the three parameters changed the maximum of calculated values of R_A by 2.8, 1.8, and 1.7%, supporting the assumption of constant parameters.

R_C was obtained by subtracting R_A from the total resistance (R_T), which was calculated from a rearranged Penman-Monteith equation after Blanken and Black (2004):

$$R_T = \frac{s}{\gamma}\beta R_A + \frac{\rho c_p D}{\hat{\rho}\gamma\lambda E_C} \quad (m^2\ s\ mmol^{-1}) \tag{8}$$

where s is the slope of the saturation vapor pressure with T_a (kPa K^{-1}), γ is the psychrometric constant (kPa K^{-1}), β is the Bowen ratio (ratio of sensible to latent heat fluxes), ρ is the density of air (kg m^{-3}), c_p is the specific heat of air (J kg^{-1} K^{-1}), D is the vapor pressure deficit (kPa), λ is the latent heat of vaporization (J g^{-1}), and E_C is the canopy transpiration (g H_2O m^{-2} (ground area) s^{-1}). Typical values of β for temperate forests (lower in deciduous than in conifer forests) ranged from 0.4 to 0.8 (Novel, 2005; Wilson et al., 2002). Since a change of β by 0.1 within the range resulted in only 2.5% difference in R_T under the selected conditions in this study, β was assumed to be constant (0.5). E_C was estimated with J_S from outer sensors (depth of 0-20 mm; g H_2O m^{-2}

(sapwood area) s^{-1}) and cross-sectional sapwood area per unit ground area (A_S; cm^2 m^{-2}) weighed using radial profiles of J_S. The weighed A_S of each species was obtained from allometric relationship between diameter at breast height and sapwood area (Oishi et al., 2008; Oishi et al., 2010).

To assess the importance of R_{bl} in this stand, species mean R_{bl} values were calculated using an equation for the resistance of vapor transport in forced convection (Campbell and Norman, 1998), which dominates over free convection in this canopy (Stoy et al., 2006):

$$R_{bl} = \frac{\nu^{1/6}}{0.664\hat{\rho}D_v^{2/3}}\sqrt{\frac{d_l}{u}} = 0.0068\sqrt{\frac{d_l}{u}} \quad (m^2\ s\ mmol^{-1}) \qquad (9)$$

where ν is the kinematic viscosity of air (m^2 s^{-1}), D_v is the molecular diffusivity of water vapor in air (m^2 s^{-1}), d_l is the leaf characteristic dimensions (0.011 – 0.083 m; Table 3.2), and u is the vertically averaged U within canopy (m s^{-1}). A constant value of 0.0068 $m^2 s^{1/2}$ $mmol^{-1}$ was used for $\nu^{1/6}(664\hat{\rho}D_v^{2/3})^{-1}$ (Campbell and Norman, 1998). u was estimated based on U profiles within canopy and LAI profile when canopy leaf area was at its stable seasonal plateau (DOY 154):

$$u = \frac{\sum_{h=1}^{H} U(h)\mathrm{LAI}(h)}{\sum_{h=1}^{H} \mathrm{LAI}(h)} \qquad (10)$$

where $U(h)$ and LAI(h) are U and LAI at a height h within canopy, and H is the canopy height (m). The U profiles were calculated as (Campbell and Norman, 1998):

$$U(h) = u_0 \, \mathrm{e}^{a\left(\frac{h}{H}-1\right)} \tag{11}$$

where u_0 is the U at the top of the canopy and a is an attenuation coefficient (assumed to be 2.5). The LAI profile was estimated from measurements at ~2 m intervals from 1 to 45 m along a tower using an optical plant canopy analyzer (LAI-2000, LI-COR, Lincoln, NE, USA; Stoy et al., 2005).

Also, to understand the coupling between the air within and above the canopy volume, the decoupling coefficient for the canopy (Ω) was considered. In this study Ω was calculated using Jarvis and McNaughton (1986):

$$\Omega = \frac{\frac{s}{\gamma}+1}{\frac{s}{\gamma}+1+\frac{R_C}{R_A}} \tag{12}$$

Ω approaches zero when the ratio R_C/R_A approaches infinity, a condition of perfect coupling between the air in the canopy volume and the bulk air above the canopy (i.e. very efficient mass and energy exchange), resulting in essentially identical T_a and humidity in these two locations. If R_A is much larger than R_C, Ω approaches one, reflecting the isolation of the air in the canopy volume from that aloft.

3.3 Results and Discussion

3.3.1 Sap flux density

We first examined the relationship between U and J_S. We used a subset of the available data to minimize the effects of other variables including light, temperature, and

soil water. The means (and ranges) of T_a, PAR, θ, *D*, and *U* of the selected data were 29.0 (25.0 – 35.1) °C, 1662 (1500 – 2047) μmol m^{-2} s^{-1}, 0.30 (0.20 – 0.50) m^3 m^{-3}, 1.69 (0.09 – 3.09) kPa, and 2.16 (0.44 – 5.09) m s^{-1}, respectively. Although the size of the subset is only 5.3% of total daytime of the stable LAI period (but see below), the range of *U* includes 98.3% of the range of *U* during daytime hours of the growing season above this stand. The average J_S of *L. tulipifera*, *L. styraciflua*, *C. tomentosa*, *Q. alba*, *Q. michauxii*, and *Q. phellos* after the filtering were 26.0, 22.1, 20.9, 38.5, 37.8, and 35.0 g H_2O m^{-2} (sapwood area) s^{-1}, respectively.

Figure 3.2 shows the relationship between 30 minute average J_S of the six species and *U* during the growing season. Over the wide range of *U*, J_S of *L. tulipifera* and *Q. phellos* did not change significantly. For *L. styraciflua*, *C. tomentosa*, *Q. alba*, and *Q. michauxii*, the relationships were weak (R^2 = 0.01 to 0.28) and inconsistent in sign. The sensitivity of J_S to *U* can be influenced by different leaf size among species because specific leaf dimension (i.e. leaf width in the direction of the wind) changes the leaf boundary layer thickness (Campbell and Norman, 1998). However, no effect of leaf size on the J_S-*U* sensitivity was observed among species (p = 0.796).

Observations of the relationship between *U* and sap flux (or tree transpiration) were diverse. For example, increasing *U* by up to 2 m s^{-1} by partially harvesting a boreal stand composed of *Picea glauca*, *P. balsamifera*, and *Butula papyrifera* increased transpiration per unit leaf area (Bladon et al., 2006), but sap flux of hybrid poplar (*P. nigra* L. × *P. maximowiczii* A. Henry) was negatively correlated to *U* (Zalesny et al., 2006). Komatsu et al. (2006) found no difference of sap flux of *Cryptomeria japonica*

under a given D at all $U > 0.7$ m s^{-1}. In a study of 7-year-old *Eucalyptus globulus* the ratio of sap flux of edge trees to that of trees far from the edge increased with U when R_C of edge trees was sufficiently low to cause leaf temperature to equal T_a (Taylor et al., 2001). Similarly at the individual crown scale, simulated transpiration of 20-year-old *Juglans regia* foliage increased slightly as U increased from 1 to 5 m s^{-1} in shaded leaves but was insensitive to U in sunlit leaves that had higher leaf temperature than T_a (Daudet et al., 1999). The results of these studies demonstrate the complex effect U can have on stand transpiration.

3.3.2 Total, aerodynamic, and canopy resistance

In order to examine how U affected resistances, we first calculated R_T for each species from its J_S and A_S, as if the stand was entirely composed by that species (Fig. 3.3). The mean R_T values of each species (*L. tulipifera*, *L. styraciflua*, *C. tomentosa*, *Q. alba*, *Q. michauxii*, and *Q. phellos*) were 0.83×10^{-2}, 0.89×10^{-2}, 0.87×10^{-2}, 0.75×10^{-2}, 0.81×10^{-2}, and 0.83×10^{-2} m^2 (ground area) s $mmol^{-1}$, respectively. R_T weakly increased with U for two species in the stand (*L. tulipifera* and *Q. michauxii*; Fig. 3.3).

Stand-level R_T based on the actual species composition was calculated using sap flux-scaled canopy transpiration (E_C). E_C was unrelated to U in three PAR intervals (0-500, 500-1000, and 1000-1500 μmol m^{-2} s^{-1}) when analyzed along the entire range of U found in each interval (p = 0.0746, 0.3710, and 0.0707; Fig. 3.4a). In the highest PAR interval (≥ 1500 μmol m^{-2} s^{-1}), a weak positive relationship was observed between E_C and U (p = 0.0069, R^2 = 0.02). However, the increase of E_C associated with ~7-fold increase

of U was only 6.5%. Thus, we must reject **H1**: Under most conditions, stand transpiration did not increase with *U*.

Although R_T increased with *U* for two species, the relationship between stand-level R_T and *U* was not significant (p = 0.3650; Fig. 3.4b). Because of the observed lack of or limited sensitivity of E_C to *U* in any PAR range, we concentrate our analyses on only the one set of conditions in which no environmental variable was limiting, thus reducing the variation in the calculated resistances. The direct effect of *U* on water transport through the air layer above the canopy is reflected in R_A. The average R_A of this stand was 4.62×10^{-4} m^2 (ground area) s $mmol^{-1}$, within the range of values from other broadleaved forest stands (Köstner et al., 1992; Kumagai et al., 2004; Lindroth, 1993; Pereira et al., 2010). The estimated values of R_A over the canopy decreased from 1.31×10^{-3} to 1.95×10^{-4} m^2 (ground area) s $mmol^{-1}$ as *U* increased from ~0.7 to ~4.7 m s^{-1} (Fig. 3.4c). However, consistent with **H2**, R_A was a relatively small component of R_T, decreasing from 15% to 1.6% with increasing *U* except three half-hourly values with 18.8, 23.5 and 37.8% due to exceptionally low *D* (0.10, 0.31 and 0.97 kPa; Fig. 3.4d). When *D* was low, R_T was generally lower under all *U* condition, and thus the ratio of R_A to R_T increased somewhat with decreasing *D* (see Fig. 3.4b and 3.4d).

R_C, calculated by subtracting R_A from R_T, increased with *U* in the stand (p = 0.0132; R^2 = 0.2; Fig. 3.4e). The mean R_C of the stand was 7.61×10^{-3} m^2 (ground area) s $mmol^{-1}$, similar to values observed in other broadleaved forest stands (Blanken and Black, 2004; Hinckley et al., 1994). In a *Coffea arabica* plantation, R_C normalized by

PAR also increased with increasing U from 1 to 2.5 m s^{-1} (Gutiérrez et al., 1994), as it did, albeit weakly, in a *Zea mays* field (Irmak and Mutiibwa, 2010).

We assessed the contribution of R_{bl} to R_C modeling the wind velocity profile down the canopy based on leaf-area profile and characteristic leaf dimensions (Fig. 3.5a and b). The maximum values of R_{bl} of the six species ranged from 2.76×10^{-4} to 7.64×10^{-4} m^2 (ground area) s $mmol^{-1}$, an order of magnitude smaller than R_C over much of the range of U in this stand (Fig. 3.4e and 3.5c). Indeed, R_{bl} was less than half of R_A at low U, becoming similar to R_A only at very high U when the sum of both resistances was a very small component of the total. Thus, R_{stom} is much greater than R_{bl} and can be assumed equivalent to R_C. We test this assumption when we address **H3** in the last section.

The small absolute decrease of R_A with increasing U, and the low ratio of R_A to R_T at our stand indicate that the stand was generally well-coupled to the atmosphere (mean $\Omega = 0.22$; Fig. 3.6a) despite its high tree density (~866 total trees per hectare), extensive vertical distribution of foliage (~685 of ~866 trees were in the sub-canopy) and high LAI (~7 m^2 m^{-2}). Transpiration in a stand with low Ω value is largely influenced by air humidity and stomatal response rather than available energy (Jarvis and Mcnaughton, 1986; Lindroth, 1993), which in our analysis was set to a limited range (approximately $1500 \leq PAR \leq 2050$ μmol m^{-2} s^{-1}, and $25 \leq T_a \leq 35$ °C). Thus, we assessed further the concurrent variation of D and R_{stom}.

3.3.3 Vapor pressure deficit and its effect on resistances

D functions as a driving gradient for water vapor exchange through stomata, where carbon assimilation driven by CO_2 concentration gradient occurs concurrently.

Understanding the effect of U on transpiration is complicated because wind affects not only R_A and R_{bl}, but also D, and thus R_{stom} (Fig. 3.1; Table 3.1; Dixon and Grace, 1984). Gutiérrez et al. (1994) suggested that increased leaf-to-air D at the leaf surface with U generated a positive relationship between normalized R_C and U, but evidence of such relationships is rare. In this study, the slight increase in canopy-atmosphere coupling of the stand was sufficient to produce a significant positive relationship ($p < 0.0001$) between U and D (Fig. 3.6b). Grace et al. (1975) estimated that as U increased from 0.1 to 1.0 m s^{-1}, the effective D at leaf surface increased by 38%. Within the range of our data, the increase of D within the canopy volume averaged ~11% per 1 m s^{-1} increase in U, with greater increases at the lower end. At low D, its increase tends to drive higher canopy transpiration (Daudet et al., 1999; Kupper et al., 2011). However, further increases in D lead to stomatal closure (decrease in leaf stomatal conductance) such that transpiration does not increase through the entire range of D commonly observed in temperate forests (Oishi et al., 2010; Oren and Pataki, 2001; Oren et al., 1999; Pataki and Oren, 2003). Phillips and Oren (2001) explained the small variation observed in canopy transpiration of *Pinus taeda* during periods of daytime $D > 0.9$ kPa based on compensation of the direct (positive) and indirect (negative) effects of D. Indeed, Roberts (1983) suggested the negative feedback between R_{stom} and D as the reason transpiration is a conservative hydrological process in forests.

More common are studies showing increased R_{stom} or R_C of broadleaved stands with increased D (Blanken and Black, 2004; Clausnitzer et al., 2011; Granier et al., 2000; Irmak and Mutiibwa, 2010; Jonard et al., 2011; Köstner et al., 1992; Oren and Pataki,

2001; Pataki and Oren, 2003; Schäfer et al., 2000). The response of R_{stom} to D can be estimated as (Lohammar et al., 1980; Oren et al., 1999):

$$R_{stom} = \frac{R_{Sref}}{1 - m\ln(D)} \quad (13)$$

where R_{Sref} is a reference resistance at D = 1 kPa, m is the slope of the relationship between reference conductance ($1/R_{Sref}$) and the sensitivity of stomatal conductance to D ($-dG_{Stom}/dln(D)$). This response is consistent with hydraulic theory and reflects the decreased sensitivity to D of R_{stom} with increasing R_{stom} at low D (Katul et al., 2009). We estimated R_{Sref} and m from coefficients of linear regression between canopy conductance (a reciprocal of R_C) and the natural log of D. The estimated value of m, 0.74, was higher by about 9% than that estimated in similar forest stands in the area (Oren and Pataki, 2001). Based on R_{Sref} and m we estimated the expected increase of R_{stom} with D (Fig. 3.6c). Based on this analysis, as D increases from 0.1 to 3.0 kPa, R_{stom} should increase about ten-fold, increasing two-fold between 1.0 and 2.0 kPa, similar to observation in a 35-year-old oak stand (Granier and Bréda, 1996).

We examined the expected response of R_{stom} to U by converting D in equation 13 to U based on the relationship between D and U (from Fig. 3.6b). Estimated R_{stom} increased 38% over the range of U and fell close to or within the 95% confidence intervals of the relationship between R_C and U (Fig. 3.4e). As a result of the small contribution of R_A to R_T, the variation of R_T was also highly correlated ($p < 0.0001$, R^2 = 0.79) with the response of R_{stom} to D; the slope was very close to unity, with R_T averaging only 2.8% higher than the expected values of R_{stom} (Fig. 3.7). Thus, we failed to reject

H3, concluding that the direct effect of *D*, acting as a driving gradient for plant transpiration, relative to its indirect effect, inducing stomatal closure (Fig. 3.1), dominates the response of transpiration to *U*. The average *D*, even in calm wind conditions of less than < 1 m s^{-1}, was > 1 kPa in this study, suggesting that much of the time the direct effect of *D* was offset by R_{stom} response to *D*, resulting in a constant E_C over the observed range of *U*.

3.4. Conclusion

This study assessed the responses of J_S (as a surrogate for transpiration) to *U* in a mixed hardwood stand under optimal meteorological condition for transpiration based on T_a and θ. J_S of the six species were insensitive or weakly responded to increasing *U*; stand-level transpiration appeared not to significantly change with *U* (**H1**). The canopy of the broadleaved stand was well-coupled to the atmosphere, and thus had a low R_A. Further decrease in R_A with increasing *U* was readily offset by an increasing R_C (**H2**). The increase in R_C was consistent with the theoretical increase in R_{stom} with *D* – which in turn increased with *U* – keeping transpiration constant despite the increase of the driving force (**H3**). These results suggest that in similar forests the effect of *U* on canopy transpiration is negligible. However, due to its effect on *D* within the canopy and thus R_{stom}, *U* could have an important influence on CO_2 uptake.

Table 3.1. Field studies that have investigated relationships between transpiration (or sap flow) and wind velocity

Correlation	Site description (species)	Wind velocity ($m\ s^{-1}$)	Tree stage (age in years)	LAI [1]	SLA [2] ($cm^2\ g^{-1}$)	Source
Positive	Hardwood, South Australia (*Eucalyptus globulus*)	-	young (7)	-	62 – 192 [4]	Taylor et al. (2001)
	Boreal mixedwood, Alberta, Canada (*Picea glauca, P. balsamifera, Betula papyrifera*)	0 - 2	mature (45 - 50)	-	-	Bladon et al. (2006)
	Shrub, Tengger desert, China *(Artemisia ordosica)*	-	(10)	0.5 – 0.9	-	Lei et al. (2010)
	Temperate hardwood, Estonia (*B. pendula, P. tremula + P. tremuloides* [3])	0 - 4	seedling (1)	-	-	Kupper et al. (2011)
	Temperate hardwood, China (*Populus alba*)	0 - 0.6	young (7 - 10)	0 - 2	100 – 120 [4]	Xu et al. (2011)
Negative	Shrub, island of Kauai, USA (*Coffea arabica L.)*	1 - 3	(1 – 5.3)	0.7 – 6.7	-	Gutiérrez et al. (1994)
	Hardwood, Wisconsin, USA (*P. nigra + P. maximowiczii* [3])	0 - 4.5	young	-	-	Zalesny et al. (2006)
Weak or none	Hardwood, Plauzat, France (*Juglans regia*)	0 - 4	mature (20)	9	82 - 398 [4]	Daudet et al. (1999)
	Softwood, Chiba, Japan (*Cryptomeria japonica*)	0 - 1.5	young (8)	3.7	-	Komatsu et al. (2006)
	Crop, Nebraska, USA (Zea mays L.)	0 - 7		1 - 5	-	Irmak and Mutiibwa (2010)
	Temperate hardwood, Durham, USA (*Liriodendron tulipifera, Liquidambar styraciflua, Carya tomentosa, Quercus alba, Q. michauxii, Q. phellos*)	0.8 - 4.7	mature (80 - 100)	7.03	102 - 174	This study

[1] Leaf Area Index

[2] Specific Leaf Area

[3] Hybrid between the two species

[4] General values from various studies

Table 3.2. Characteristics of sampled trees at the Duke Forest hardwood site. Standard deviations are shown in parentheses.

Species	DBH [1]	LAD [2]	J_S [3]	A_S [4]	SLA [5]	d [6]	Number of trees
L. tulipifera	39.3	0.017	42.36	2.37	161.8	8.3	10
	(14.96)		(15.21)				
L. styraciflua	36.58	0.020	29.44	2.09	102.4	8.1	10
	(12.16)		(13.10)				
Other diffuse porous	-	-	-	1.48	173.3	-	-
C. tomentosa	34.12	0.062	36.32	2.11	131.9	4.7	5
	(20.86)		(15.30)				
Q. alba	32.34	0.018	42.30	0.52	112.2	5.4	5
	(18.46)		(12.61)				
Q. michauxii	33.68	0.014	37.55	0.59	128.9	6.8	5
	(16.80)		(10.40)				
Q. phellos	49.48	0.003	43.88	0.27	101.9	1.1	5
	(9.02)		(10.28)				
Other ring porous	-	-	-	0.60	-	-	-

[1] Diameter at Breast Height (cm)

[2] Leaf Area Density ($m^2\ m^{-3}$)

[3] Average sap flux density (g $H_2O\ m^{-2}s^{-1}$) from selected data

[4] Sapwood area ($cm^2\ m^{-2}$) weighed based on radial profiles of J_S (Oishi et al., 2008)

[5] Specific Leaf Area ($cm^2\ g^{-1}$)

[6] Leaf Characteristic Dimension (cm; Harlow et al., 1996)

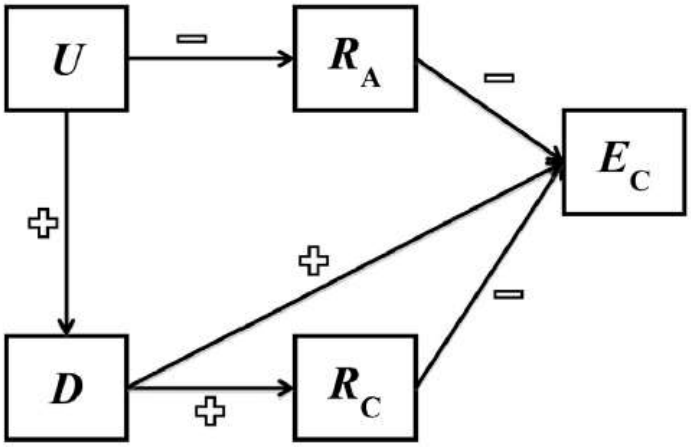

Figure 3.1. Diagram showing the effect of wind velocity, U, on transpiration, E_C in a big-leaf framework. The sign represents the relationship between the two parameters at the arrow tip and tail (D – vapor pressure deficit; R_A – aerodynamic resistance; R_C – canopy resistance). For example, an increase in U results in a decrease in R_A because of the negative relationship between U and R_A and, in turn, the decrease in R_A leads to an increase in E_C because of the negative relationship between R_A and E_C.

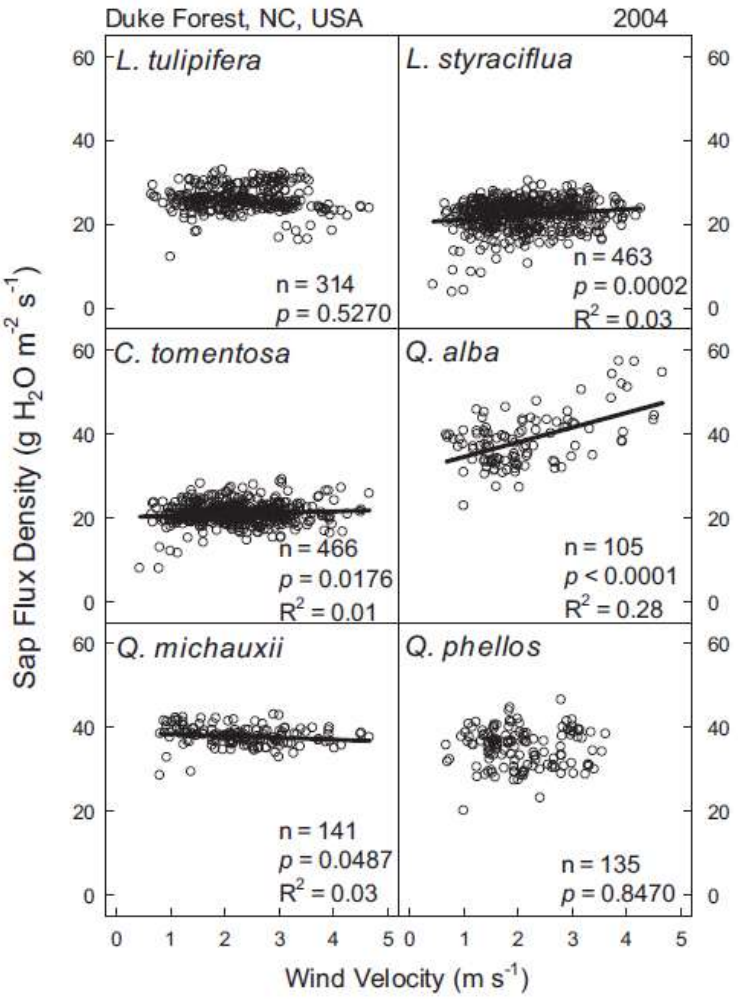

Figure 3.2. The effect of wind velocity on sap flux density of six species in the Duke Forest hardwood site. Solid lines represent significant relationships at $p < 0.05$.

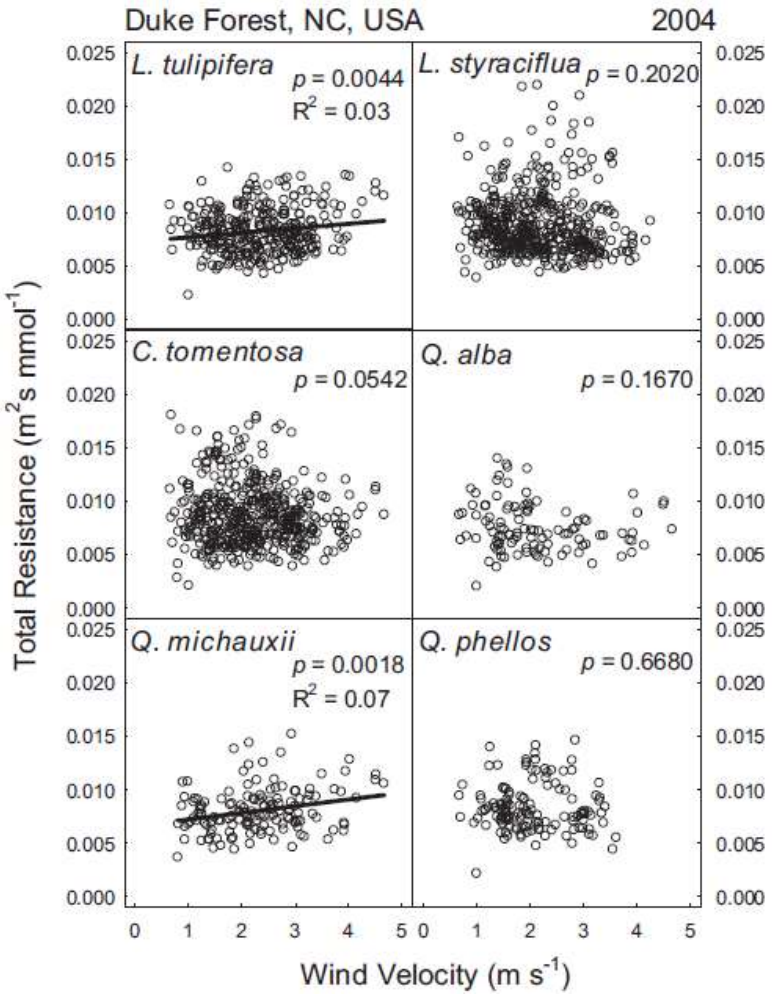

Figure 3.3. The relationship between wind velocity and total resistance. Solid lines represent significant relationships at $p < 0.05$.

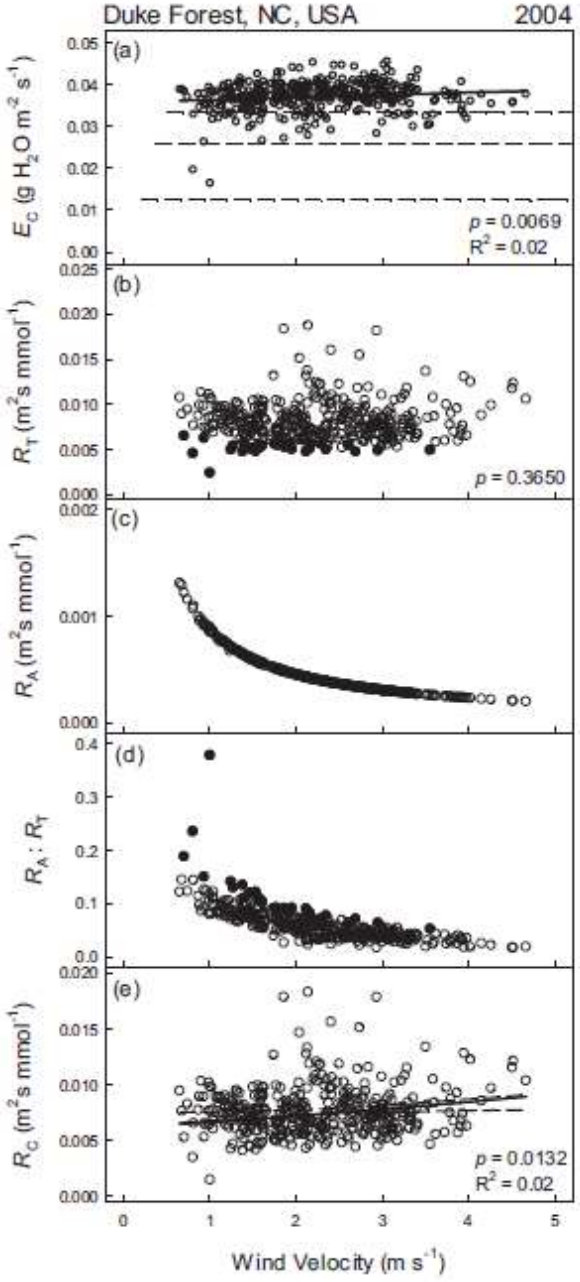

Figure 3.4. Changes in stand-level transpiration and resistances with increasing wind velocity (*U*). (a**)** Canopy transpiration (E_C); lines from the bottom up represent light conditions of 500 μmol m^{-2} s^{-1} intervals from 0 to 1500 μmol m^{-2} s^{-1}, while the data points

represent conditions of > 1500 μmol m^{-2} s^{-1}. Only one PAR interval (> 1500 μmol m^{-2} s^{-1}) showed significant yet very weak correlation. (b) total resistance (R_T); filled circles represent R_T when vapor pressure deficit (D) is low (< 1 kPa), (c) aerodynamic resistance (R_A), (d) proportion of R_A to R_T; filled circles represent the proportion when D is low (< 1 kPa), and (e) canopy resistance (R_C) with 95% confidence intervals for individual estimates (dashed lines) and expected R_{stom} based on the relationship between R_{stom} and vapor pressure deficit (D), and between D and U (solid line; see text).

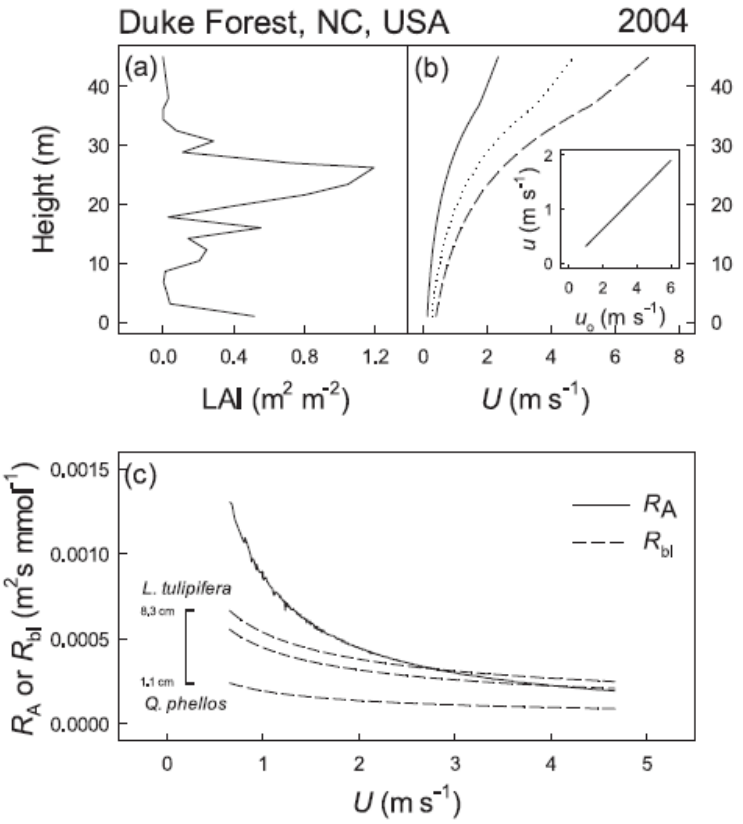

Figure 3.5. (a) Leaf area index (LAI) profile (DOY 154). (b) Calculated wind velocity (*U*) profiles above and within the canopy when *U* at measurement height (39.8 m) are 2 (solid line), 4 (dotted line), and 6 (dashed line) m s^{-1}. Inset figure shows the relationship between *U* above canopy (u_0) and average *U* within canopy weighted by leaf area profile (*u*). (c) Aerodynamic resistance (R_A; solid line) and leaf boundary layer resistance (R_{bl}; dashed lines) estimated using *U* and leaf characteristic dimensions of the six species, ranged from 1.1 cm for *Q. phellos* to 8.6 cm for *L. tulipifera* (see Table 3.2); the dashed lines from the top represent R_{bl} estimates of *L. tulipifera*, weighed average, and *Q. phellos*.

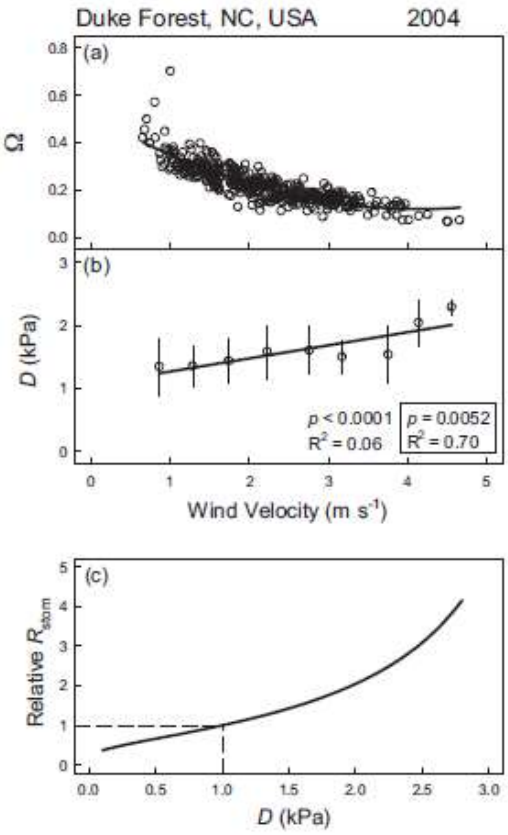

Figure 3.6. (a) Responses of the decoupling coefficient (Ω) to wind velocity (*U*). (b) Responses of vapor pressure deficit (*D*) to *U* (data are mean vapor pressure deficit grouped in *U* intervals of 0.5 m s^{-1}; *p*-value and R^2 within the box were calculated from mean values rather than individual data). (c) The theoretical, hydraulically controlled increase of stomatal resistance (R_{stom}) with *D*, normalized by the resistance at *D* = 1 kPa.

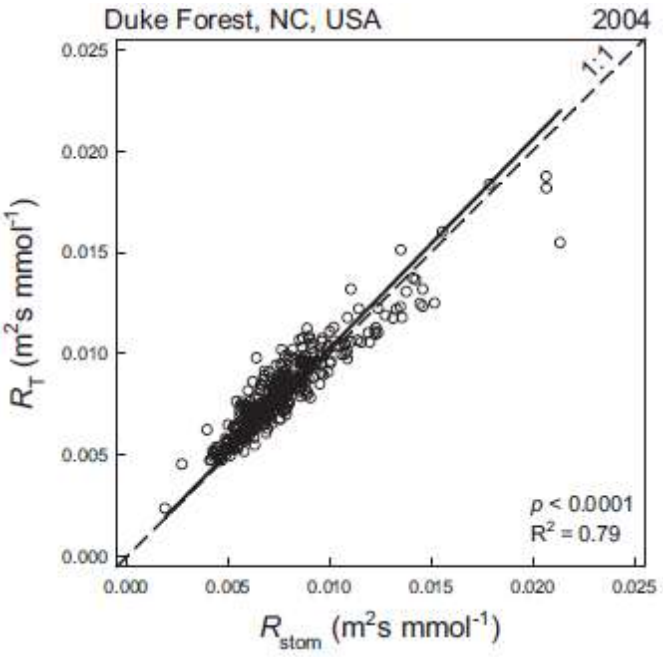

Figure 3.7. The relationship between predicted stomatal resistance (R_{stom}) and total resistance (R_T) estimated from sap flux and associated measurements. R_{stom} was calculated using equation 10, with $R_{Sref} = 0.51 \times 10^{-2}$ m^2 (ground area) s mmol^{-1} and m = 0.74. Solid line and dashed line represent a linear fit without intercept and 1:1 line.

4. Response of stomatal conductance to termination of Long-term CO_2 enrichment

4.1 Introduction

Stomata are the common pathway of carbon uptake and water vapor loss in plant, therefore how environmental factors, including in high atmospheric CO_2 condition, affect stomatal conductance (G_S) have implications for tree (or stand) water use and photosynthesis (or primary production). Stomatal apertures are expected to respond to various environmental stimuli, such as light, temperature, humidity, water potential, and CO_2 concentration (Jarvis, 1976). The recent rise of atmospheric CO_2 concentration has drawn particular attention to the prediction of the stomatal response to atmospheric CO_2 (Morison, 1998).

The stomatal response to elevated CO_2 can be divided into direct and indirect responses. The direct response is caused by the increase in intercellular CO_2 concentration (c_i), which leads to stomatal closure. The indirect response is related to allometric (change in leaf area) or hydraulic adjustment, which leads to changes in specific hydraulic conductivity, leaf to sapwood area ratio, and whole-tree hydraulic conductance (Uddling et al., 2009). The characteristics of the direct and indirect effects may induce different responses among species. Deciduous trees tend to show stronger and quicker responses to long-term (>1 year) exposure to elevated CO_2 than coniferous trees (Medlyn et al., 2001; Norby and Zak, 2011). Reduction of G_S due to direct

responses to elevated CO_2 (i.e. stomatal closure) were observed for many deciduous trees in both short and long-term Free Air CO_2 Enrichment (FACE) treatment (Keel et al., 2007; Noormets et al., 2001; Tricker et al., 2005; Wullschleger et al., 2002). However, this response was not significant for *Pinus taeda* under FACE treatment for 3.5 years (Ellsworth, 1999; Ellsworth et al., 1995; Schäfer et al., 2002). However, at the same stand Ward (2013) observed reduced G_S after 11 years of exposure to elevated CO_2. Wang *et al*. (2005) observed that decrease in crown conductance of 30-year-old *P. sylvestris* in closed-top chambers became greater with longer (>2 years) exposure to elevated CO_2, reducing sap flow, while the opposite (increase in sap flow) was observed due to small decrease of the conductance compensated by increased leaf area with one year of exposure. Domec *et al*. (2009) suggested that the adjustment of hydraulic pathway in response to elevated CO_2 can be important for coniferous trees to stimulate stomatal closure, thus it requires longer exposure to observe a significant reduction of water transport. The authors also found a significant effect of nitrogen fertilization on liquid phase water transport, which represents a structural change demanding nitrogen. For better understanding of the importance of the indirect effect of elevated CO_2 on *P. taeda*, investigation of stomatal responses of coniferous and deciduous trees under the same condition is necessary.

The objective of this study is to investigate the responses of the dominant (*P. taeda*) and a major sub-canopy species (*Liquidambar styraciflua*) over two years following the termination of CO_2 enrichment. Lack of G_S response to short-term manipulation of atmospheric CO_2 concentration showed that G_S was unaffected by a

rapid response due to direct stomatal reaction (Tor-ngern *et al.* 2015). Decrease in leaf area may alter the hydraulic allometry, and influence on G_S indirectly. However, since changes in leaf area and xylem hydraulic properties are not rapid, a complete indirect response of G_S to termination of CO_2 enrichment is unlikely. Therefore, the overall effect on G_S during the period after the termination of CO_2 enrichment should be dominated by slower and incomplete adjustments reflecting changes in leaf area and xylem hydraulics. Thus, we can hypothesize that (**H1**) G_S of *P. taeda* in previously elevated CO_2 will increase when the hydraulic adjustment is made. Because broadleaved species showed stronger response to elevated CO_2 than conifers (Medlyn *et al.* 2001), (**H2**) G_S of *L. styraciflua* in previously elevated CO_2 will increase to the ambient level faster than *P. taeda*. The increase in G_S and reduction of leaf area may compensate each other. Thus, (**H3**) canopy transpiration in previously elevated CO_2 may be maintained unless further structural adjustments occur.

4.2 Materials and Methods

4.2.1 Site description

The study was conducted at the Duke FACE experiment site, Orange county, North Carolina (35° 58´ N, 79° 05´ W, 163 m asl) from 2009 to 2012. The mean annual precipitation and air temperature for the area are approximately 1140 mm and 15.5 °C.

The experiment site was established with 3-year old *P. taeda* seedlings in 1983. Four 30m-diameter plots under ambient atmospheric CO_2 concentration and four plots

under elevated atmospheric CO_2 concentration (target at 200 μmol mol^{-1} above ambient condition) composed the site. The CO_2 enrichment began with a prototype plot in 1994, and extended to four plots in 1996. The enrichment for the four plots concluded in October, 2010. Each plot was divided into two sections with a barrier inserted in the soil, and nitrogen fertilization (11.2 g N m^{-2} yr^{-1}) for one section of each plot was applied. The fertilization began with the prototype plot and its replicate in 1998, and extended to other plots in 2005. After the termination of CO_2 enrichment, all above- and belowground biomass in one half (including one fertilized and one unfertilized quadrant) of each plot was harvested from late 2010 to mid-2011. Further details about the site can be found at the Duke Forest FACE website (http://face.env.duke.edu).

4.2.2 Data collection

Air temperature (*T*) and relative humidity were measured at two-thirds of canopy height in each plot with temperature/RH probes (HMP series, Campbell Scientific, Logan, UT, USA), and used to calculate vapor pressure deficit (*D*). Photosynthetic photon flux density (*Q*; LI-190, LI-COR Biosciences, Lincoln, NE, USA) and net radiation (R_n; REBS Q7, Radiation and Energy Balance Systems Inc., Seattle, WA, USA) were measured at the top of the canopy in two plots (plot 4 and 7). Volumetric soil water content (*M*) of the upper 30 cm soil layer was measured at four different locations in each plot (CS615 or CS616L, Campbell Scientific, Logan, UT, USA). All measurements were collected every 30 seconds. 30-minute averages were stored in a data logger (CR-21X or CR-23X, Campbell Scientific, Logan, UT, USA) in each plot.

Leaf area index (L) was estimated from total leaf litterfall and specific leaf area, measured using a digital scanner (McCarthy et al., 2007). Leaf litterfall was collected once or twice (October to January due to high volume of leaf litter) per month from 12 (three per sector) 0.16 m^2 litter baskets in each plot. Details on L estimation are given in McCarthy et al. (2007). Sapwood area (A_S) was obtained from annual surveys of DBH and proportion of sapwood area to total area, which was measured from trees harvested in 2011.

Sap flow at three different depths (outer 0-20 mm; middle 20-40 mm; inner 40-60 mm) was measured using thermal dissipation probes (Granier, 1987). The sap flow sensors were classified by species, treatment, depth and year (Table 4.1). Sensors which were installed on trees planned to be harvested were removed in late 2010. To account for nocturnal flux, the measurements from the probes were converted into sap flux density (J_S) using baseline values representing negligible transpiration (Oishi et al., 2008).

Although measurements of J_S were supposed to be collected every 30 minutes, occasional sensor failure and power outage created gaps in data, missing values. The hierarchical Bayesian state-space approach was used to accommodate the gaps with the temporal structure of the data. The model was also used to access responses of G_S to environmental conditions and to detect changes after the termination of CO_2 enrichment.

4.2.3 Model structure

Using the hierarchical Bayesian state-space framework, we modeled G_S of each species under each treatment as a multiplicative function of reference G_S (G_{Sref}), vapor

pressure deficit f_D, photosynthetic photon flux density f_Q and soil moisture f_M (Jarvis, 1976; Oren et al., 1999):

$$G_S = G_{Sref} f_D f_Q f_M \tag{4.1}$$

where G_{Sref} is a reference stomatal conductance at D = 1 kPa, high Q and high M (Oren et al., 1999), and f_D, f_Q and f_M are functions for the response of G_S to D, Q and M. f_D depends on D and sensitivity of G_S to D (λ):

$$f_D = 1 - \lambda ln\, D \tag{4.2}$$

f_Q and f_M are relative effect of the variables on G_S, and were taken as:

$$f_Q = 1 - \beta_1 \exp\left\{\frac{-Q}{\beta_2}\right\} \tag{4.3}$$

$$f_M = \begin{cases} \exp\left\{-0.5\left(\frac{M-\beta_4}{\beta_3}\right)^2\right\} & \text{if } M < \beta_4 \\ 1 & \text{if } M \geq \beta_4 \end{cases} \tag{2.5}$$

Details on model description, a Gibbs sampling algorithm and model diagnostics are given in Bell (2011) and Ward et al. (2013).

4.3 Results and Discussion

4.3.1 Environmental variables and leaf area index

Figure 4.1 showed temporal patterns of photosynthetically active radiation (PAR), T, D and M from 2009 to 2012. Growing season PAR was similar during the four years ($p = 0.421$), averaging 732.7 μmol m^{-2} s^{-1}. Growing season T in 2009 (19.4 °C) was lower than that in other years (21.9 °C; $p < 0.001$). Growing season M was the lowest in 2010

(0.20) and the highest in 2012 (0.27). Maximum *L* of *P. teade* during the study period were 3.44, 3.57, 2.93, 3.70 m^2 m^{-2} in ambient CO_2 and 4.32, 4.22, 3.13, 3.79 m^2 m^{-2} in elevated CO_2 (Fig. 4.2). In 2009 and 2010, *L* of *P. taeda* in elevated CO_2 was ~22% greater ($p < 0.001$) than that in ambient CO_2 under native soil; the enhancement of *L* was consistent with 19% increase in *L* over previous 11 years (Ward *et al.* 2013). Under N-fertilized conditions, mean enhancement of *L* was only ~9% ($p < 0.001$) because *L* of *P. taeda* may have reached the site maximum with CO_2 enrichment ($p = 0.753$; McCarthy *et al.* 2007). When the long-term FACE was terminated, the difference reduced to ~7 and ~4% under native soil and N-fertilized condition during the first year and became not significant in the second year ($p = 0.409$ and 0.467). *L* of broadleaved deciduous species were unresponsive to elevated CO_2 during both before and after the termination of FACE ($p = 0.154$ and 0.187). Due to the unresponsive *L* of broadleaved deciduous species, the response of canopy *L* in elevated CO_2 (~20%) was slightly smaller than that of *P. taeda*; the enhancement was not observed in both years after the termination of FACE ($p = 0.245$ and 0.558). Under N-fertilized condition, *L* of broadleaved deciduous species in elevated CO_2 was ~40% greater than that in ambient CO_2 ($p < 0.001$); the difference became not significant after the termination of FACE ($p = 0.541$). The response of *L* of broadleaved deciduous species led ~13% increase ($p < 0.001$) in canopy *L* in elevated CO_2 under N-fertilized condition. The increase became not significant as the enhancement of *L* of broadleaved deciduous species disappeared.

4.3.2 Response of stomatal conductance

Annual mean daytime G_S of *P. teade* under native soil fertility were 84.6, 68.0, 71.5 and 79.1 mmol m^{-2} s^{-1} in ambient CO_2 and 50.8, 53.7, 76.5 and 87.6 mmol m^{-2} s^{-1} in elevated CO_2 during the study period (Fig. 4.3). Ratio of monthly daytime mean G_S of *P. teade* in elevated CO_2 to that in ambient CO_2 were less than one for 21 of 22 months under native soil condition and 16 of 22 months under N-fertilized condition before the termination of FACE (Fig. 4.4). Mean G_S ratio of *P. teade* under native soil and N-fertilized condition before the termination of FACE (0.69 and 0.74) were slightly lower than means over previous 11 years (0.87 and 0.78; Ward *et al.* 2013), but within the yearly variations. The mean G_S ratio increased to 1.12 and 0.97 under native soil and N-fertilized condition after the termination of FACE ($p < 0.001$), which may agree with **H1**. Tor-ngern *et al.* (2015) observed no direct response of G_S to short-term manipulation of atmospheric CO_2 concentration, and suggested that the reduction of G_S in elevated CO_2 was mainly driven by indirect responses, such as hydraulic conductance and leaf shading (McCarthy *et al.* 2007; Domec *et al.* 2010). Because the difference in water potential between soil and leaf was unresponsive to elevated CO_2 and change in hydraulic conductance of the xylem required structural adjustment (Domec *et al.* 2009; Domec *et al.* 2010), the increase in ratio may be from changes in the hydraulic allometry, especially decrease in leaf area.

The mean ratio of *L. styraciflua* was slightly higher after than before the termination (0.94 and 0.84, respectively) under native soil condition ($p = 0.023$); the ratio increased from 0.64 to 1.11 under N-fertilized condition ($p < 0.001$). In the second year after the termination of CO_2 enrichment, differences of monthly mean daytime G_S of *L.*

styraciflua in ambient and elevated CO_2 were not significant for most of months. The response of the ratio of *L. styraciflua* was not particularly faster than that of *P. teade*, thus we may reject **H2**.

4.3.3 Response of transpiration and canopy conductance

Figure 4.5 shows monthly integrated transpiration of *P. teade* and *L. styraciflua*. Annual transpiration of *P. teade* in ambient CO_2 under native soil fertility was 327, 297, 294 and 301 kg m^{-2} during the study period. Assuming the G_S response of all broadleaved deciduous species at the site were the same, annual canopy transpiration in ambient CO_2 under native soil fertility was 432-561 kg m^{-2} during the study period. The values are slightly lower than canopy transpiration estimated with eddy covariance method at the same site (Schäfer *et al.* 2002; Stoy *et al.* 2006), but within the yearly variations. Difference in total canopy transpiration between ambient and elevated CO_2 were not significant both before and after the termination of CO2 enrichment ($p = 0.421$ and 0.872), which is consistent with findings from previous study (Tor-ngern *et al.* 2015).

Agreeing with **H3**, the responses of canopy transpiration were not far from the unaltered long-term mean response (Tor-ngern *et al.* 2015). After the termination of CO_2 enrichment, the difference of canopy transpiration between ambient CO_2 plots and plots previously under elevated CO_2 on native soil were not significant in both years ($p = 0.788$ and 0.157). Under N-fertilized condition, 13% greater canopy transpiration in previously elevated CO_2 plots was observed in the first year following termination, but the difference became not significant in the second year ($p = 0.252$). Total canopy conductance (G_C) showed that the growing season ratio of G_C were not significantly

different from 1.0 both before and after the termination of CO_2 enrichment regardless of N fertility, except N-fertilized condition in 2009 (Fig. 4.6). Given no change in c_i/c_a (Medlyn *et al.* 2001; Ellsworth *et al.* 2012), the growing season ratio of G_C after the termination indicates that trees in previously elevated CO_2 assimilated at least the same amount of carbohydrates as those in ambient CO_2.

Table 4.1. The number of sap flow sensors by species in ambient and elevated CO_2 under native soil (AN and EN) and nitrogen-fertilized condition (AF and EF)

Period	Species	Depth (mm)	AN	AF	EN	EF
Before harvest	*P. taeda*	0 – 20	23	25	24	24
		20 – 40	9	17	12	12
		40 – 60	6	6	6	7
	L. styraciflua	0 – 20	12	12	12	12
		20 – 40	5	4	4	4
		40 – 60	0	0	0	0
After harvest *	*P. taeda*	0 – 20	16	16	19	18
		20 – 40	9	8	9	9
		40 – 60	3	2	6	5
	L. styraciflua	0 – 20	9	8	7	7
		20 – 40	4	4	4	3
		40 – 60	0	0	0	0

* Sensors, installed on trees planned to be harvested, were removed in advance of the harvest.

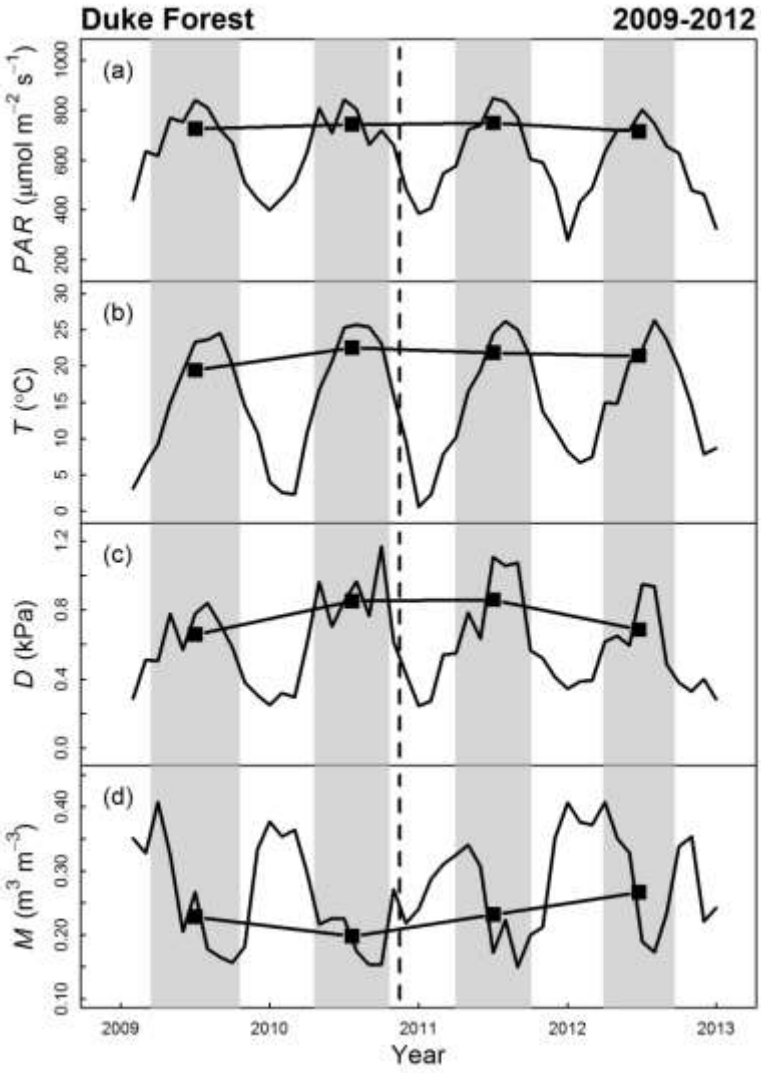

Figure 4.1. Changes in (a) photosynthetically active radiation (*PAR*), (b) air temperature (*T*), (c) vapor pressure deficit (*D*), and (d) volumetric soil moisture (*M*) in 2009-2012. Grey area indicates growing season, and closed squares are growing season means. Vertical dashed line separates before and after the termination of long-term CO_2 enrichment.

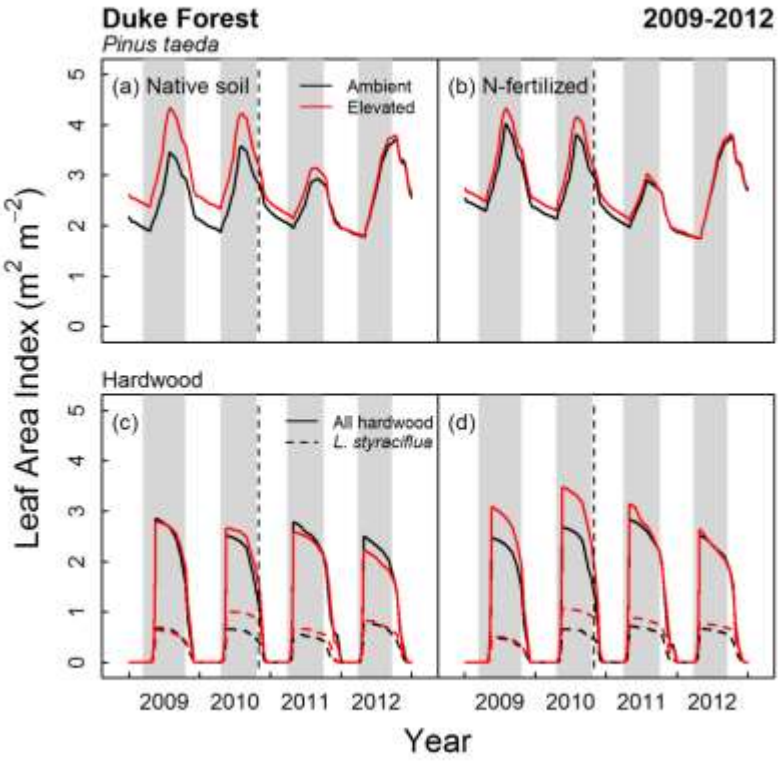

Figure 4.2. Leaf area index (*L*) of *Pinus taeda* (a, b) and all hardwood combined (c, d) in ambient (black lines) and elevated CO_2 (red lines) under native soil and N-fertilized conditions. Dashed lines in c and d are *L* of *Liquidambar styraciflua*. Grey area indicates growing season, and vertical dashed line separates before and after the termination of long-term CO_2 enrichment.

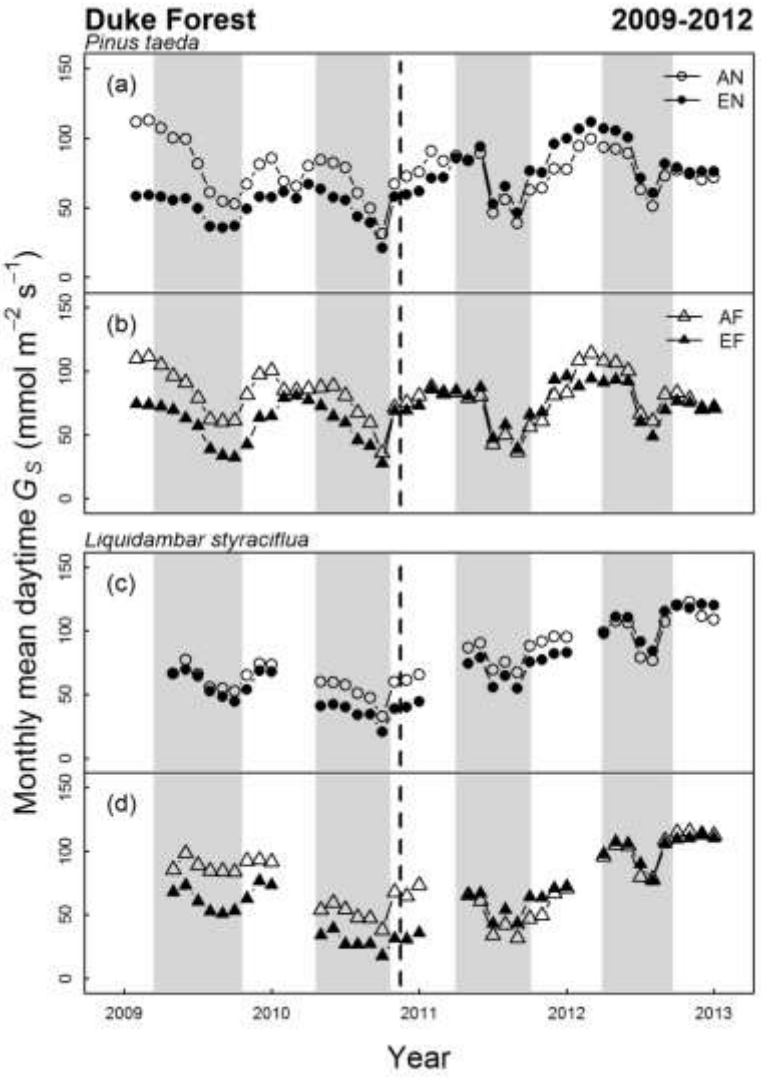

Figure 4.3. Monthly mean daytime stomatal conductance (G_S) of *Pinus taeda* (a, b) and *Liquidambar styraciflua* (c, d) in ambient (open symbols) and elevated CO_2 (closed symbols) under native soil (circles) and N-fertilized conditions (triangles). Grey area indicates growing season, and vertical dashed line separates before and after the termination of long-term CO_2 enrichment.

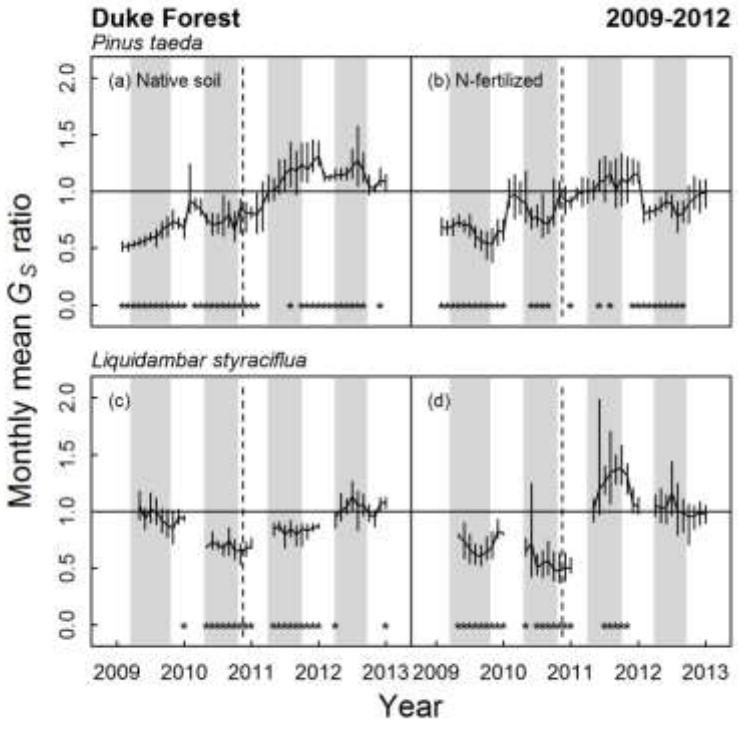

Figure 4.4. Monthly mean ratio of daytime stomatal conductance (G_S) of *Pinus taeda* (a, b) and *Liquidambar styraciflua* (c, d). Vertical bars represent 95% confidence intervals. Asterisks indicate ratios significantly different from 1. Grey area indicates growing season, and vertical dashed line separates before and after the termination of long-term CO_2 enrichment.

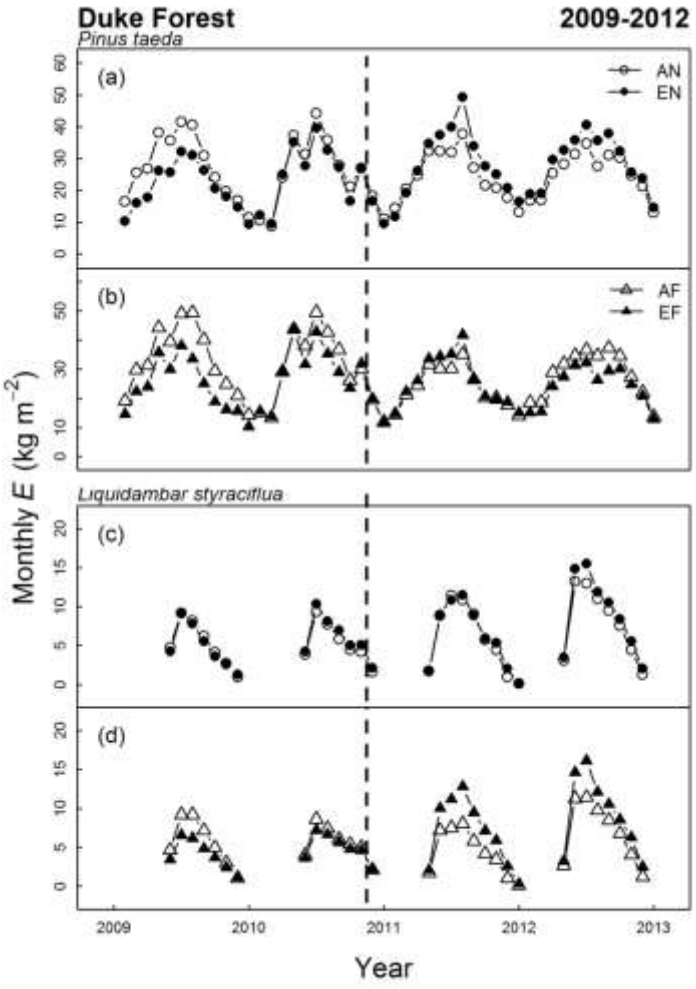

Figure 4.5. Monthly integrated transpiration (*E*) of *Pinus taeda* (a, b) and *Liquidambar styraciflua* (c, d) in ambient (open symbols) and elevated CO_2 (closed symbols) under native soil (circles) and N-fertilized conditions (triangles). Vertical dashed line separates before and after the termination of long-term CO_2 enrichment.

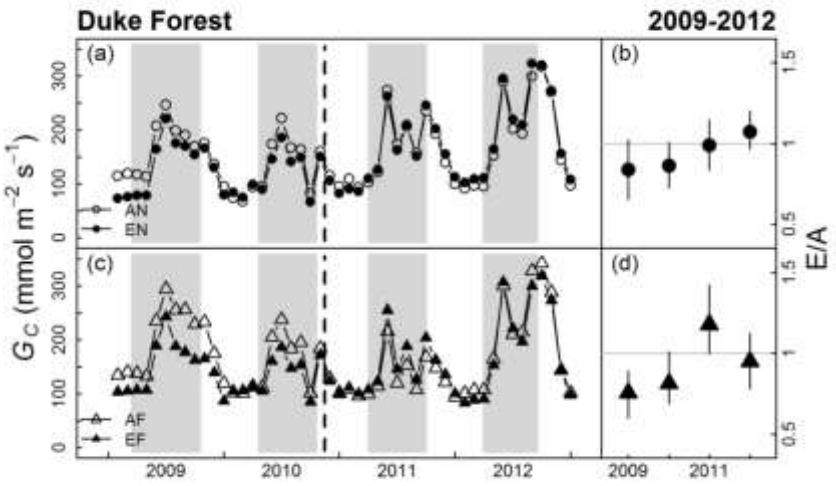

Figure 4.6. Monthly mean (a, c) and growing season mean (b, d) canopy conductance (G_C) in ambient (open symbols) and elevated CO_2 (closed symbols) under native soil (circles) and N-fertilized conditions (triangles). Vertical dashed lines separate before and after the termination of long-term CO_2 enrichment. In b and d, vertical lines indicate 95% confidence intervals.

5. Dynamics of soil CO_2 efflux under varying atmospheric CO_2 concentrations reveal dominance of slow processes

5.1 Introduction

Carbon (C) sequestration in forest ecosystems comprises a small difference between two large fluxes – photosynthesis and respiration (Schlesinger & Andrews 2000; Valentini *et al.* 2000; Bond-Lamberty & Thomson 2010). The largest, and most complex component of forest ecosystem respiration takes place in the soil and forest floor (R_S), were fine roots, fungi and other microorganisms dominating the living biomass, feed on either recently fixed carbohydrates, or on necromass produced in the soil as these constituents turn over, and on litter dropped on the forest floor. Thus, forest floor CO_2 efflux (F_{CO2}) is determined by the delivery of substrate, the mass of respiring populations, as well as the hydration state and temperature of the forest floor and soil profile in which roots and microorganisms reside. Complicating matters, in addition to the temporal variation in relations to climate condition (Oishi *et al.* 2013), and the spatial variation in relation to soil resources (Palmroth *et al.* 2005), R_S reflects the combined effects of seasonal dynamics of substrate availability and population mass, as well as the temperature acclimation of respiration rates (Reich *et al.* 2016). Thus, for example, variation in temperature and moisture affect leaf-scale photosynthesis, the activity and population size of microorganisms, and diffusivity of CO_2 in the soil (Stoy *et al.* 2007). But canopy-scale sugar production is further affected by leaf-area dynamics and solar angle (Schäfer *et al.* 2003), and the allocation of sugar belowground depends also on the

dynamics of growth aboveground (Schäfer *et al.* 2003; Palmroth *et al.* 2006; Novick *et al.* 2012). Additionally, although improved N availability enhances leaf area, and litter delivery to the forest floor, the increased C consumption aboveground is at the expense of reduces C allocation belowground (Palmroth *et al.* 2006; Lim *et al.* 2015); the net effect is lower forest floor F_{CO2} (Butnor *et al.* 2003; Oishi *et al.* 2013). Indeed, the number of processes interacting to ultimately produce a measured rate of F_{CO2} frustrates efforts to isolate the effect of each process; it is not surprising that studies conclude without clear attribution of F_{CO2} to a particular process, impeding efforts to properly model soil F_{CO2} and ecosystem respiration.

Ecosystem-scale, free-air CO_2 enrichment (FACE) experiment permit altering primarily the amount of carbohydrates allocated to belowground, litterfall, and the population size of the soil constituents contributing to respiration, without affecting weather conditions and soil hydration and temperature, and the seasonal dynamics of photosynthesis, growth and litter production (Schäfer *et al.* 2003; Palmroth *et al.* 2006; McCarthy *et al.* 2010). These experiments can be used to obtain empirical estimates of C pool size in, and F_{CO2} from the forest-floor-soil system, for constraining modeled results. Perhaps even more importantly, these experiments can help isolate the effects of short-term variation of recently-fixed carbohydrate supply from longer term adjustments of the respiring biomass in the soil and forest floor, thus providing insights into processes regulating carbon flow to, and release from belowground, and improved specification of mechanisms in models. In contrast to the majority of studies designed to assess the dynamics of F_{CO2} and its contributing constituents in response to a step decrease of

carbohydrate supply to belowground (mostly girdling and trenching experiments), eCO_2 experiments do not destructively modified the system, providing insight into processes dominating intact systems. From these experiments we learned that eCO_2 increases F_{CO2} (Table B2). The increase was attributed to a number of causes, including increased root biomass, specific root respiration rates, root exudates, and root turnover rate (Table 5.1; Allen *et al.* 2000; King *et al.* 2001; Norby *et al.* 2002; Lukac *et al.* 2003; Drake *et al.* 2008; Jackson *et al.* 2009). It was also shown that increasing the availability of soil nitrogen (N) resulted in a decrease of all of these contributors to soil respiration (Jackson *et al.* 2009; Pritchard *et al.* 2014), which was reflected in decreasing F_{CO2} under both ambient and elevated atmospheric CO_2 (aCO_2 and eCO_2, respectively; Palmroth *et al.* 2006; Oishi *et al.* 2013).

In contrast, reductions in the supply of recently-produced carbohydrate to belowground by girdling or trenching overlap with an increased mortality as roots and mycorrhizal fungi run out of carbohydrates. Furthermore, concurrent increase of soil moisture (relative to unaltered reference) due to reduced water absorption by severed or degrading root systems may increase the decomposition rate of the bigger necromass pool. The onset and rate of root mortality depend on the amount of carbohydrates stored in the tissue prior to treatment initiation, and the temperature of the tissue (Marshall & Waring 1985), and decomposition may increase or decrease with increasing soil moisture. Shading experiments can reduce carbon allocation to belowground less destructively, allowing evaluation of the effect of reduced carbohydrates source and, in combination with enhanced N supply, of altered carbohydrate sinks on both aboveground

and belowground process (Hasselquist *et al.* 2016). However, the approach cannot be implemented over a long periods without making the ecosystem too different from, and thus unrepresentative of intact ecosystems, and can be employed only over short-statured forests. Stem chilling (Johnsen *et al.* 2007) and the recently developed pressure girdling (Henriksson *et al.* 2015) provides a reversible method for reducing carbohydrate transport to belowground. While the former is impractical for long-term ecosystem-scale manipulation, upon further testing and improvements the latter may become more broadly applicable.

Experimental reduction in C flow belowground often monitor F_{CO2} at high frequency beginning before treatment application, facilitating detection of the onset of changes in fast processes, those depending on recently produced carbohydrates, before slower processes such as mortality and decomposition begin and complicate interpretation (Högberg et al. 2010). Unfortunately, these early dynamics were poorly quantified in FACE experiments. The ^{13}C signature was followed at Duke FACE, and showed changes at 20 cm depth 7 days after commencement of enrichment; the enrichment signature moved progressively down the soil profile (Andrews & Schlesinger 2001). The vertical dynamics was consistent with CO_2 released through respiration in the upper horizon, some of which dissolving in water moving down the profile at rates determined by soil physical properties and hydration. However, measurements of F_{CO2} from the soil surface were made at coarser intervals, thus potentially missing effects on fast process found within days in C flow reduction experiments.

We employed a nondestructive approach to quantify the effect of short-term manipulation of atmospheric CO_2 on the F_{CO2} from the forest-floor at the Duke FACE experiment during periods of high and low soil moisture, at the end of the growing season. A follow-up, two-year study on the response to termination of CO_2 enrichment, permitted separating the effects of short and longer term reduction in belowground C allocation on R_S. At the end of the growing season, carbohydrates are preferentially allocated to belowground, thus the study should be taken a measure of maximum effect. A $^{13}CO_2$-labeling experiment has shown for a boreal *Pinus sylvestris* that belowground C allocation increases fivefold in this period relative to mid-growing season allocation (Hogberg *et al.* 2010), and a study on southeastern US *Pinus taeda* showed that stem-chilling during the height of the growing season had little effect on C transport belowground, but that at the end of the season it had a marked effect (Johnsen *et al.* 2007). The manipulation we imposed was a high frequency (five days long), step changes of CO_2 concentration (from ambient to ~80% above ambient), which based on a previous work would cause similar changes in canopy-scale photosynthesis (Tor-ngern *et al.* 2015), on the background of low frequency (seasonal and years long) adjustments of belowground biomass. The high frequency changes were made when soil is moist and dry, searching for interaction effects, thus increasing the temporal scope of inference. The plots under CO_2 manipulation were split, and half of each received increased N supply for at least 5 growing season, thus increasing the spatial scope of inference of such a study.

A combination of eddy-covariance, atmospheric and soil conditions measurements, with modeling CO_2 transport from the soil suggests that climate signature on photosynthesis can be observed within three days in F_{CO2} (Stoy *et al.* 2007). We thus hypothesized that (**H1**) the effect of five-day CO_2 changes during the end of the growing season will be reflected in corresponding changes of F_{CO2}. We further hypothesized that, if eCO_2 confers some protection from drought effects, the effect of **H1** will be relatively greater during low soil moisture, high vapor pressure (*D*) conditions. The reduction of F_{CO2} has been explained not only by a decrease in sugar flow to belowground, but also in terms of rapidly decreasing biomass of mycorrhizae and fine roots (Table B2; Högberg *et al.* 2001; Drake *et al.* 2012; Jing *et al.* 2015; Hasselquist *et al.* 2016). Reductions of mycorrhizae may occur within a week (Högberg *et al.* 2001), and those of fine roots are observed after three months (Jing *et al.* 2015). Thus we hypothesized that, (**H2**) following the termination of eCO_2 at the Duke FACE, F_{CO2} (reflecting R_S) will decline to that of the reference within approximately three months, remaining at that level for the following two years of monitoring. Alternatively, a larger pool of carbohydrate reserves in roots may buffer against short-term variation in photosynthesis, and a pulse of dying roots may provide for greater microbial activity, maintaining greater F_{CO2} in plots previously subjected to eCO_2.

5.2 Materials and Methods

5.2.1 Site description

The study was conducted at the Duke Forest FACE site, North Carolina, USA (36° 58′ N, 79° 06′ W) from 2009 to 2012. The annual mean precipitation and air temperature of the site are approximately 1145 mm and 15.5 ºC, respectively. *P. taeda* seedlings (3-year-old) were planted after clear-cutting and burning in 1983, and the average height of *P. taeda* reached ~21 m in 2010. Naturally regenerated broadleaved species including *Liquidambar styraciflua*, *Ulmus alata*, *Acer rubrum*, and *Fraxinus americana* accounted for ~41% of total leaf area of the site 2009 during growing season. Most broadleaved trees were presented in the mid- to lower-canopy, but some extended to the upper-canopy (McCarthy *et al.* 2007).

A total of eight 30-m-diameter circular plots were established. The FACE experiment started in a prototype plot under CO_2 enrichment (targeted at 200 μmol mol^{-1} above ambient atmospheric CO_2 concentration) and its reference in 1993, and extended to eight plots (four elevated and four ambient plots) in 1996. Annual N fertilization with ammonium nitrate pellets (NH_4CO_3; 11.2 g N m^{-2} yr^{-1}) began on one half of each plot in 1998 for the prototype plot and its reference, and extended to the other six plots in 2005; each plot was divided with an impermeable barrier inserted to 70 cm from the ground, which is the depth of the fine root system of the site (Matamala & Schlesinger 2000). In 2010, short-term CO_2 response study was conducted using stepwise changes of atmospheric CO_2 concentration in elevated plots from late August to early October, day of year (DOY) 242-282. One out of five target CO_2 concentrations (ambient, 100, 150, 200 and 300 μmol mol^{-1} above ambient) were set at an interval of five (or six for the last period) days. The CO_2 enrichment returned to the long-term target (+200 μmol mol^{-1}) on

October 10, and concluded on October 31, 2010. All above- and belowground biomass in 40% of each plot, half in native soil quadrant and half in N-fertilized quadrant, was harvested from late 2010 to early 2011. The annual N fertilization continued for the remaining half of each plot until 2012.

5.2.2 Data collection

Soil temperature was measured with thermistors (334-NTC102-RC, Xicon Passive components, Masnfield, TX, USA) buried at 10 cm in each plot. Volumetric soil water content (θ) of the upper 30 cm soil layer was measured with time-domain reflectometry probes (CS615 or CS616L, Campbell Scientific, Logan, UT, USA) at four different locations in each plot. Soil water availability for trees was expressed as relative extractable water (REW; Granier 1987):

$$\mathrm{REW} = \frac{\theta - \theta_m}{\theta_{FC} - \theta_m} \quad (1)$$

where θ_m is the hygroscopic point where soil water is unavailable for plants (0.125 m^3 m^{-3}) and θ_m is θ at field capacity (0.35 m^3 m^{-3}).

F_{CO2} was measured using automated carbon efflux system (ACES) developed by the United States Department of Agriculture (USDA) Forest Service (Butnor *et al.* 2003). The ACES is chamber-based, multiport respiration measurement system that linked an infrared gas analyzer (EGM-3 or EGM-4, PP Systems, Amesbury, MA, USA) to 11 soil chambers (six under native soil fertility and five under N-fertilized condition), randomly distributed in each plot. Each soil chamber had a diameter of 25 cm (491 cm^2 measurement area) and a height of 10 cm, and was moved to one of two fixed positions at

least once a week to minimize chamber effects on litter input, precipitation and the microenvironment inside the chamber. Each chamber was sampled for 10 minutes, for a maximum of nine times a day. After allowing the condition within the chamber to equilibrate with ambient condition, measurements of the last three minutes, when fluxes are stable, were used to calculate mean F_{CO2}. If air flow rates, or CO_2 concentrations, were unstable or out of a specific range, the data were removed from analysis. Fluxes which can be considered as abnormal (lower than 0.1 or higher than 30 μmol CO_2 m^{-2} s^{-1}) were also excluded. When more than half of daily measurements from a soil chamber were available, daily mean of the soil chamber was used for further analyses.

Filtering out fluxes with unstable or abnormal air flow rates or CO_2 concentrations created gaps in data. Occasional failure of the gas analyzer, disconnection or leakage of tubing between the ACES and soil chamber, malfunctioning ACES components, power outage, and periodic maintenance for recalibration, also caused missing data. Bayesian state space models were used to fill gaps in data and to investigate treatment effects. The method is beneficial because it can compute the uncertainties of parameter estimates (Clark *et al.* 2011). We modeled log R_S of a chamber at time t (x_t) as a function of soil temperature (T_t), REW (M_t), daytime mean CO_2 concentration (C_t), N treatment (N_t) and relaxation period (P_t):

$$x_t \sim N(f(T_t, M_t, C_t, N_t, P_t), \sigma^2) \quad (1)$$

$$y_t \sim N(x_t, \tau^2) \quad (2)$$

where σ^2 represents process error, y_t represents log of observed soil respiration, and τ^2 represents observation error. In addition to current daytime mean CO_2 concentration, CO_2

concentration with time lags were also tested to identify potential time lags associated with photosynthesis and F_{CO2} (Stoy *et al.* 2007).

5.3 Results

The Bayesian state space model, parameterized based on soil temperature, REW, daytime mean CO_2 concentration data from 2009 and 2010, and nitrogen fertilization explained most of the variations in daily mean F_{CO2}. Focusing on 2009, the last complete year of data before the termination of eCO_2, the model shows only a slight underestimation of the rarely measured high fluxes (Fig. B1). The model was also parameterized separately for each of the two years following termination of eCO_2, allowing for slow adjustment of the plots that beforehand were exposed to eCO_2, and for the two years combined. The outcome from both approaches was the same for both aCO_2 and eCO_2 estimates (Fig. B2). Thus, the parameters obtained based on data collected during the combined two last years of enrichment and during the combined two years post enrichment were used to gap fill data for both the analyses of the response to short-term, stepwise manipulation of CO_2, and analyses of long-term response to termination of eCO_2.

The short-term CO_2 response study was divided into two periods representing distinct difference of soil moisture, before and after a major rainfall event followed by several smaller events (mean REW during low and high soil moisture periods were 0.03 and 0.78, respectively; for detailed representation of conditions during the short-term experiment, see Tor-Ngern *et al.*, 2015). We evaluated the five-day steps in CO_2

concentrations in three ways: (1) to evaluate whether there is a gradual response, we analyzed F_{CO2} in each 5-day period, searching for an increasing or decreasing rates for a corresponding step-change in CO_2 concentration – among the 48 available changes for all plots, we found only two significant. Given these results, (2) we tested whether the change of F_{CO2} was consistent in both amount and direction to the change in CO_2 concentration – we found that, after eliminating six of 48 points during which soil moisture increased rapidly and greatly, thus causing evacuation of soil-CO_2, there was no response corresponding to the changes of CO_2 concentration ($p = 0.162$). Lastly, (3) we assessed the daily mean F_{CO2} in relation to CO_2 concentration (Fig. 5.1). We found that, the posteriors of the coefficients for both main and interaction effects involving CO_2 concentration were close to zero. Regardless of soil moisture, daily mean F_{CO2} did not respond to changes in CO_2 concentration at five-day intervals (Fig. 5.1). Yet, consistent with the long-term behavior observed at the site, plots receiving eCO_2 for many years, maintained higher F_{CO2} when measured under ambient concentration than plots receiving long-term aCO_2 – the difference was significant in all but the most restrictive condition of low moisture and N addition (Fig. 5.1c; compare open and closed symbols under aCO_2 concentrations). As commonly observed, respiration was higher when REW was greater.

The gap-filled data showed a typical dynamics corresponding roughly those of soil temperature, slightly lagging air temperature, with excursions above and below the general pattern corresponding to variation of soil moisture (Fig. B3). The difference (and thus ratio) of F_{CO2} under eCO_2 versus aCO_2 increased with the flux to a maximum in mid-growing season and decreased to a minimum in winter. After terminating eCO_2 in late

fall, 2010, F_{CO2} in plots of the two treatments converged as in previous winters, remaining similar in the following spring. However, by mid-summer, F_{CO2} of previously eCO_2 plots was less than that of aCO_2 plots, a pattern becoming even more obvious in 2012 growing season. The dynamics of F_{CO2} in the N-fertilized portions of the plots were similar but the amplitude was smaller, without affecting the ratio of F_{CO2} in eCO_2 relative to aCO_2 plots. We summarized the long-term responses into annual values, and merged with previous data obtained at the site based on the same methodology (Fig. 5.2). F_{CO2} was higher under eCO_2 in most years before termination of enrichment, depressed similarly by N addition under aCO_2 and eCO_2, showing slightly (but not significantly) higher enhancement ratio under N-fertilized conditions than under native soil conditions. Consistent with the response of the seasonal dynamics (Fig. B3), following termination of enrichment the annual F_{CO2} of previously enriched plots decreased to less than that of aCO_2 plots, with the decrease apparently greater under native soil (Fig. 5.2). Analysis of the high frequency data showed that F_{CO2} of previously eCO_2 plots decreased below those of aCO_2 plots approximately five weeks following termination of enrichment, and despite some seasonal variations, remained lower for the remainder of the study (Fig. 5.3). During the last two years of enrichment, annual F_{CO2} under eCO_2 was ~210 g m^{-2} more than under aCO_2 regardless of soil fertility, while during the two years following termination F_{CO2} decreased in previously enriched plots to ~250 g m^{-2} less than aCO_2 in native fertility plot portions, but to only ~100 g m^{-2} less than aCO_2 in N-fertilized portions (Table B3). The change from before to after termination was from an E/A F_{CO2} of 1.20 to 0.77 under native soil, and 1.27 to 0.89 under N-fertilized conditions, or a

reduction of ~35% following termination, slightly more for native soil fertility than N-fertilized conditions.

The underlying causes for the change were reflected in the model parameters (Table 5.1), showing 10% higher base respiration (at 15 ºC) at eCO_2, becoming 22% lower following termination under native soil conditions (+14% and -11%, respectively, in N-fertilized plot portions). In contrast, the temperature sensitivity of F_{CO2} was the same in both CO_2 treatments during the enrichment period, but decreased 9% after termination, regardless of soil fertility. The sensitivity to soil moisture was ~5% lower under eCO_2, and did not change after termination.

To further investigate potential causes of the large decrease in F_{CO2} after the termination of enrichment, we related the flux to estimates of leaf area index (*L*) obtained from the same data and methodology as in McCarthy *et al.* (2007), available throughout the study (Fig. 5.4). We found that, under aCO_2, maximum monthly mean *L* was somewhat lower (~0.5 m^2 m^{-2}) in the final two years of observation relative to the previous two years, yet monthly F_{CO2} at a given *L* increased significantly, slightly more in N-fertilized than native soil plot portions (Fig. 5.3a and 5.3c). In contrast, termination of eCO_2 caused a large decrease in *L* and in F_{CO2} at a given *L*, with the effect slightly less pronounced in N-fertilized portions. These observations were consistent in all plots. Attempting to lag-correlate the two time series reduced the proportion of variation in F_{CO2} accounted by *L* by >30%.

5.4 Discussion

Synthesis of results from FACE experiments showed that eCO_2 increases F_{CO2}, and that the increase is higher in young than old stands (Table B1; King *et al.* 2004). In young stands, the extra carbohydrates under eCO2 facilitate a rapid exploitation of the soil volume by roots and mycorrhizae, as they quickly occupy the canopy volume (Norby *et al.* 2005), while in older stands extra carbohydrates are used to increase the efficiency of resource utilization (Finzi *et al.* 2015) because they already access most of the incoming light and soil resources. Nevertheless, even following crown closure, contributing to higher F_{CO2} under eCO_2 are larger coarse, fine root and mycorrhizal mass and litterfall (DeLucia *et al.* 1999; Matamala & Schlesinger 2000; Lukac *et al.* 2003; King *et al.* 2004; Pritchard *et al.* 2008; Pritchard *et al.* 2014); more biomass, combined with faster turnover of fine roots and mycorrhizae under eCO_2 (Lukac *et al.* 2003; Pritchard *et al.* 2008) increases necromass, leading to higher microbial respiration and R_S. Increased litterfall with eCO_2 makes more forest floor substrate available for decomposition above the soil surface, enhancing F_{CO2} (Allen *et al.* 2000), even without concurrent increase in belowground carbohydrate allocation (Subke *et al.* 2004). Thicker litter layer may also limit soil evaporation, thus increasing soil moisture, further enhancing soil microbial activity and R_S (Schäfer *et al.* 2002). These changes in the forest floor-soil system occur slowly, taking months to years to be observed and affect F_{CO2} (Allen *et al.* 2000; Andrews & Schlesinger 2001; King *et al.* 2004). However, changes in photosynthetic rates affect the delivery of carbohydrates belowground within days (Andrews *et al.* 1999; Stoy *et al.* 2007).

On poor sandy soils, temporary blockage of sugar transport to roots resulted a reduction of F_{CO2} within ~6 days, but only in fall (Johnsen *et al.* 2007; Henriksson *et al.* 2015), when recently produced carbohydrates are used in the production of fine roots and mycorrhizae (Högberg *et al.* 2001). At that time, non-structural carbohydrates reserves in fine roots is typically low (Oren *et al.* 1988), which may be the reason for the strong coupling observed between the activity of the belowground constituents in these ecosystem and the supply of recently assimilated carbohydrates. However, when CO_2 concentration was manipulated in eCO_2 plots to between ambient and nearly 80% over ambient, causing a similar effect on carbohydrate production because stomata did not respond (Tor-ngern *et al.* 2015), F_{CO2} did not change in either soil N availability regime (Fig. 5.1), thus refuting **H1**. This suggests that carbohydrate reserves in the roots under eCO_2 was sufficiently large to buffer the activity of the belowground constituent during periods of lower photosynthesis when CO_2 concentration was brought below the long term mean enrichment, and that no limitation on carbohydrates availability was alleviated when CO_2 concentration was increased above the long term mean enrichment. This was true regardless of soil water conditions; during the first period of the short-term manipulation, the soil was dry, and stomatal conductance was very low (Tor-ngern *et al.* 2015). Although lower photosynthesis when the soil was dry likely reduced carbohydrates supply belowground, a somewhat lower belowground activity at that time (Fig. 5.1) meant that the carbohydrate reserve under eCO_2 was sufficient to meet the demand, and the large fluctuations of photosynthetic rates imposed by step changes of CO_2 concentration had no effect on F_{CO2}. Carbohydrate concentrations in fine roots were

unrelated to any treatment at the Duke FACE, although no measurements were made in the fall (Drake *et al.* 2008). If the similarity of carbohydrate reserves among treatments held through the fall, the results suggest that carbohydrate demand was less than the combined availability from reserves and the up to ~30% lower photosynthesis (to ~30% below the long term average in eCO2 plots; Schäfer *et al.* 2003).

When eCO_2 plots were subjected to aCO_2, F_{CO2} was higher than that of aCO_2 plots, under all but dry soil, N-fertilized conditions (Fig 5.1), reflecting the difference in belowground biomass and activity (~50% more fine root biomass and 90% more mycorrhizal standing crop in native soil, and 20% more fine roots in N-fertilized soil; Drake *et al.* 2008; Pritchard *et al.* 2014). Thus, while carbohydrate reserves under eCO_2 may be sufficient to buffer short-term fluctuations in CO_2 concentration, a prolonged reduction of photosynthesis must have starved the large biomass of belowground constituents residing in eCO_2 plots. The soils of the site are relatively warm, which should cause a fast utilization of root carbohydrate reserves (Marshall & Waring 1985), followed by a large contraction of the root system. This proposed response is consistent with the large drop of base respiration (Table 5.1), somewhat less in N-fertilized sub-plots in which the root-mycorrhizal system complex did not increase as much under eCO_2. The concurrent reduction in the temperature sensitivity of respiration (Table 5.1) may reflect down-regulation to match the curtailed carbohydrate supply. The changes in base respiration and temperature sensitivity were reflected in a fast decline of F_{CO2} (Fig. 5.2 and 5.3). Although averaged for the first dormant period after termination (Fig. 5.3), F_{CO2} of formerly eCO_2 plots was similar to that under aCO_2, as in the last winter of

enrichment, the daily data showed that E/A response of F_{CO2} dropped below unity by about five weeks after termination of enrichment, and remain approximately 20% less than in aCO_2 plots for the remaining two years, forcing a rejection of **H2**.

The contraction of the root-mycorrhizal system exceeded what can be expected by simply scaling to lowered canopy photosynthesis. Because the ratio of the leaf-internal to external concentration of CO_2 was largely unaffected by eCO_2, canopy photosynthesis before termination was ~40% higher in eCO_2 than aCO_2 plots, largely reflecting the higher atmospheric CO_2 concentration (Schäfer *et al.* 2003), and marginally ~17% greater *L* (McCarthy *et al.* 2007). A synthesis of gas exchange data showed show ~10% down-regulation of net photosynthesis in leaves produced under eCO_2 (Ellsworth *et al.* 2012), and soil moisture and atmospheric conditions were similar in all treatments (Oishi *et al.* 2014). Thus, total canopy photosynthesis following eCO_2 termination should be related to *L* in a saturating fashion, because mutual shading increases with *L* (Palmroth *et al.* 2006). Even with slightly lower net photosynthesis, deeply shaded leaves may no longer be able to support themselves, and will certainly not be able to export carbohydrates to support the root-mycorrhizal system. Thus, reductions in both *L* and F_{CO2} can be expected, as was observed (Fig. 5.2 and 5.3). However, while the reduction of *L* in previously eCO_2 plots resulted in *L*, and likely photosynthesis, becoming similar to that observed in aCO_2 plot, the reduction of R_S brought F_{CO2} of previously eCO_2 plots to ~20% less than that under aCO_2 (Fig. 5.2). Resources were not available to directly quantify the response of belowground constituents to reductions in carbohydrate availability, but seasonal analysis may shed some light on the dynamics of the response.

In *P. taeda* stands, maximum canopy-scale photosynthesis occurs in mid-June, preceding the peak *L* time by four months. Even though the dynamics of *L* and photosynthesis are not synchronized, those of *L* and F_{CO2} are both before and after termination of enrichment (Fig. 5.4). Compared to 2009-2010, the data from 2011-2012 show a small reduction in *L*, and a small increase of F_{CO2} at a given *L* (~25% change in slopes) in aCO_2 plots of both fertility regimes. The increase in F_{CO2} is consistent with warmer and wetter conditions in the latter pair of years (Table B4). Termination of enrichment in eCO_2 plots resulted in a much greater reduction of *L*, as well as a large reduction of F_{CO2} at a given *L*. The reduction in *L*, normalized by that of aCO_2 plots, was ~15%, while the reduction in the slope (similarly normalized), was ~50%. Assuming, based on the above, that canopy photosynthesis following termination was similar in all plots, as was C allocation belowground, as reflected in the similarity of *L*, and thus leaf biomass production, the reduction of F_{CO2} of previously eCO_2 plots at the same level of *L* suggests a large contraction of the live fine root-mycorrhizal system that is both disproportionate to the contraction of canopy *L*, and not balanced by an increased mass and activity of organism decomposing the swelling necromass pool. Our post enrichment monitoring did not last long enough to determine how long it will take the belowground system to recover a similar activity to aCO_2 plots, and the end of time series may have confounded dormant season F_{CO2} with recovery (Fig. 5.3).

Interpretation of time series measurements requires that the length of the measurement series and the frequency of the data collected correspond to the time necessary for relevant process to play out. For example, the decreasing enhancement ratio

of F_{CO2} during the early years at the Duke FACE (1999 – 2003) were interpreted as consistent with decreasing R_S as forests age (Bernhardt *et al.* 2006), while the increasing ratio in the latter years (2003 – 2009) as consistent with increasing fine root biomass in eCO2 relative to aCO_2 (Jackson *et al.* 2009). However, the entire time series (Fig. 5.2) shows no clear pattern; the variation were unrelated to variation in root biomass or soil conditions, and the ratio was not significantly higher or lower in any year since the year after the replicated study came on line (1996), until the enrichment was terminated. Clearly, there must have been a period of time initially during which the system adjusted to eCO_2, and F_{CO2} progressively increased relative to aCO_2 plots. This period could be shorter than a year, requiring frequent monitoring to capture.

The necromass pool of roots and associated mycorrhizae enlarges when carbohydrate allocation to belowground increases, because the live biomass pool increases in size and turns over faster (Lukac *et al.* 2003; Drake *et al.* 2008); the necromass pool enlarges also when belowground allocation decreases, because of extensive fine root and mycorrhizal mortality of the contracting root system. In contrast to the similarity of the response of the necromass pool to both increasing and decreasing belowground allocation, the amount of living, respiring fine root (and associated mycorrhizae) increases or decreases in concert with carbohydrate allocation (Table B2; Högberg *et al.* 2001; Jing *et al.* 2015; Hasselquist *et al.* 2016). We analyzed data available from four FACE experiments in forests and those from various approaches to reduce or eliminate carbohydrate movement belowground (Fig. 5.5). We found that the aforementioned changes, and associated changes in rhizosphere microorganisms, living

on root exudates and necromass, cause treatments enhancing carbohydrate allocation belowground to increase R_S at appreciably longer temporal lag than treatments reducing the allocation, even though the same constituents are involved. Reducing carbohydrate production upon termination of eCO_2 had an intermediate lag. These asymmetric responses pose a tractable challenge to process based models attempting to isolate the effect of individual processes.

Table 5.1. Means and 95% credible intervals of base respiration (β_0), temperature sensitivity (β_T) under non-limiting soil moisture condition and moisture sensitivity (β_M) under mean soil temperature condition before and after the termination of CO_2 enrichment

Parameter	Period	Native			N-fertilized		
		Ambient	Elevated	E/A	Ambient	Elevated	E/A
β_0	Before	2.70	2.98	1.10*	2.29	2.60	1.14*
(μmol CO_2 m^{-2} s^{-1})		(2.68, 2.72)	(2.96, 3.01)		(2.27, 2.31)	(2.58, 2.63)	
	After	2.63	2.06	0.78*	2.23	1.99	0.89*
		(2.62, 2.65)	(2.04, 2.09)		(2.21, 2.25)	(1.96, 2.02)	
β_T	Before	1.48		1.00	1.48		1.00
		(1.47, 1.49)			(1.47, 1.49)		
	After	1.42	1.29	0.91*	1.42	1.29	0.91*
		(1.41, 1.43)	(1.29, 1.30)		(1.41, 1.43)	(1.29, 1.30)	
β_M	Before	1.01	0.97	0.96*	1.01	0.97	0.96*
		(1.01, 1.01)	(0.97, 0.97)		(1.01, 1.01)	(0.97, 0.97)	
	After	1.01	0.96	0.95*	1.01	0.96	0.95*
		(1.01, 1.01)	(0.96, 0.97)		(1.01, 1.01)	(0.96, 0.97)	

* Ratio is significantly different from 1.

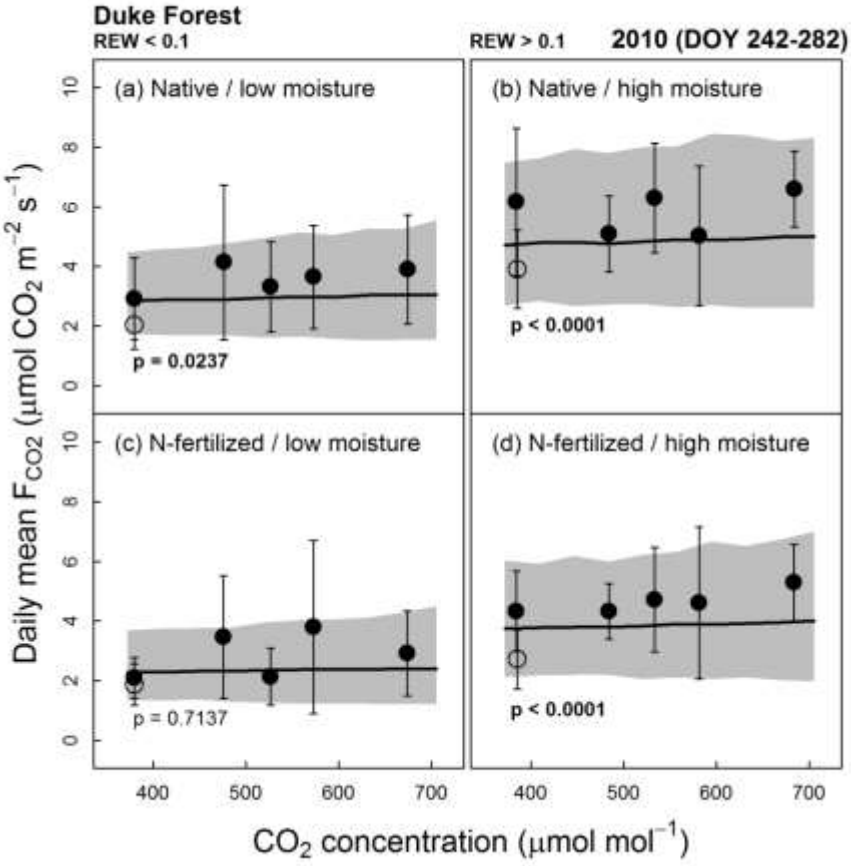

Figure 5.1. Response of daily mean soil CO_2 efflux (F_{CO2}) to atmospheric CO_2 concentration ranged from ambient to ambient + 300 ppm under native soil (a, b) and N-fertilized (c, d) conditions. Vertical lines are 95% confidence intervals of observed F_{CO2}. Solid lines and grey area are mean predicted values and 95% prediction intervals. P values are for testing difference of F_{CO2} between ambient and elevated CO_2 plots under ambient CO_2 concentration.

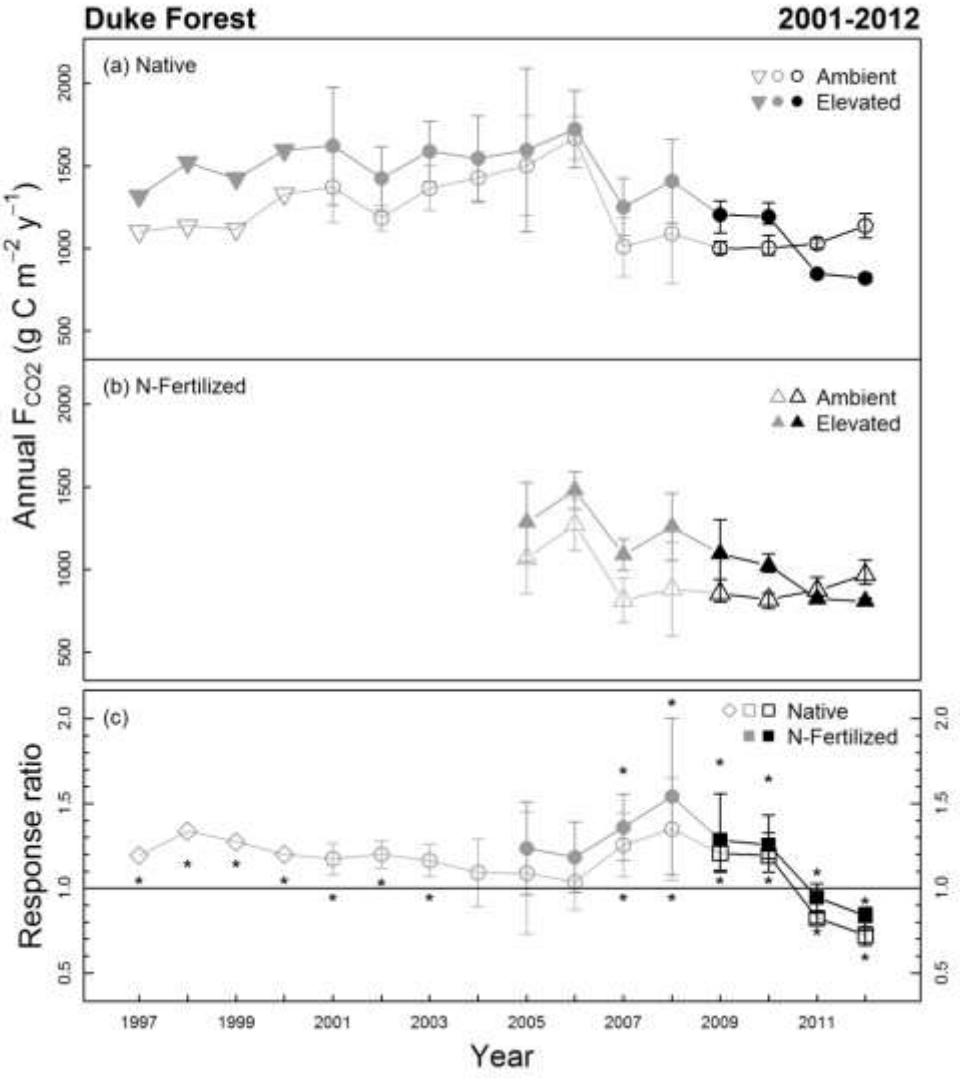
Duke Forest
2001-2012
(a) Native
Ambient
Elevated
(b) N-Fertilized
Ambient
Elevated
(c)
Native
N-Fertilized
Annual F_{CO2} (g C m^{-2} y^{-1})
Response ratio
Year
500
1000
1500
2000
0.5
1.0
1.5
2.0
1997
1999
2001
2003
2005
2007
2009
2011

Figure 5.2. (a) Annual soil CO_2 efflux (F_{CO2}) under native soil fertility, (b) annual F_{CO2} under N-fertilized condition, and (c) F_{CO2} response ratio from 1997 to 2012. Vertical lines are 95% confidence intervals. Values in 2001-2008 are from Oishi *et al.* (2014); values in 1997-2000 are adjusted means from King *et al*. (2004), Bernhardt *et al*. (2006) and Jackson *et al*. (2009). Asterisks were placed for significant difference of the response ratio to one.

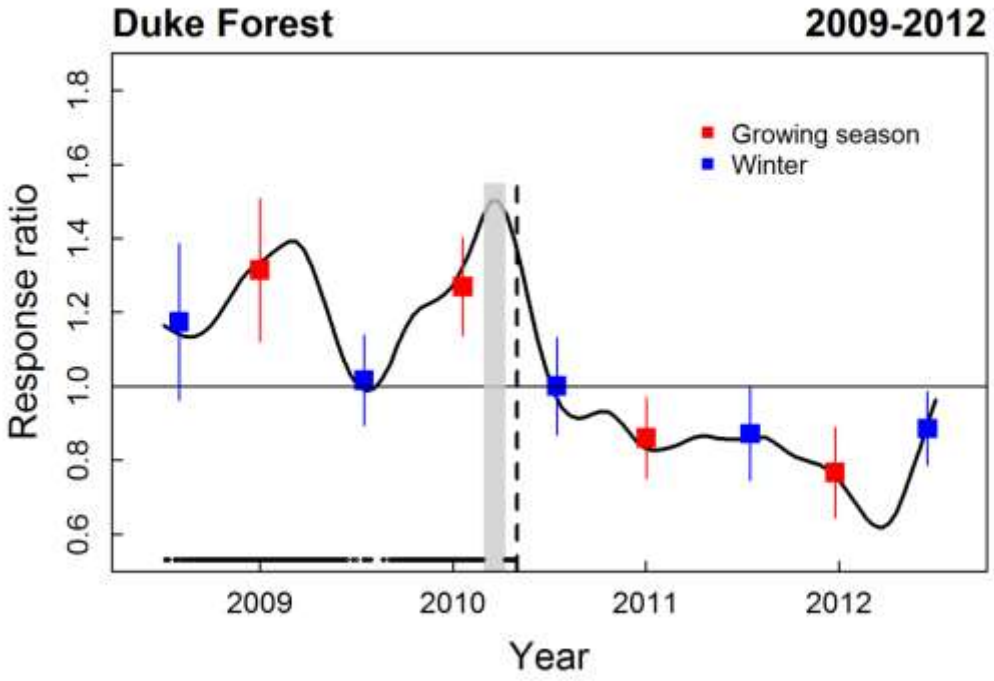

Figure 5.3. Soil CO_2 efflux (F_{CO2}) response ratio before and after the termination of CO_2 enrichment. Blue and red symbols indicate values during growing season and winter. Vertical dashed line shows when CO_2 enrichment was terminated. Grey area represents short-term CO_2 response study period. Dots on the bottom indicate dates with CO_2 enrichment (ambient + 200 ppm).

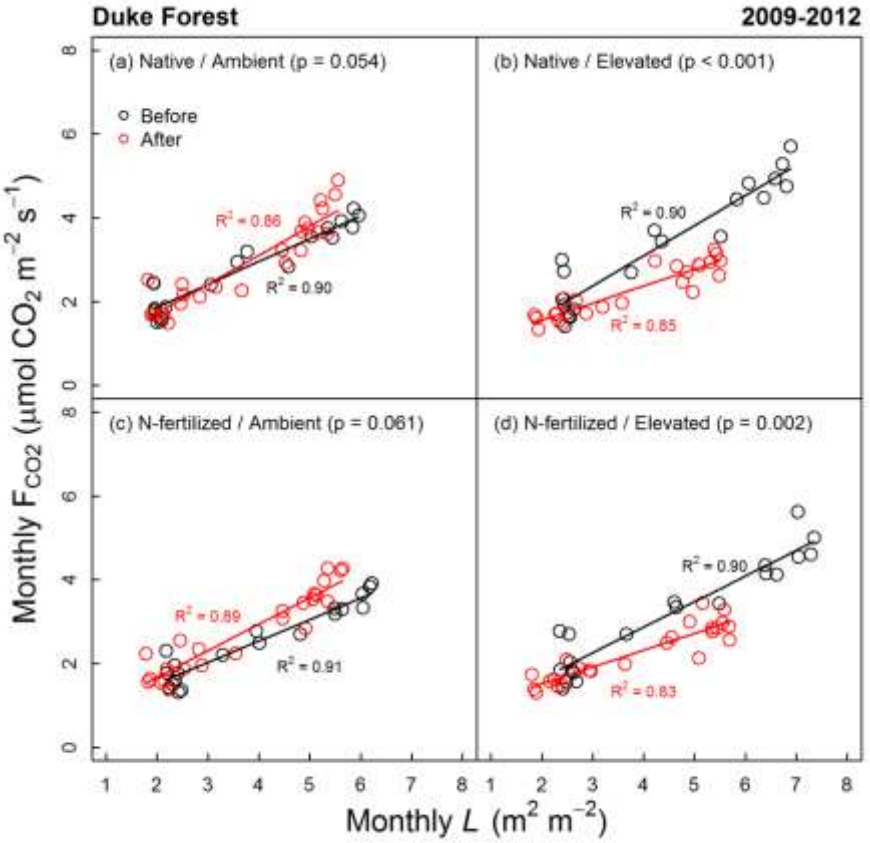

Figure 5.4. Response of monthly mean soil CO_2 efflux (F_{CO2}) to monthly mean leaf area index (L) under native soil (a, b) and N-fertilized (c, d) conditions. Solid lines represent significant relationships.

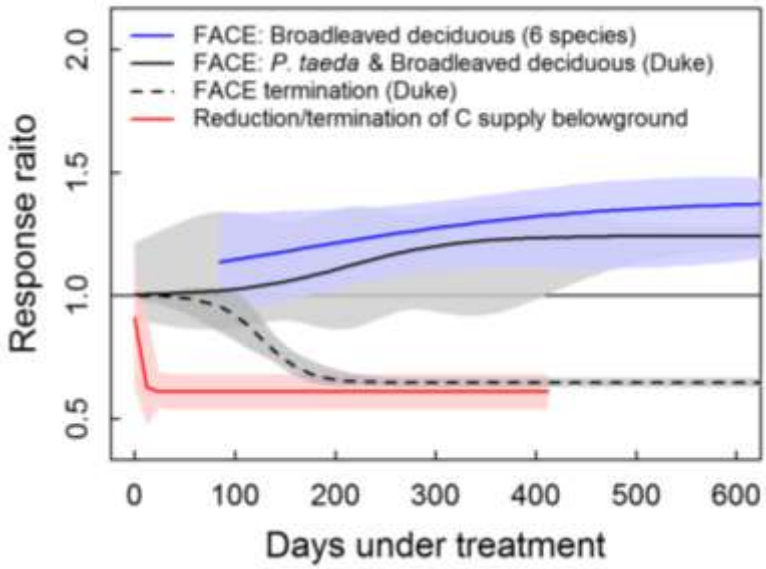

Figure 5.5. Temporal patterns of response ratios following the initial free-air CO_2 enrichment (FACE; black and blue solid lines), the termination of long-term FACE (dashed line) and the reduction of carbohydrate supply belowground (red solid line). Grey, blue and red area represent 95% confidence intervals. Data and sources are in Table B1 and B2.

Appendix A

Table A1. Response of understory vegetation to elevated CO_2 in previous studies at FACE sites

Site	Overstory	Functional group [a]	Response [b]	Sources
ORNL	*Liquidambar styraciflua*	Groundcover	Increase or no change in ANPP	Belote *et al.* (2004)
		Vine	Increase in ANPP	Belote *et al*. (2004)
		Seedling	no change in ANPP	Belote *et al*. (2004)
		Groundcover + Vine + Seedling	Increase or no change in ANPP	Belote *et al*. (2004); Sanders *et al.* (2004)
		Groundcover + Vine + Broadleaved	Increase in aboveground biomass	Souza *et al.* (2010)
Aspen	*Populus tremuloides*, *Betula papyrifera*	Groundcover	No change of biomass	Bandeff *et al.* (2006)
			Increase or no change in natural abundance	Awmack *et al.* (2007)
			Decrease in root and shoot biomass	Awmack *et al.* (2007)
Duke	*Pinus taeda*	Broadleaved	Increase in photosynthesis	DeLucia and Thomas (2000); Naumburg and Ellsworth (2000); Singsaas *et al.* (2000); Ellsworth *et al.* (2012)
		Broadleaved	Increase in photosynthesis	Springer and Thomas (2007)

	Broadleaved	Little change of growth rate	Mohan *et al.* (2007)
	Vine	Increase in photosynthesis and biomass	Mohan *et al.* (2006); Mohan *et al.* (2008); Schnitzer *et al.* (2008)

Table A2. Mean (and standard deviation) of understory aboveground biomass and density in four treatments (native soil / ambient CO_2; native soil / elevated CO_2; N-fertilized / ambient CO_2; N-fertilized / elevated CO_2) at Duke FACE site

	Native soil		N-fertilized	
	Ambient	Elevated	Ambient	Elevated
Aboveground biomass (g m^{-2})				
Total	1696.70	1509.85	1772.32	1240.83
	(418.12)	(592.82)	(664.63)	(395.82)
Groundcover	0.11	0.02	0.03	0.29
	(0.10)	(0.01)	(0.02)	(0.51)
Vine	102.44	83.20	95.69	121.48
	(150.14)	(47.55)	(87.09)	(146.86)
Lonicera japonica	4.42	0.09	0.60	0.30
	(3.11)	(0.09)	(0.78)	(0.21)
Parthenocissus quinquefolia	0.70	0.77	17.10	23.62
	(1.29)	(1.39)	(20.26)	(43.94)
Smilax rotundifolia	0.98	5.00	0.48	3.78
	(1.78)	(5.63)	(0.78)	(5.23)
Toxicodendron radicans	0.31×10^{-3}	0.02	0.02	10.81
	(0.63×10^{-3})	(0.02)	(0.02)	(21.61)
Vitis spp.	95.22	77.09	77.50	77.70
	(147.82)	(53.36)	(103.20)	(119.38)
All other vines	1.12	0.24	0.49×10^{-3}	5.28
	(2.23)	(0.30)	(0.98×10^{-3})	(10.08)
Broadleaved species	1594.15	1426.63	1676.60	1119.05
	(549.23)	(566.78)	(708.59)	(486.14)
Regenerating canopy species	948.49	748.75	1123.84	709.41
	(660.96)	(415.31)	(779.63)	(696.61)
Acer rubrum	91.93	66.97	351.52	73.93

	(96.34)	(41.04)	(402.68)	(141.20)
Fraxinus americana	50.25	203.60	80.22	141.55
	(43.84)	(218.82)	(158.93)	(259.74)
Liquidambar styraciflua	662.46	423.86	605.77	427.68
	(503.10)	(339.36)	(554.72)	(525.71)
Carya ovata	13.63	10.25	3.05	15.43
	(15.79)	(17.05)	(4.04)	(19.79)
Carya tomentosa	38.88	21.34	21.92	22.92
	(36.18)	(36.98)	(40.34)	(44.28)
All other regenerating canopy species	91.34 (100.87)	22.73 (29.71)	61.38 (110.12)	27.90 (51.65)
Subcanopy species	645.66	677.88	552.75	409.64
	(286.31)	(472.25)	(201.07)	(218.95)
Ulmus alata	113.38	224.51	309.88	262.06
	(26.17)	(234.70)	(155.98)	(263.89)
Carpinus caroliniana	19.00	69.22	13.47	44.82
	(38.01)	(138.44)	(26.93)	(89.64)
Cercis canadensis	208.13	37.16	150.89	55.99
	(226.85)	(74.31)	(113.63)	(111.98)
Diospyros virginiana	0.84×10^{-3}	0.38	1.48	1.65
	(1.68×10^{-3})	(0.76)	(2.96)	(3.29)
Prunus serotina	102.39	120.66	17.48	2.41
	(170.78)	(215.35)	(34.96)	(4.82)
All other subcanopy species	202.75	225.95	59.55	42.71
	(313.34)	(331.53)	(113.49)	(72.12)
Density (m^{-2})				
Total	1.32	1.05	0.74	0.58
	(0.74)	(0.08)	(0.15)	(0.25)
Groundcover	0.34	0.12	0.04	0.07
	(0.37)	(0.03)	(0.02)	(0.08)
Vine	0.19	0.28	0.16	0.22

	(0.14)	(0.13)	(0.11)	(0.19)
Seedling	0.002	0.004	0.034	0.002
	(0.005)	(0.005)	(0.055)	(0.005)
Advanced generation	0.19	0.28	0.12	0.21
	(0.14)	(0.13)	(0.12)	(0.19)
Lonicera japonica	0.05	0.03	0.03	0.01
	(0.03)	(0.04)	(0.04)	(0.01)
Parthenocissus quinquefolia	0.01	0.01	0.01	0.03
	(0.01)	(0.01)	(0.01)	(0.05)
Smilax rotundifolia	0.10	0.12	0.07	0.12
	(0.10)	(0.12)	(0.09)	(0.16)
Toxicodendron radicans	0.24×10^{-2}	0.05	0.02	0.01
	(0.48×10^{-2})	(0.06)	(0.03)	(0.02)
Vitis spp.	0.03	0.06	0.02	0.03
	(0.02)	(0.08)	(0.01)	(0.02)
All other vines	0.45×10^{-2}	1.12×10^{-2}	0.24×10^{-2}	1.00×10^{-2}
	(0.91×10^{-2})	(1.34×10^{-2})	(0.49×10^{-2})	(0.82×10^{-2})
Broadleaved species	0.80	0.58	0.44	0.36
	(0.40)	(0.15)	(0.28)	(0.21)
Seedling	1.45×10^{-2}	3.12×10^{-2}	0.19×10^{-2}	0.71×10^{-2}
	(1.16×10^{-2})	(2.69×10^{-2})	(0.39×10^{-2})	(0.86×10^{-2})
Advanced generation	0.78	0.55	0.44	0.35
	(0.39)	(0.15)	(0.28)	(0.21)
Regenerating canopy species	0.53	0.33	0.28	0.24
	(0.31)	(0.15)	(0.21)	(0.22)
Seedling	0.77×10^{-2}	0.21×10^{-2}	0.19×10^{-2}	0.28×10^{-2}
	(0.95×10^{-2})	(0.43×10^{-2})	(0.39×10^{-2})	(0.56×10^{-2})
Advanced generation	0.52	0.33	0.27	0.24
	(0.31)	(0.14)	(0.21)	(0.23)
Acer rubrum	0.04	0.05	0.06	0.02

	(0.02)	(0.01)	(0.04)	(0.02)
Fraxinus americana	0.03	0.06	0.01	0.03
	(0.03)	(0.02)	(0.01)	(0.03)
Liquidambar styraciflua	0.22	0.11	0.10	0.11
	(0.30)	(0.04)	(0.14)	(0.16)
Carya ovata	0.10	0.07	0.02	0.04
	(0.12)	(0.13)	(0.02)	(0.04)
Carya tomentosa	0.07	0.02	0.04	0.02
	(0.06)	(0.02)	(0.03)	(0.02)
All other regenerating canopy species	0.06 (0.02)	0.02 (0.02)	0.04 (0.03)	0.03 (0.03)
Subcanopy species	0.27	0.24	0.17	0.11
	(0.09)	(0.14)	(0.08)	(0.04)
Seedling	0.68×10^{-2}	2.24×10^{-2}	-	-
	(1.36×10^{-2})	(2.98×10^{-2})		
Advanced generation	0.26	0.22	0.17	0.11
	(0.08)	(0.12)	(0.08)	(0.04)
Ulmus alata	0.11	0.12	0.10	0.07
	(0.08)	(0.13)	(0.09)	(0.05)
Carpinus caroliniana	0.24×10^{-2}	2.75×10^{-2}	0.73×10^{-2}	1.06×10^{-2}
	(0.48×10^{-2})	(5.50×10^{-2})	(1.46×10^{-2})	(1.60×10^{-2})
Cercis canadensis	5.12×10^{-2}	0.81×10^{-2}	3.40×10^{-2}	0.28×10^{-2}
	(5.05×10^{-2})	(1.11×10^{-2})	(2.32×10^{-2})	(0.56×10^{-2})
Diospyros virginiana	0.23×10^{-2}	0.39×10^{-2}	0.24×10^{-2}	0.53×10^{-2}
	(0.45×10^{-2})	(0.79×10^{-2})	(0.49×10^{-2})	(0.62×10^{-2})
Prunus serotina	1.42×10^{-2}	0.84×10^{-2}	0.28×10^{-2}	0.29×10^{-2}
	(1.84×10^{-2})	(1.21×10^{-2})	(0.55×10^{-2})	(0.58×10^{-2})
All other subcanopy species	8.49×10^{-2}	7.61×10^{-2}	2.16×10^{-2}	1.89×10^{-2}
	(3.52×10^{-2})	(2.54×10^{-2})	(0.58×10^{-2})	(1.61×10^{-2})

Table A3. Shade tolerance of broadleaved species and shrubs in understory at Duke FACE site

Scientific name	Common name	Shade tolerance*
Acer rubrum	Red maple	tolerant
Carpinus caroliniana	American hornbeam	tolerant
Carya glabra	Pignut hickory	intolerant
Carya ovata	Shagbark hickory	intolerant
Carya tomentosa	Mockernut hickory	intolerant
Cercis canadensis	Eastern redbud	tolerant
*Celtis tenuifolia***	Dwarf hackberry	tolerant
Chionanthus virginicus	White fringetree	tolerant
Cornus florida	Flowering dogwood	tolerant
Diospyros virginiana	Common persimmon	tolerant
Elaeagnus umbellata	Autumn olive	tolerant
Fraxinus americana	white ash	intolerant
Ilex decidua	Meadow holly	tolerant
Ilex opaca	American holly	tolerant
Juniperus virginiana	Eastern redcedar	intolerant
Ligustrum sinense	Chinese privet	tolerant
Liquidambar styraciflua	Sweetgum	intolerant
Liriodendron tulipifera	Yellow-poplar	intolerant
*Morus rubra***	Red mulberry	tolerant

Nyssa sylvatica	Black tupelo	tolerant
Prunus serotina	Black cherry	intolerant
Quercus alba	white oak	intolerant
Quercus falcata	Southern red oak	intolerant
Quercus phellos	Willow oak	intolerant
Quercus velutina	Black oak	intolerant
Ulmus alata	Winged elm	tolerant
Ulmus rubra	Slippery elm	tolerant
Vaccinium spp.		tolerant
Viburnum prunifolium	Blackhaw	tolerant
Viburnum rafinesquianum	Downy arrowwood	tolerant

[*] sources: Burns (1990); Farrar (1995); Harlow *et al.* (1996)

[**] A recent literature (Nowacki & Abrams, 2015) classified them as shade intermediate, but those species were classified as shade tolerant in this study.

Table A4. Results of ANOVA and ANCOVA of aboveground biomass and density by CO_2 enrichment, nitrogen (N) fertilization nested within CO_2 and five-year (2005-2009) average growing season diffuse radiation (diffuse non-interceptance; DIFN)

Model	Response variable		p-values			
			CO_2	CO_2 × N	DIFN [a]	CO_2 × DIFN
ANOVA (N nested within CO_2)						
	Ground cover	Biomass	0.507	0.350	-	-
		Density [b]	0.375	0.252	-	-
	Vine	Biomass	0.956	0.895	-	-
		Density	0.335	0.774	-	-
	Broadleaved regeneration	Biomass	0.238	0.748	-	-
		Density	0.290	0.143	-	-
ANCOVA with DIFN as covariate						
	Total understory [c]	Biomass	0.112	0.991	0.017 [d]	-
		Density	0.333	0.187	0.265	-
ANCOVA with DIFN and DIFN × CO_2 as covariate						
	Total understory	Biomass	0.128	0.992	0.022 [d]	0.659
		Density	0.278	0.134	0.213	0.106

[a] Centered diffuse non-interceptance (DIFN) were used.

[b] Individuals per unit ground area (m^{-2})

[c] Log of aboveground biomass ($g\ m^{-2}$) were used for ANCOVA.

[d] $p < 0.05$

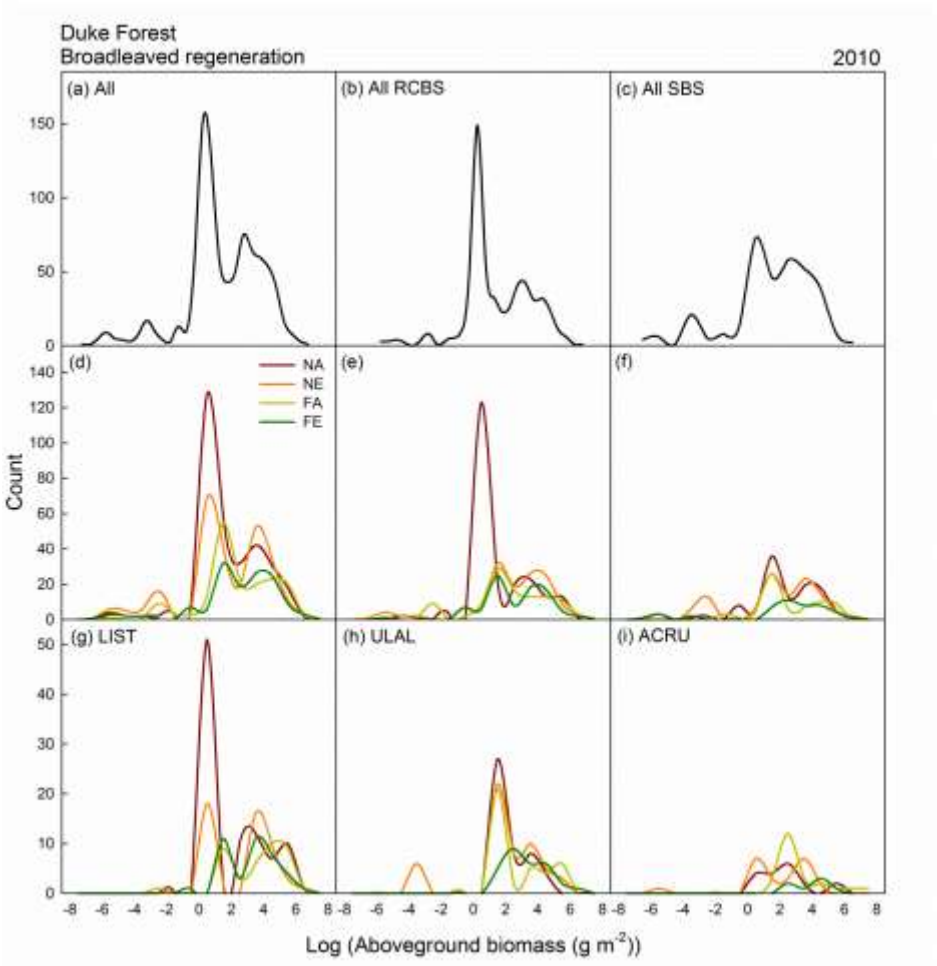

Figure A1. Distribution of aboveground biomass (log transformed) across (a) all broadleaved regeneration, (b) all regenerating canopy broadleaved species (RCBS), (c) all subcanopy broadleaved species (SBS) and those by treatment (d-f; NA: native soil / ambient CO_2; NE: native soil / elevated CO_2; FA: N-fertilized / ambient CO_2; FE: N-fertilized / elevated CO_2). (g-i) shows log transformed aboveground biomass of *Liquidambar styraciflua* (LIST), *Ulmus alata* (ULAL) and *Acer rubrum* (ACRU) across all treatments.

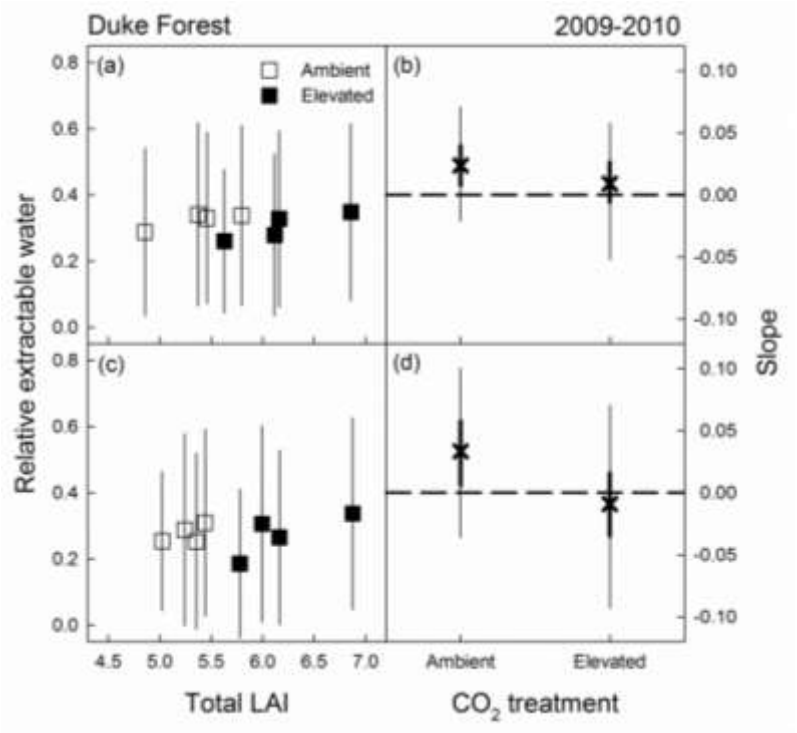

Figure A2. Relationship between relative extractable water in the root zone and total leaf area index (LAI) in 2009 (a, b) and 2010 (c, d). In (b) and (d), means, 50% (thick lines) and 95% (thin lines) posterior credible intervals of slopes are presented. The horizontal dashed lines are the zero lines.

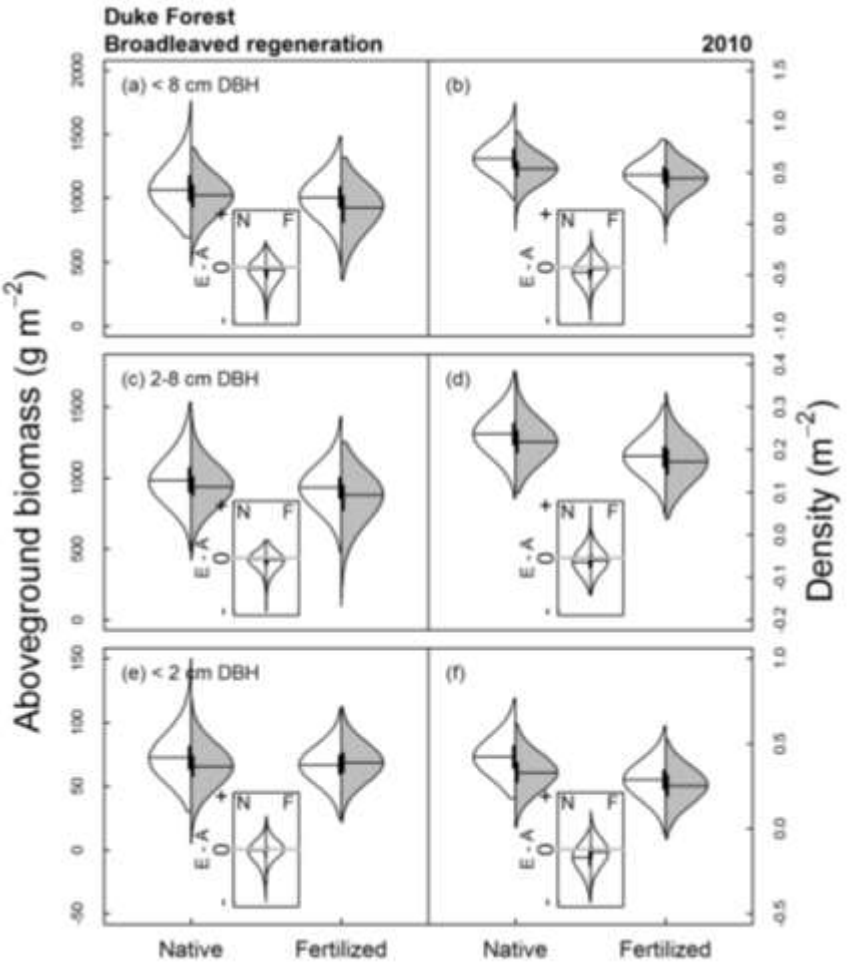

Figure A3. Aboveground biomass and density of broadleaved regeneration with diameter at breast height (DBH) < 8 cm (a, b), DBH 2-8 cm (c, d) and DBH < 2 cm (e, f) in ambient (white, left) and elevated CO_2 (grey, right) under native soil and N-fertilized conditions. Means (horizontal solid lines) and 50% posterior credible intervals (boxes) are presented. Inset figures are posterior distributions of differences (elevated - ambient). The horizontal grey lines in the inset figures are the zero difference lines.

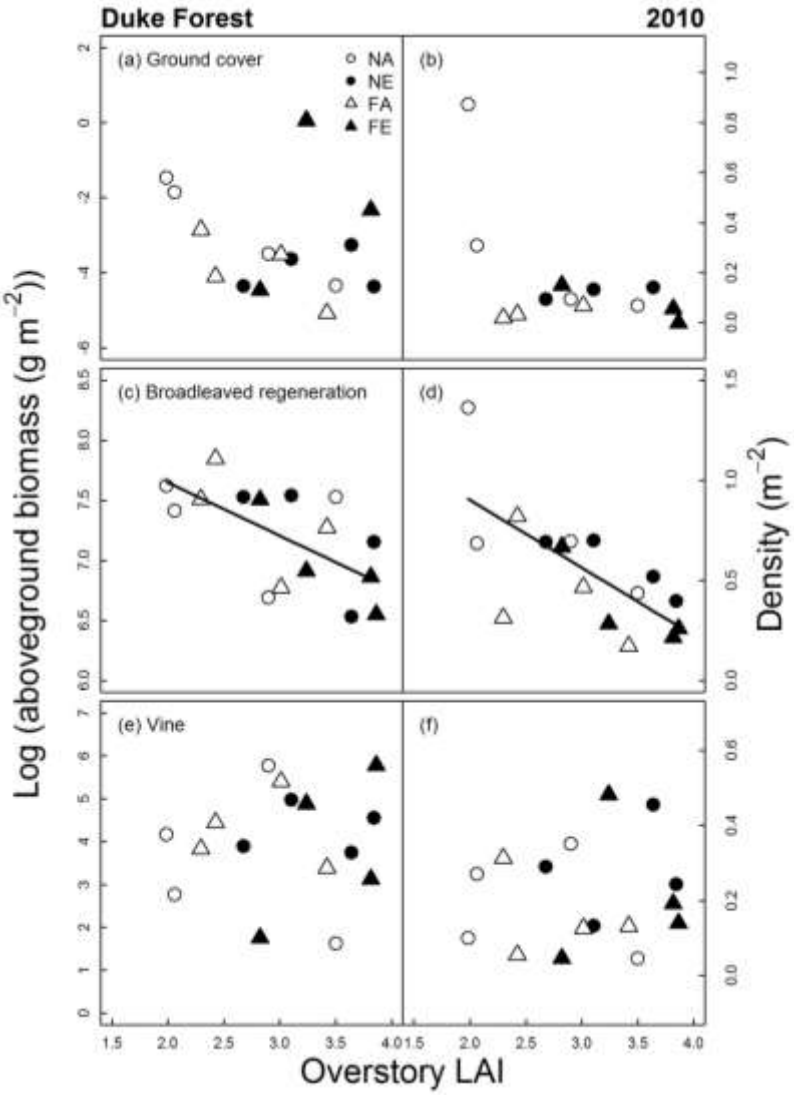

Figure A4. Responses of aboveground biomass (log transformed) and density of ground cover plants (a, b), broadleaved regeneration (c, d) and vine (e, f) in ambient (open symbols) and elevated (closed symbols) CO_2 under native soil (circles) and N-fertilized (triangles) conditions to 5-year average growing season canopy leaf area index (LAI). Solid lines show significant relationships.

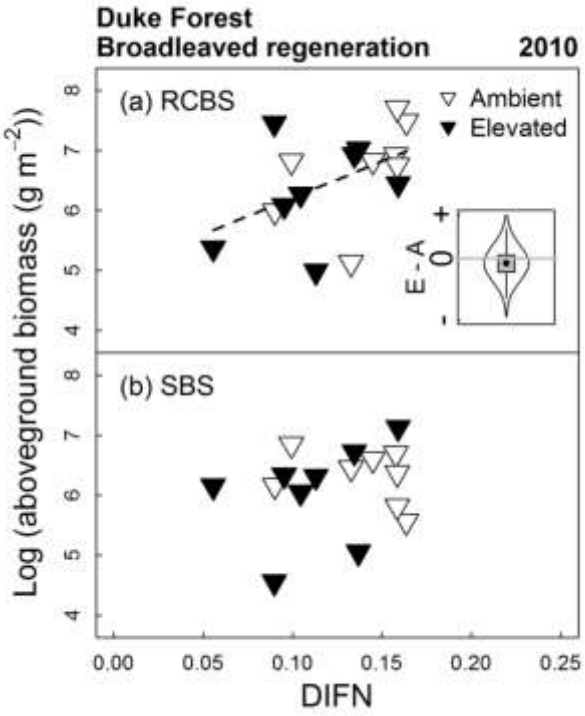

Figure A5. Responses of aboveground biomass (log transformed) of regenerating canopy broadleaved species (RCBS; a) and subcanopy broadleaved species (SBS; b) in ambient (open symbols) and elevated (closed symbols) CO_2 to diffuse radiation (diffuse non-interceptance; DIFN). Dashed lines represent close to significant relationships. Inset figure in (a) shows posterior distribution of mean difference (elevated - ambient) of slope; a box is 50% posterior credible interval and grey horizontal dashed line is the zero line.

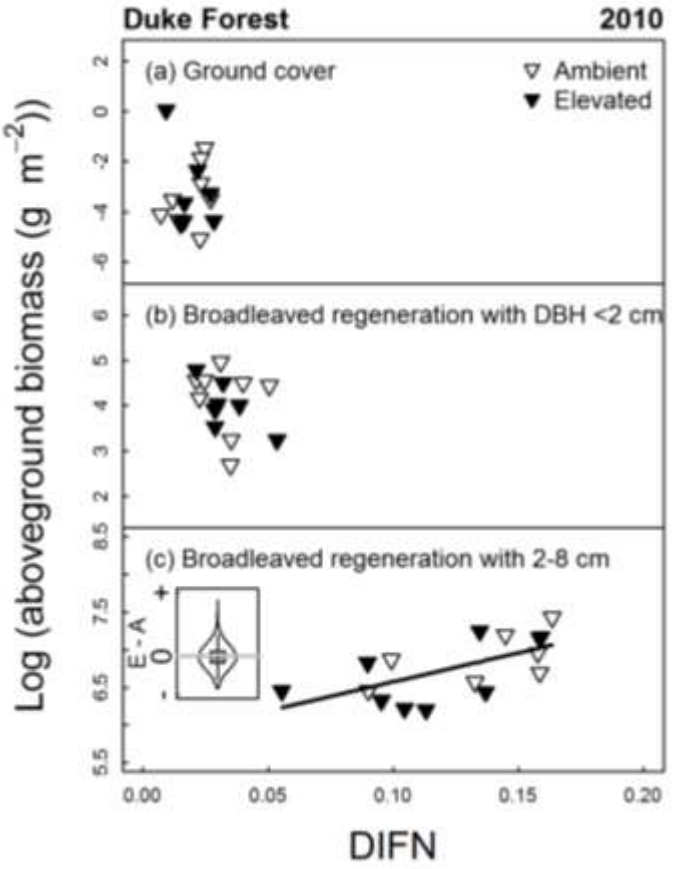

Figure A6. Responses of aboveground biomass (log transformed) of ground cover plants (a), broadleaved regeneration with diameter at breast height (DBH) <2 cm (b) and broadleaved regeneration with DBH 2-8 cm (c) in ambient (open symbols) and elevated (closed symbols) CO_2 to diffuse radiation (diffuse non-interceptance; DIFN). Solid line represents a significant relationship. Inset figure in (c) shows posterior distribution of mean difference (elevated - ambient) of slope; a box is 50% posterior credible interval and grey horizontal dashed line is the zero line.

Appendix B

Table B1. Effect of free-air CO_2 enrichment (FACE) on soil respiration (R_S) and major contributors to R_S

Component	Site [a]	Stand age at initial exposure [b]	Stand age studied	Percent response to elevated CO_2 (%)			Source
				Rate	Annual integrated	Pattern	
R_S	Duke FACE	16	15-17	26-59 (summer), 8-15 (winter) [c]			Andrews & Schlesinger (2001)
			17	24	11 (marginal)		Andrews & Schlesinger (2001)
			18	43	27		Andrews & Schlesinger (2001)
			17-18	marginal			Allen *et al*. (2000)
			17-21	16	10-39		King *et al*. (2004)
			17-23		10-19	Decreasing	Bernhardt *et al*. (2006)
			17-28	23		Increasing	Jackson *et al*. (2009)
			21-30		17		Oishi *et al*. (2014)
	ORNL FACE	11	10-14	12	11-17		King *et al*. (2004)
	Aspen FACE	2	2-5	24-54	3-60		King *et al*. (2004)
	POPFACE	1	2-3	32-45	34-50		King *et al*. (2004)
NPP	Duke FACE	16	18		26		DeLucia *et al*. (1999)

	ORNL FACE	11	11-13	16-25	Norby *et al*. (2002)
Leaf litterfall	Duke FACE	16	16-17	0	Allen *et al*. (2000)
			18	15	Allen *et al*. (2000)
	ORNL FACE	11	11-13	11	Norby *et al*. (2002)
Fine root biomass	Duke FACE	16	17-28	24	Jackson *et al*. (2009)
	ORNL FACE	11	11-13	56	Norby *et al*. (2002)
	Aspen FACE	2	2-3	83-113	King *et al*. (2001)
	POPFACE	1	1-3	35-84	Lukac *et al*. (2003)
Fine root turnover	Duke FACE	16	17-18	26 (not significant)	Allen *et al*. (2000)
	POPFACE	1	1-3	27-55	Lukac *et al*. (2003)
Coarse root biomass	Duke FACE	16	17-28	17	Jackson *et al*. (2009)
	ORNL FACE	11	11-13	12	Norby *et al*. (2002)
	Aspen FACE	2	2-3	72	King *et al*. (2001)
Microbial C	Duke FACE	16	17-18	0	Allen *et al*. (2000)

[a] Dominant species are *Pinus taeda* at the Duke FACE site, *Liquidambar styraciflua* at the ORNL site, *Populus tremuloides*, *Acer saccharum* and *Betula papyrifera* at the Aspen FACE site, and *P. alba*, *P. nigra* and *P.* × *euramericana* at the PopFACE site.

[b] Prototype experiment or pre-treatment tests were conducted when stand age was 14 at the Duke FACE site, 10 at the ORNL FACE site, and 1 at the Aspen FACE site.

[c] Values are from prototype experiment, and adjusted to remove the effect of 0.1-8.1% differences in surface soil (3 cm depth) temperature.

Table B2. Effects of manipulations of carbon transport to soil on soil respiration (R_S) and major contributors to R_S

Manipulation	Site description (species)	Study period	Responses (Time after manipulation)		Source
			Contributor to R_S	R_S	
Trenching	Temperate forest, Kamloops, Canada (*Betula papyrifera*, *Pseudotsuga menziesii*)	Growing season	-50% EM fungi richness and diversity (16 mo) [b]		Simard *et al*. (1997)
	Temperate forest, Achenkirch, Austria	Growing season	-9% fine root biomass (5 mo) -30% fine root biomass (15 mo)	-20% (0-5 mo) -30% (11-16 mo)	Díaz-Pinés *et al*. (2010)
	Boreal forest, Brevens bruk, Sweden (*Picea abies*)	Jun.-Oct.		-33% (13 d)	Comstedt *et al*. (2011)
	Temperate forest, Durham, USA (*Pinus taeda*)	Growing season	-28% fine root biomass (7 mo) [a] -15% microbial respiration (7 mo)	-46% (7 mo)	Drake *et al*. (2012)
Girdling	Boreal forest, Åheden, Sweden (*Pinus sylvestris* L.)	Jun.	-99% EM fungi sporocarp biomass (72 d) -66% fine root starch (28 d) -78% fine root starch (68 d) -88% fine root starch (130 d)	-27% (5 d) -52% (8 wk) -30 to -60% (1 yr)	Högberg *et al*. (2001); Bhupinderpal-Singh *et al*. (2003)
		Aug.	-52% EM fungi sporocarp biomass (2-3 d) -71% fine root starch (59 d)	-37% (5 d.) -56% (2 wk.) -40 to -70% (1 yr)	

	Boreal forest, Flakaliden, Sweden (*Picea abies*)	Jun. – Oct.	-66% fine root starch (40 d) -94% coarse root starch (40 d)	-60% (2.5 mo)	Olsson *et al*. (2005)
	Temperate forest, Pura, Switzerland (*Castanea sativa* Mill.)	Aug. – Oct.	-90% fine root starch (37 d) No difference in fine root biomass No difference in organic C content	-36% (9 d) -13% (37d)	Frey *et al*. (2006)
	Temperate forest, Durham, USA (*P. taeda*)	Spring		No response	Johnsen *et al*. (2007)
		Autumn		-7 to -26% (6 d)	
	Temperate forest, York, England (*Tsuga heterophylla*)	Sep.		-35% (2 wk)	Subke *et al*. (2011)
		Winter		-25% (4 mo)	
	Temperate forest, Ghent, Belgium (*Quercus robur*)	Aug. – Sep.	- 21% xylem CO_2 concentration (5 d) -39% fine root starch (40 d)	-22% (5 d) -35% (25 d)	Bloemen *et al*. (2014)
	Boreal forest, Åheden, Sweden (*P. sylvestris* L.)	Jul. – Sep.	-65% phloem C (7 d)	-50% (18 d)	Henriksson *et al*. (2015)
	Temperate forest, China	Jun. – Sep.	-82% fine root biomass (3 mo) -83% fine root soluble sugar (3 mo) -74% fine root starch (3 mo)	-33% (4 d) -40% (3 mo)	Jing *et al*. (2015)
Stem	Boreal forest, Åheden, Sweden	Growing season	-65% phloem C (7 d) [c]	-20% (3 d) [d]	Henriksson *et al*.

compression	(*P. sylvestris*)			-34 to -40% (3-27 d)	(2015)
Shading	Boreal forest, Åheden, Sweden (*P. sylvestris*)	Jul. – Sep.	-60% photosynthetic C gain (4 wk) -25% EM fungi biomass (4 wk) -40% EM fungi sporocarp (4 wk)	-30% (4 wk)	Hasselquist *et al*. (2016)
Chilling	Temperate forest, Durham, USA (*P. taeda*)	spring		No response	Johnsen *et al*. (2007)
		autumn	-39% soil soluble C (0-15 d)	-9% (3 d)	Johnsen *et al*. (2007)

[a] Live fine root biomass decreased by 57% while dead fine root biomass increased by 110%.

[b] EM: Ectomycorrhizal

[c] Phloem C content returned to normal by 19 days after the release of stem compression.

[d] R_S returned to normal within 1 day after the release of stem compression.

Table B3. Annual mean (and standard deviation) of soil CO_2 efflux (g C m^{-2} y^{-1}) in ambient and elevated CO_2 under native and N-fertilized conditions

Year	Native			N-Fertilized		
	Ambient	Elevated	p-value	Ambient	Elevated	p-value
2009	999.28 (24.37)	1205.10 (67.82)	<**0.0001**	856.25 (47.73)	1095.66 (128.87)	<**0.0001**
2010	1002.76 (44.65)	1193.18 (49.41)	<**0.0001**	817.35 (31.76)	1023.09 (40.39)	<**0.0001**
2011	1029.10 (18.95)	847.45 (10.20)	<**0.0001**	873.26 (53.07)	822.80 (11.74)	<**0.0001**
2012	1137.35 (61.70)	820.44 (12.86)	<**0.0001**	968.02 (54.51)	806.71 (10.52)	<**0.0001**

Table B4. Annual mean (and standard deviation) of air temperature, soil temperature and growing season relative extractable water (REW)

Year	Air temperature (°C)	Soil temperature (°C)	Growing season REW
2009	14.5 (8.4)	14.2 (5.1)	0.44 (0.34)
2010	14.9 (9.8)	14.1 (6.3)	0.32 (0.27)
2011	15.7 (8.5)	15.2 (6.7)	0.45 (0.33)
2012	15.7 (7.6)	15.7 (5.7)	0.58 (0.34)

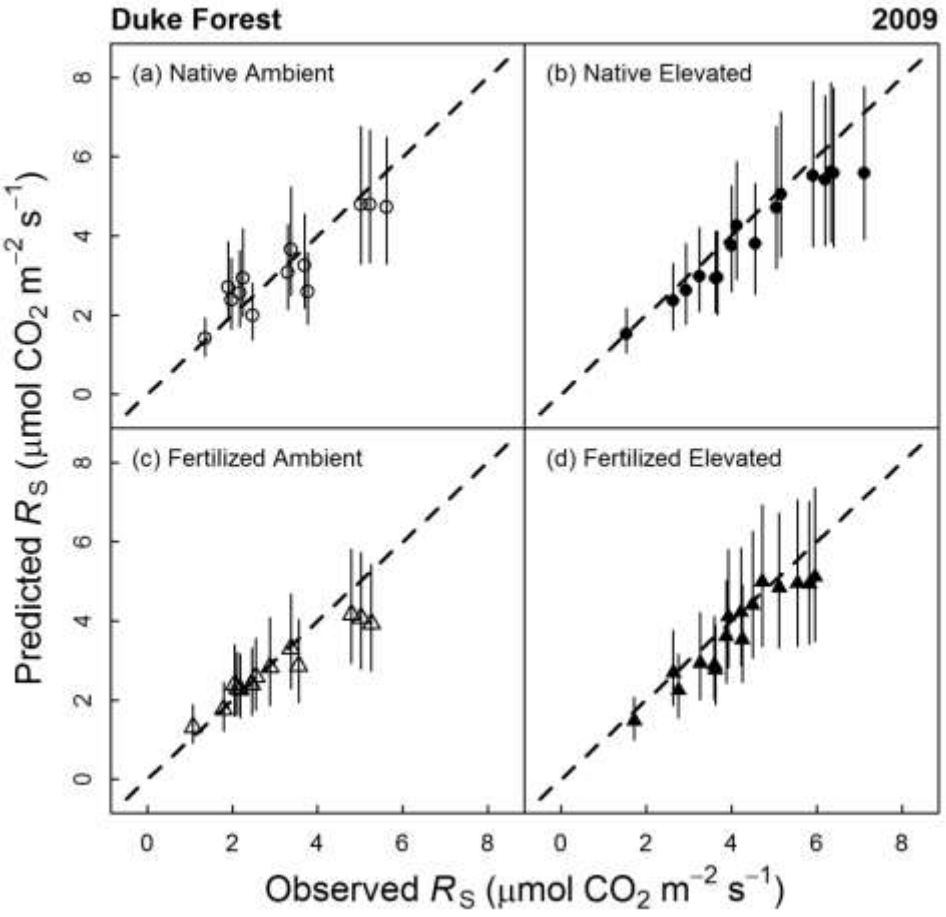

Figure B1. Comparison of observed and predicted soil respiration (R_S) in 2009 under (a) ambient CO_2 native soil, (b) elevated CO_2 native soil, (c) ambient CO_2 N-fertilized, and (d) elevated CO_2 N-fertilized conditions. Observed values were aggregated with soil temperature (0-25 °C with 5°C intervals) and soil moisture ranges (relative extractable water, REW 0-1 with 0.2 intervals). Dashed lines are 1:1 lines. Vertical lines represent 95% confidence intervals.

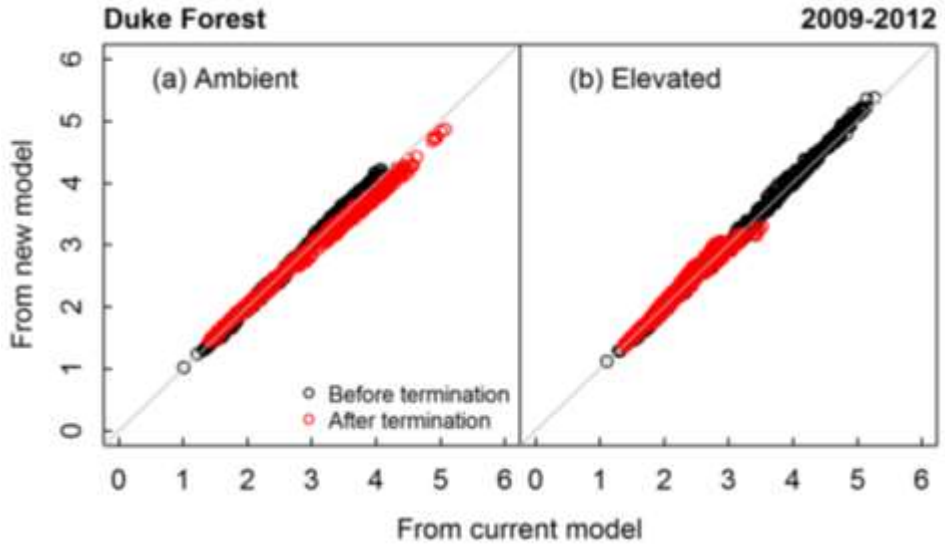

Figure B2. Comparison of outcomes from models parameterizing data after the termination of CO_2 enrichment as two separate years (current) and a combined period (new) in (a) ambient and (b) elevated CO_2.

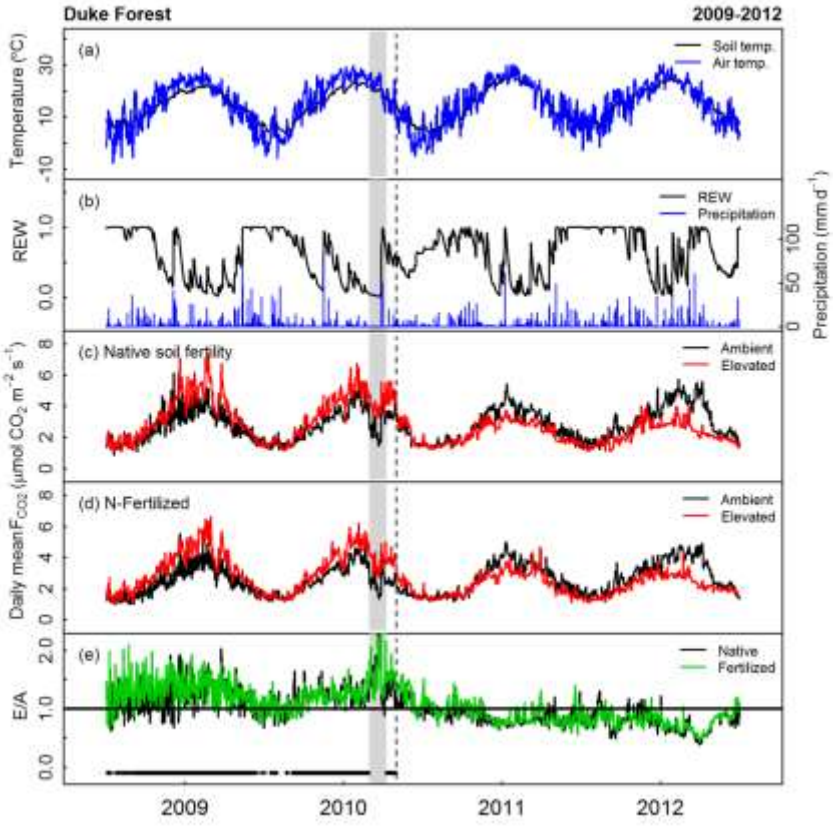

Figure B3. (a) Mean air and soil temperature, (b) relative extractable water (REW) and precipitation, (c) daily mean soil CO_2 efflux (F_{CO2}) in ambient (black lines) and elevated CO_2 (red lines) under native soil fertility, (d) daily mean F_{CO2} under N-fertilized condition, and (e) ratio of F_{CO2} in elevated over ambient CO_2. Vertical dashed line shows when CO_2 enrichment was terminated. Grey area represents short-term CO_2 response study period. Horizontal solid line is 1:1 line. Dots on the bottom of (e) indicate dates with CO_2 enrichment (ambient + 200 ppm).

References

Ainsworth E.A. & Long S.P. (2005). What have we learned from 15 years of free-air CO_2 enrichment (FACE)? A meta-analytic review of the responses of photosynthesis, canopy. New Phytologist, **165**, 351-371.

Ainsworth E.A. & Rogers A. (2007). The response of photosynthesis and stomatal conductance to rising [CO_2]: mechanisms and environmental interactions. Plant Cell and Environment, **30**, 258-270.

Allen A.S., Andrews J.A., Finzi A.C., Matamala R., Richter D.D. & Schlesinger W.H. (2000). Effects of free-air CO_2 enrichment (FACE) on belowground processes in a Pinus taeda forest. *Ecol Appl*, 10, 437-448.

Allen R.G. (2005). Penman-Monteith Equation. In: D. Hillel (Editor), Encyclopedia of Soils in the Environment. Elsevier, pp. 180-188.

Andrews J.A., Harrison K.G., Matamala R. & Schlesinger W.H. (1999). Separation of root respiration from total soil respiration using carbon-13 labeling during Free-Air Carbon Dioxide Enrichment (FACE). *Soil Sci Soc Am J*, 63, 1429-1435.

Andrews J.A. & Schlesinger W.H. (2001). Soil CO2 dynamics, acidification, and chemical weathering in a temperate forest with experimental CO_2 enrichment. *Global Biogeochem Cy*, 15, 149-162.

Aphalo P.J. & Jarvis P.G. (1993). The boundary layer and the apparent responses of stomatal conductance to wind speed and to the mole fractions of CO_2 and water vapor in the air. Plant Cell Environ., 16(7): 771-783.

Asshoff R., Zotz G. & Korner C. (2006). Growth and phenology of mature temperate forest trees in elevated CO_2. Global Change Biology, **12**, 848-861.

Awmack C.S., Mondor E.B. & Lindroth R.L. (2007). Forest understory clover populations in enriched CO_2 and O_3 atmospheres: Interspecific, intraspecific, and indirect effects. Environmental and Experimental Botany, **59**, 340-346.

Avissar R. & Werth D. (2005). Global hydroclimatological teleconnections resulting from tropical deforestation. J. Hydrometeorol., 6(2): 134-145.

Bader M.K.F. & Korner C. (2010). No overall stimulation of soil respiration under mature deciduous forest trees after 7 years of CO_2 enrichment. Global Change Biology, 16(10): 2830-2843.

Bandeff J.M., Pregitzer K.S., Loya W.M., Holmes W.E. & Zak D.R. (2006). Overstory community composition and elevated atmospheric CO_2 and O_3 modify understory biomass production and nitrogen acquisition. Plant and Soil, **282**, 251-259.

Bauerle W.L. & Bowden J.D. (2011). Predicting transpiration response to climate change: insights on physiological and morphological interactions that modulate water exchange from leaves to canopies. Hortscience, 46(2): 163-166.

Bell D.M. (2011). Longterm approaches to assessing tree community responses to resource limitation and climate variation. Doctoral Dissertation, University Program in Ecology, Duke University, Durham, NC, USA

Belote R.T., Weltzin J.F., Norby R.J. (2004). Response of an understory plant community to elevated [CO2] depends on differential responses of dominant invasive species and is mediated by soil water availability. New Phytologist, **161**, 827-835.

Bernhardt E.S., Barber J.J., Pippen J.S., Taneva L., Andrews J.A. & Schlesinger W.H. (2006). Long-term effects of free air CO2 enrichment (FACE) on soil respiration. *Biogeochemistry*, 77, 91-116.

Bindi M., Fibbi L., Miglietta F. (2001). Free Air CO2 Enrichment (FACE) of grapevine (Vitis vinifera L.): II. Growth and quality of grape and wine in response to elevated CO2 concentrations. European Journal of Agronomy, **14**, 145-155.

Bladon K.D., Silins U., Landhausser S.M. and Lieffers V.J. (2006). Differential transpiration by three boreal tree species in response to increased evaporative demand after variable retention harvesting. Agric. For. Meteorol., 138(1-4): 104-119.

Blanken P.D. & Black T.A. (2004). The canopy conductance of a boreal aspen forest, Prince Albert National Park, Canada. Hydrol. Processes, 18(9): 1561-1578.

Bond-Lamberty B. & Thomson A. (2010). Temperature-associated increases in the global soil respiration record. *Nature*, 464, 579-U132.

Butnor J.R., Johnsen K.H., Oren R. & Katul G.G. (2003). Reduction of forest floor respiration by fertilization on both carbon dioxide-enriched and reference 17-year-old loblolly pine stands. *Global Change Biology*, 9, 849-861.

Caldwell M.M. (1970). Plant gas exchange at high wind speeds. Plant Physiol., 46(4): 535-537.

Campbell-Clause J.M. (1998). Stomatal response of grapevines to wind. Aust. J. Exp. Agric., 38(1): 77-82.

Campbell G.S. & Norman J.M. (1998). An introduction to environmental biophysics. Springer, New York.

Chapin F.S. III (2002). Principles of terrestrial ecosystem ecology. Springer, New York.

Chu C.R., Hsieh C.I., Wu S.Y. & Phillips N.G. (2009). Transient response of sap flow to wind speed. J. Exp. Bot., 60(1): 249-255.

Clark J.S., Agarwal P., Bell D.M., Flikkema P.G., Gelfand A., Nguyen X.L., Ward E. & Yang J. (2011). Inferential ecosystem models, from network data to prediction. *Ecol Appl*, 21, 1523-1536.

Clausnitzer, F., Kostner, B., Schwarzel, K. & Bernhofer, C., (2011). Relationships between canopy transpiration, atmospheric conditions and soil water availability-Analyses of long-term sap-flow measurements in an old Norway spruce forest at the Ore Mountains/Germany. Agric. For. Meteorol., 151(8): 1023-1034.

Curtis P.S. & Wang X.Z. (1998) A meta-analysis of elevated CO2 effects on woody plant mass, form, and physiology. Oecologia, **113**, 299-313.

da Silva R.R., Bohrer G., Werth D., Otte M.J. & Avissar R. (2006). Sensitivity of ice storms in the southeastern United States to Atlantic SST - Insights from a case study of the December 2002 storm. Mon Weather Rev, 134, 1454-1464.

Daudet F.A., Le Roux X., Sinoquet H. and Adam B., (1999). Wind speed and leaf boundary layer conductance variation within tree crown - Consequences on leaf-to-atmosphere coupling and tree functions. Agric. For. Meteorol., 97(3): 171-185.

Dawes M.A., Hagedorn F., Handa I.T., Streit K., Ekblad A., Rixen C., Körner C. & Hättenschwiler S. (2013). An alpine treeline in a carbon dioxide-rich world:

synthesis of a nine-year free-air carbon dioxide enrichment study. Oecologia, **171**, 623-637.

DeLucia E.H., Hamilton J.G., Naidu S.L., Thomas R.B., Andrews J.A., Finzi A.C., Lavine M., Matamala R., Mohan J.E., Hendrey G.R. & Schlesinger W.H. (1999). Net primary production of a forest ecosystem with experimental CO2 enrichment. *Science*, 284, 1177-1179.

DeLucia E.H. & Thomas R.B. (2000). Photosynthetic responses to CO2 enrichment of four hardwood species in a forest understory. Oecologia, **122**, 11-19.

Dietze M.C. (2014). Gaps in knowledge and data driving uncertainty in models of photosynthesis. Photosynthesis Research, **119**, 3-14.

Dixon, M. & Grace, J. (1984). Effect of wind on the transpiration of young trees. Ann. Bot., 53(6): 811-819.

Domec, J.C., Palmroth S., Ward E., Maier C.A., Thérézien M. & Oren R. (2009). Acclimation of leaf hydraulic conductance and stomatal conductance of *Pinus taeda* (loblolly pine) to long-term growth in elevated CO_2 (free-air CO_2 enrichment) and N-fertilization. Plant Cell and Environment, 32(11): 1500-1512.

Domec J.C., Schäfer K., Oren R., Kim H.S., Mccarthy H.R. (2010). Variable conductivity and embolism in roots and branches of four contrasting tree species and their impacts on whole-plant hydraulic performance under future atmospheric CO_2 concentration. Tree Physiology, **30**, 1001-1015.

Drake J.E., Oishi A.C., Giasson M.A., Oren R., Johnsen K.H. & Finzi A.C. (2012). Trenching reduces soil heterotrophic activity in a loblolly pine (Pinus taeda) forest exposed to elevated atmospheric [CO_2] and N fertilization. *Agr Forest Meteorol*, 165, 43-52.

Drake J.E., Stoy P.C., Jackson R.B. & DeLucia E.H. (2008). Fine-root respiration in a loblolly pine (Pinus taeda L.) forest exposed to elevated CO(2) and N fertilization. *Plant Cell Environ*, 31, 1663-1672.

Efron B. (1978). Controversies in Foundations of Statistics. American Mathematical Monthly, **85**, 231-246.

Ellsworth, D.S., Oren, R., Huang, C., Phillips, N. and Hendrey, G.R. (1995). Leaf and Canopy Responses to Elevated Co2 in a Pine Forest under Free-Air CO_2 Enrichment. Oecologia, 104(2): 139-146.

Ellsworth, D.S. (1999). CO2 enrichment in a maturing pine forest: are CO_2 exchange and water status in the canopy affected? Plant Cell and Environment, 22(5): 461-472.

Ellsworth D.S., Thomas R., Crous K.Y., Palmroth S., Ward E., Maier C., DeLucia E. & Oren R. (2012). Elevated CO_2 affects photosynthetic responses in canopy pine and subcanopy deciduous trees over 10 years: a synthesis from Duke FACE. Global Change Biology, **18**, 223-242.

Etheridge D.M., Barnola J.M. & Morgan V.I. (1996). Natural and anthropogenic changes in atmospheric CO2 over the last 1000 years from air in Antarctic ice and firn. Journal of Geophysical Research-Atmospheres, 101(D2): 4115-4128.

Ewers B.E. & Oren R. (2000). Analyses of assumptions and errors in the calculation of stomatal conductance from sap flux measurements. Tree Physiology, 20, 579-589.

FAO (2012). *Global forest land-use change, 1990-2005,* Rome, Food and Agriculture Organization of the United Nations.

Finzi A.C., DeLucia E.H., Hamilton J.G., Richter D.D., Schlesinger W.H. (2002). The nitrogen budget of a pine forest under free air CO2 enrichment. Oecologia, **132**, 567-578.

Finzi A.C., Abramoff R.Z., Spiller K.S., Brzostek E.R., Darby B.A., Kramer M.A. & Phillips R.P. (2015). Rhizosphere processes are quantitatively important components of terrestrial carbon and nutrient cycles. *Global Change Biology*, 21, 2082-2094.

Gelman A. & Hill J. (2007). *Data analysis using regression and multilevel/hierarchical models*, New York, Cambridge University Press.

Gelman A., Hill J., Yajima M. (2012). Why We (Usually) Don't Have to Worry About Multiple Comparisons. Journal of Research on Educational Effectiveness, **5**, 189-211.

Gelman A. & Tuerlinckx F.A. (2000). Type S error rates for classical and Bayesian single and multiple comparison procedures. Computational Statistics, **15**, 373-390.

Gini C. (1912). *Variabilità e mutabilità: contributo allo studio delle distribuzioni e delle relazioni statistiche. [*Tipogr. di P. Cuppini.

Grace J., Malcolm D.C. & Bradbury I.K. (1975). Effect of wind and humidity on leaf diffusive resistance in Sitka spruce seedlings. J. Appl. Ecol., 12(3): 931-940.

Grace J. & Russel G. (1982). The effect of wind and a reduced supply of water on the growth and water relations of Festuca-Arundinacea Schreb. Ann. Bot., 49(2): 217-225.

Granier A. (1987). Sap flow measurements in Douglas-fir tree trunks by means of a new thermal method. Ann. Sci. For., 44(1): 1-14.

Granier A. & Bréda N. (1996). Modelling canopy conductance and stand transpiration of an oak forest from sap flow measurements. Ann. Sci. For., 53(2-3): 537-546.

Granier A., Loustau D. & Bréda N. (2000). A generic model of forest canopy conductance dependent on climate, soil water availability and leaf area index. Ann. For. Sci., 57(8): 755-765.

Gregory J.M., Jones C.D., Cadule P. & Friedlingstein P. (2009). Quantifying Carbon Cycle Feedbacks. Journal of Climate, **22**, 5232-5250.

Gunderson C.A., Sholtis J.D., Wullschleger S.D., Tissue D.T., Hanson P.J. & Norby R.J. (2002). Environmental and stomatal control of photosynthetic enhancement in the canopy of a sweetgum (*Liquidambar styraciflua* L.) plantation during 3 years of CO2 enrichment. Plant Cell and Environment, 25(3): 379-393.

Gutiérrez M.V., Meinzer F.C. and Grantz D.A. (1994). Regulation of transpiration in coffee hedgerows - covariation of environmental variables and apparent responses of stomata to wind and humidity. Plant Cell Environ., 17(12): 1305-1313.

Harlow W.M., Harrar E.S., Hardin J.W. and White F.M. (1996). Textbook of dendrology. McGraw-Hill series in forest resources. McGraw-Hill, New York.

Harrington T.B. & Edwards H.B. (1999). Understory vegetation, resource availability, and litterfall responses to pine thinning and woody vegetation control in longleaf pine plantations. Canadian Journal of Forest Research-Revue Canadienne De Recherche Forestiere, **29**, 1055-1064.

Hasselquist N.J., Metcalfe D.B., Inselsbacher E., Stangl Z., Oren R., Näsholm T. & Högberg P. (2016). Greater carbon allocation to mycorrhizal fungi reduces tree nitrogen uptake in a boreal forest. *Ecology*, 97, 1012-1022.

Hättenschwiler S. (2001). Tree seedling growth in natural deep shade: functional traits related to interspecific variation in response to elevated CO2. Oecologia, **129**, 31-42.

Hättenschwiler S. & Körner C. (1997). Growth of autotrophic and root-hemiparasitic understory plants under elevated CO2 and increased N deposition. Acta Oecologica-International Journal of Ecology, **18**, 327-333.

Hättenschwiler S. & Körner C. (2000) Tree seedling responses to in situ CO2-enrichment differ among species and depend on understorey light availability. Global Change Biology, **6**, 213-226.

Henriksson N., Tarvainen L., Lim H., Tor-Ngern P., Palmroth S., Oren R., Marshall J. & Nasholm T. (2015). Stem compression reversibly reduces phloem transport in Pinus sylvestris trees. *Tree Physiology*, 35, 1075-1085.

Hegarty E.E. & Caballe G. (1991). Distribution and abundance of vines in forest communities. In: *The Biology of vines.* (eds Mooney HA, Putz FE) pp Page. Cambridge ; New York, Cambridge University Press.

Hendrey G.R., Ellsworth D.S., Lewin K.F., Nagy J. (1999). A free-air enrichment system for exposing tall forest vegetation to elevated atmospheric CO2. Global Change Biology, **5**, 293-309.

Hinckley T.M., Brooks J.R., Čermák J., Ceulemans R., Kučera J., Meinzer F.C. and Roberts D.A. (1994). Water flux in a hybrid poplar stand. Tree Physiol., 14(7-9): 1005-1018.

Högberg M.N., Briones M.J.I., Keel S.G., Metcalfe D.B., Campbell C., Midwood A.J., Thornton B., Hurry V., Linder S., Nasholm T. & Högberg P. (2010). Quantification of effects of season and nitrogen supply on tree below-ground carbon transfer to ectomycorrhizal fungi and other soil organisms in a boreal pine forest. *New Phytol*, 187, 485-493.

Högberg P., Nordgren A., Buchmann N., Taylor A.F.S., Ekblad A., Högberg M.N., Nyberg G., Ottosson-Lofvenius M. & Read D.J. (2001). Large-scale forest

girdling shows that current photosynthesis drives soil respiration. *Nature*, 411, 789-792.

Holmgren B., Ovhed M. and Karlsson P.S. (1996). Measuring and modeling stomatal and aerodynamic conductances of Mountain birch: Implications for treeline dynamics. Arct. Alp. Res., 28(4): 425-434.

Horn H.S. (1966) Measurement of Overlap in Comparative Ecological Studies. American Naturalist, **100**, 419-424.

Horsley S.B., Long R.P., Bailey S.W., Hallett R.A., Wargo P.M. (2002). Health of eastern North American sugar maple forests and factors affecting decline. Northern Journal of Applied Forestry, **19**, 34-44.

Huntingford C., Lowe J.A., Booth B.B.B., Jones C.D., Harris G.R., Gohar L.K., Meir P. (2009). Contributions of carbon cycle uncertainty to future climate projection spread. Tellus Series B-Chemical and Physical Meteorology, **61**, 355-360.

Irmak S. & Mutiibwa D. (2010). On the dynamics of canopy resistance: generalized linear estimation and relationships with primary micrometeorological variables. Water Resour. Res., 46.

Jarvis P.G. (1976). The interpretation of the variations in leaf water potential and stomatal conductance found in canopies in the field. Philos. Trans. R. Soc. London, Ser. B Biol. Sci., 273(927): 593-610.

Jarvis P.G. & Mcnaughton K.G. (1986). Stomatal control of transpiration - Scaling up from leaf to region. Adv. Ecol. Res., 15: 1-49.

Jackson R.B., Cook C.W., Pippen J.S. & Palmer S.M. (2009). Increased belowground biomass and soil CO2 fluxes after a decade of carbon dioxide enrichment in a warm-temperate forest. *Ecology*, 90, 3352-3366.

Jing Y.L., Guan D.X., Wu J.B., Wang A.Z., Jin C.J. & Yuan F.H. (2015). An Experimental Comparison of Two Methods on Photosynthesis Driving Soil Respiration: Girdling and Defoliation. *Plos One*, 10.

Johnsen K., Maier C., Sanchez F., Anderson P., Butnor J., Waring R. & Linder S. (2007). Physiological girdling of pine trees via phloem chilling: proof of concept. *Plant Cell Environ*, 30, 128-134.

Jonard F., Andre F., Ponette Q., Vincke C. and Jonard M. (2011). Sap flux density and stomatal conductance of European beech and common oak trees in pure and mixed stands during the summer drought of 2003. J. Hydrol., 409(1-2): 371-381.

Jones H.G. (1992). Plants and microclimate: a quantitative approach to environmental plant physiology. Cambridge University Press, Cambridge [England] , New York, NY, USA.

Juang J.Y., Porporato A., Stoy P.C., Siqueira M.S., Oishi A.C., Detto M., Kim H.S. and Katul G. (2007). Hydrologic and atmospheric controls on initiation of convective precipitation events. Water Resour. Res., 43(3).

Karnosky D.F., Mankovska B., Percy K., Dickson R.E., Podila G.K., Sober J., Noormets A., Hendrey G., Coleman M.D., Kubiske M., Pregitzer K.S. & Isebrands J.G. (1999). Effects of tropospheric O_3 on trembling aspen and interaction with CO2: Results from an O_3-gradient and a face experiment. Water Air and Soil Pollution, **116**, 311-322.

Katsoulas N., Baille A. and Kittas C. (2007). Leaf boundary layer conductance in ventilated greenhouses: an experimental approach. Agric. For. Meteorol., 144(3-4): 180-192.

Katul G.G., Palmroth S. and Oren R. (2009). Leaf stomatal responses to vapour pressure deficit under current and CO_2-enriched atmosphere explained by the economics of gas exchange. Plant Cell Environ., 32(8): 968-979.

Keel S.G., Pepin S., Leuzinger S. and Korner C. (2007). Stomatal conductance in mature deciduous forest trees exposed to elevated CO2. Trees-Structure and Function, 21(2): 151-159.

Kelliher F.M., Leuning R., Raupach M.R. and Schulze E.D. (1995). Maximum conductances for evaporation from global vegetation types. Agric. For. Meteorol., 73(1-2): 1-16.

Kelliher F.M., Leuning R. and Schulze E.D. (1993). Evaporation and canopy characteristics of coniferous forests and grasslands. Oecologia, 95(2): 153-163.

Kerstiens G. (2001). Meta-analysis of the interaction between shade-tolerance, light environment and growth response of woody species to elevated CO2. Acta Oecologica-International Journal of Ecology, **22**, 61-69.

Keylock C.J. (2005). Simpson diversity and the Shannon-Wiener index as special cases of a generalized entropy. Oikos, **109**, 203-207.

Kim D., Oren R., Oishi A.C., Hsieh C.I., Phillips N., Novick K.A. & Stoy P.C. (2014). Sensitivity of stand transpiration to wind velocity in a mixed broadleaved deciduous forest. Agr Forest Meteorol, 187, 62-71.

Kim D., Oren R. & Qian S.S. (2016). Response to CO2 enrichment of understory vegetation in the shade of forests. Global Change Biology, 22, 944-956.

Kim H.S., Oren R. & Hinckley T.M. (2008). Actual and potential transpiration and carbon assimilation in an irrigated poplar plantation. Tree Physiol., 28(4): 559-577.

King J.S., Hanson P.J., Bernhardt E., DeAngelis P., Norby R.J. & Pregitzer K.S. (2004). A multiyear synthesis of soil respiration responses to elevated atmospheric CO2 from four forest FACE experiments. *Global Change Biology*, 10, 1027-1042.

King J.S., Pregitzer K.S., Zak D.R., Sober J., Isebrands J.G., Dickson R.E., Hendrey G.R. & Karnosky D.F. (2001). Fine-root biomass and fluxes of soil carbon in young stands of paper birch and trembling aspen as affected by elevated atmospheric Co-2 and tropospheric O-3. *Oecologia*, 128, 237-250.

Kitaya Y., Shibuya T., Yoshida M. & Kiyota M. (2004). Effects of air velocity on photosynthesis of plant canopies under elevated CO_2 levels in a plant culture system. Adv. Space Res., 34(7): 1466-1469.

Komatsu H., Kang Y.H., Kume T., Yoshifuji N. & Hotta N. (2006). Transpiration from a Cryptomeria japonica plantation, part 1: aerodynamic control of transpiration. Hydrol. Processes, 20(6): 1309-1320.

Konings A.G., Dekker S.C., Rietkerk M. & Katul G.G. (2011). Drought sensitivity of patterned vegetation determined by rainfall-land surface feedbacks. J. Geophys. Res.-Biogeo., 116.

Körner C., Asshoff R., Bignucolo O., Hättenschwiler S., Keel S.G., Peláez-Riedl S., Pepin S., Siegwolf R.T.W. & Zotz G. (2005). Carbon flux and growth in mature deciduous forest trees exposed to elevated CO_2. Science, **309**, 1360-1362.

Köstner B.M.M., Schulze E.-D., Kelliher F.M., Hollinger D.Y., Byers J.N., Hunt J.E., McSeveny T.M., Meserth R. & Weir P.L. (1992). Transpiration and canopy

conductance in a pristine broad-leaved forest of Nothofagus - an analysis of xylem sap flow and eddy-correlation measurements. Oecologia, 91(3): 350-359.

Kubiske M.E., Zak D.R., Pregitzer K.S. & Takeuchi Y. (2002). Photosynthetic acclimation of overstory Populus tremuloides and understory Acer saccharum to elevated atmospheric CO2 concentration: interactions with shade and soil nitrogen. Tree Physiology, **22**, 321-329.

Kush J.S., Meldahl R.S. & Boyer W.D. (1999). Understory plant community response after 23 years of hardwood control treatments in natural longleaf pine (Pinus palustris) forests. Canadian Journal of Forest Research-Revue Canadienne De Recherche Forestiere, **29**, 1047-1054.

Kumagai T., Saitoh T.M., Sato Y., Morooka T., Manfroi O.J., Kuraji K. & Suzuki M. (2004). Transpiration, canopy conductance and the decoupling coefficient of a lowland mixed dipterocarp forest in Sarawak, Borneo: dry spell effects. J. Hydrol., 287(1-4): 237-251.

Kupper P., Sõber J., Sellin A., Lõhmus K., Tullus A., Räim O., Lubenets K., Tulva I., Uri V., Zobel M., Kull O. & Sõber A. (2011). An experimental facility for free air humidity manipulation (FAHM) can alter water flux through deciduous tree canopy. Environ. Exp. Bot., 72(3): 432-438.

Launiainen S., Katul G.G., Kolari P., Vesala T. & Hari P. (2011). Empirical and optimal stomatal controls on leaf and ecosystem level CO_2 and H_2O exchange rates. Agric. For. Meteorol., 151(12): 1672-1689.

Liberloo M., Lukac M., Calfapietra C., Hoosbeek M.R., Gielen B., Miglietta F., Scarascoa-Mugnozza G.E. & Ceulemans R. (2009). Coppicing shifts CO2 stimulation of poplar productivity to above-ground pools: a synthesis of leaf to stand level results from the POP/EUROFACE experiment. New Phytologist, **182**, 331-346.

Lieffers V.J., Messier C., Stadt K.J., Gendron F. & Comeau P.G. (1999). Predicting and managing light in the understory of boreal forests. Canadian Journal of Forest Research-Revue Canadienne De Recherche Forestiere, **29**, 796-811.

Lim H., Oren R., Palmroth S., Tor-ngern P., Morling T., Nasholm T., Lundmark T., Helmisaari H.S., Leppalammi-Kujansuu J. & Linder S. (2015). Inter-annual variability of precipitation constrains the production response of boreal Pinus sylvestris to nitrogen fertilization. *Forest Ecology and Management*, 348, 31-45.

Lindroth A. (1993). Aerodynamic and canopy resistance of short-rotation forest in relation to leaf area index and climate. Boundary-Layer Meteorol., 66(3): 265-279-279.

Lohammar T., Larsson S., Linder S. & Falk S.O. (1980). FAST: simulation models of gaseous exchange in Scots pine. Ecol. Bull., 32: 505-523.

Lu P., Urban L. & Zhao P. (2004). Granier's thermal dissipation probe (TDP) method for measuring sap flow in trees: Theory and practice. Acta Bot. Sin., 46(6): 631-646.

Lukac M., Calfapietra C. & Godbold D.L. (2003). Production, turnover and mycorrhizal colonization of root systems of three Populus species grown under elevated CO2 (POPFACE). *Global Change Biology*, 9, 838-848.

Marshall J.D. & Waring R.H. (1985). Predicting Fine Root Production and Turnover by Monitoring Root Starch and Soil-Temperature. *Can J Forest Res*, 15, 791-800.

Matamala R. & Schlesinger W.H. (2000). Effects of elevated atmospheric CO2 on fine root production and activity in an intact temperate forest ecosystem. Global Change Biology, **6**, 967-979.

McCarthy H.R., Oren R., Finzi A.C., Ellsworth D.S., Kim H.S., Johnsen K.H. & Millar B. (2007). Temporal dynamics and spatial variability in the enhancement of canopy leaf area under elevated atmospheric CO2. Global Change Biology, **13**, 2479-2497.

McCarthy H.R., Oren R., Finzi A.C. & Johnsen K.H. (2006). Canopy leaf area constrains [CO2]-induced enhancement of productivity and partitioning among aboveground carbon pools. Proceedings of the National Academy of Sciences of the United States of America, **103**, 19356-19361.

McCarthy H.R., Oren R., Johnsen K.H., Gallet-Budynek A., Pritchard S.G., Cook C.W., Ladeau S.L., Jackson R.B. & Finze A.C. (2010). Re-assessment of plant carbon dynamics at the Duke free-air CO2 enrichment site: interactions of atmospheric [CO2] with nitrogen and water availability over stand development. New Phytologist, **185**, 514-528.

Medlyn B.E., Barton C.V.M., Broadmeadow M.S.J., Ceulemans R., De Angelis P., Forstreuter M., Freeman M., Jackson S.B., Kellomaki S., Laitat E., Rey A., Roberntz P., Sigurdsson B.D., Strassemeyer J., Wang K., Curtis P.S. & Jarvis

P.G. (2001). Stomatal conductance of forest species after long-term exposure to elevated CO2 concentration: a synthesis. New Phytol, 149, 247-264.

Medvigy D., Wofsy S.C., Munger J.W., Hollinger D.Y. & Moorcroft P.R. (2009). Mechanistic scaling of ecosystem function and dynamics in space and time: Ecosystem Demography model version 2. J Geophys Res-Biogeo, 114.

Medvigy D., Clark K.L., Skowronski N.S. & Schafer K.V.R. (2012). Simulated impacts of insect defoliation on forest carbon dynamics. Environmental Research Letters, **7**.

Medvigy D. & Moorcroft P.R. (2012). Predicting ecosystem dynamics at regional scales: an evaluation of a terrestrial biosphere model for the forests of northeastern North America. Philosophical Transactions of the Royal Society B-Biological Sciences, 367, 222-235.

Miglietta F., Peressotti A., Vaccari F.P., Zaldei A., Deangelis P. & Scarascia-Mugnozza G. (2001). Free-air CO_2 enrichment (FACE) of a poplar plantation: the POPFACE fumigation system. New Phytologist, 150, 465-476.

Mohan J.E., Clark J.S. & Schlesinger W.H. (2007). Long-term CO_2 enrichment of a forest ecosystem: Implications for forest regeneration and succession. Ecological Applications, 17, 1198-1212.

Mohan J.E., Ziska L.H., Schlesinger W.H., Thomas R.B., Sicher R.C., George K., Clark J.S. (2006). Biomass and toxicity responses of poison ivy (Toxicodendron radicans) to elevated atmospheric CO_2. Proceedings of the National Academy of Sciences of the United States of America, 103, 9086-9089.

Morin R.S., Liebhold A.M., Tobin P.C., Gottschalk K.W. & Luzader E. (2007). Spread of beech bark disease in the eastern United States and its relationship to regional forest composition. Canadian Journal of Forest Research-Revue Canadienne De Recherche Forestiere, 37, 726-736.

Morison J.I.L. (1998). Stomatal response to increased CO_2 concentration. Journal of Experimental Botany, 49: 443-452.

Morris J., Mann L. & Collopy J. (1998). Transpiration and canopy conductance in a eucalypt plantation using shallow saline groundwater. Tree Physiol., 18(8-9): 547-555.

Naumburg E. & Ellsworth D.S. (2000). Photosynthesis sunfleck utilization potential of understory saplings growing under elevated CO_2 in FACE. Oecologia, 122, 163-174.

Naumburg E., Ellsworth D.S. & Katul G.G. (2001). Modeling dynamic understory photosynthesis of contrasting species in ambient and elevated carbon dioxide. Oecologia, **126**, 487-499.

Niu S.L., Luo Y.Q., Dietze M.C., Keenan T.F., Shi Z., Li J.W. & Chapin F.S. (2014). The role of data assimilation in predictive ecology. Ecosphere, 5.

Noormets A., Sôber A., Pell E.J., Dickson R.E., Podila G.K., Sôber J., Isebrands J.G. & Karnosky D.F. (2001). Stomatal and non-stomatal limitation to photosynthesis in two trembling aspen (Populus tremuloides Michx.) clones exposed to elevated CO_2 and/or O_3. Plant Cell and Environment, 24(3): 327-336.

Norby R.J., Todd D.E., Fults J. & Johnson D.W. (2001). Allometric determination of tree growth in a CO_2-enriched sweetgum stand. New Phytologist, 150, 477-487.

Norby R.J., Hanson P.J., O'Neill E.G., Tschaplinski T.J., Weltzin J.F., Hansen R.A., Cheng W.X., Wullschleger S.D., Gunderson C.A., Edwards N.T. & Johnson D.W. (2002). Net primary productivity of a CO_2-enriched deciduous forest and the implications for carbon storage. *Ecol Appl*, 12, 1261-1266.

Norby R.J., DeLucia E.H., Gielen B., Calfapietra C., Giardina C.P., King J.S., Ledford J., McCarthy H.R., Moore D.J.P., Ceulemans R., De Angelis P., Finzi A.C., Karnosky D.F., Kubiske M.E., Lukac M., Pregitzer K.S., Scarascia-Mugnozza G.E., Schlesinger W.H. & Oren R. (2005). Forest response to elevated CO_2 is conserved across a broad range of productivity. *P Natl Acad Sci USA*, 102, 18052-18056.

Norby R.J. & Zak D.R. (2011). Ecological Lessons from Free-Air CO_2 Enrichment (FACE) Experiments. Annual Review of Ecology, Evolution, and Systematics, 42, 181-203.

Norby R.J., De Kauwe M.G., Domingues T.F., Duursma R.A., Ellsworth E.S., Goll D.S., Lapola D.M., Luus K.A., MacKenzie A.R., Medlyn B.E., Pavlick R., Rammig A., Smith B., Thomas R., Thonicke K., Walker A.P., Yang X. & Zaehle S. (2015). Model–data synthesis for the next generation of forest free-air CO_2 enrichment (FACE) experiments. New Phytologist.

Novick K.A., Katul G.G., McCarthy H.R. & Oren R. (2012). Increased resin flow in mature pine trees growing under elevated CO2 and moderate soil fertility. *Tree Physiology*, 32, 752-763.

Novel P.S. (2005). Physicochemical and environmental plant physiology. Elsevier, Burlington.

Nowacki G.J. & Abrams M.D. (2015). Is climate an important driver of post-European vegetation change in the Eastern United States? Global Change Biology, 21, 314-334.

Nowak R.S., Ellsworth D.S. & Smith S.D. (2004). Functional responses of plants to elevated atmospheric CO2 - do photosynthetic and productivity data from FACE experiments support early predictions? New Phytol, 162, 253-280.

Oishi A.C., Oren R. & Stoy P.C. (2008). Estimating components of forest evapotranspiration: a footprint approach for scaling sap flux measurement. Agric. For. Meteorol., 148(11): 1719-1732.

Oishi A.C., Oren R., Novick K.A., Palmroth S. & Katul G.G. (2010). Interannual invariability of forest evapotranspiration and its consequence to water flow downstream. Ecosystems, 13(3): 421-436.

Oishi A.C., Palmroth S., Butnor J.R., Johnsen K.H. & Oren R. (2013). Spatial and temporal variability of soil CO_2 efflux in three proximate temperate forest ecosystems. *Agr Forest Meteorol*, 171, 256-269.

Oishi A.C., Palmroth S., Johnsen K.H., Mccarthy H.R. & Oren R. (2014). Sustained effects of atmospheric [CO2] and nitrogen availability on forest soil CO_2 efflux. Global Change Biology, 20, 1146-1160.

Oksanen J., Guillaume Blanchet F., Kindt R., Legendre P., Minchin P.R., O'Hara R.B., Simpson G.L., Solymos P., Stevens M.H.H. & Wagner H. (2015). vegan: Community Ecology Package. https://github.com/vegandevs/vegan.

Oliver C.D. (1981). Forest Development in North-America Following Major Disturbances. Forest Ecology and Management, **3**, 153-168.

Oliver C.D. & Larson B.C. (1996). *Forest stand dynamics*, New York, John Wiley & Sons, Inc.

Oren R., Schulze E.D., Werk K.S., Meyer J., Schneider B.U. & Heilmeier H. (1988). Performance of 2 Picea-Abies (L) Karst Stands at Different Stages of Decline .1. Carbon Relations and Stand Growth. *Oecologia*, 75, 25-37.

Oren R., Phillips N., Katul G., Ewers B.E. & Pataki D.E. (1998). Scaling xylem sap flux and soil water balance and calculating variance: a method for partitioning water flux in forests. Ann. Sci. For., 55(1-2): 191-216.

Oren R., Sperry J.S, Katul G.G., Pataki D.E., Ewers B.E., Phillips N. & Schäfer K.V.R., (1999). Survey and synthesis of intra- and interspecific variation in stomatal sensitivity to vapour pressure deficit. Plant Cell Environ., 22(12): 1515-1526.

Oren R., Ellsworth D.S., Johnsen K.H., Phillips N., Ewers B.E., Maier C., Schäfer K.V.R., McCarthy H., Hendrey G., McNulty S.G. & Katul G.G. (2001). Soil fertility limits carbon sequestration by forest ecosystems in a CO2-enriched atmosphere. Nature, 411, 469-472.

Oren R. & Pataki D.E. (2001). Transpiration in response to variation in microclimate and soil moisture in southeastern deciduous forests. Oecologia, 127(4): 549-559.

Palmroth S., Maier C.A., McCarthy H.R., Oishi A.C., Kim H.S., Johnsen K.H., Katul G.G. & Oren R. (2005). Contrasting responses to drought of forest floor CO2 efflux in a Loblolly pine plantation and a nearby Oak-Hickory forest. *Global Change Biology*, 11, 421-434.

Palmroth S., Oren R., McCarthy H.R., Johnsen K.H., Finzi A.C., Butnor J.R., Ryan M.G. & Schlesinger W.H. (2006). Aboveground sink strength in forests controls the allocation of carbon below ground and its [CO2] - induced enhancement. *P Natl Acad Sci USA*, 103, 19362-19367.

Parton W.J., Hanson P.J., Swanston C., Torn M., Trumbore S.E., Riley W. & Kelly R. (2010). ForCent model development and testing using the Enriched Background Isotope Study experiment. J Geophys Res-Biogeo, 115.

Pataki D.E. & Oren R. (2003). Species differences in stomatal control of water loss at the canopy scale in a mature bottomland deciduous forest. Adv. Water Resour., 26(12): 1267-1278.

Pereira D.D., de Mello C.R., da Silva A.M. & Yanagi S.D.M. (2010). Evapotranspiration and estimation of aerodynamic and stomatal conductance in a fragment of Atlantic Forest in Mantiqueira Range region, Mg. Cerne, 16(1): 32-40.

Perry D.A. (2008). Forest ecosystems. Johns Hopkins University Press, Baltimore.

Poorter H. & Navas M.L. (2003). Plant growth and competition at elevated CO2: on winners, losers and functional groups. New Phytologist, 157, 175-198.

Phillips N. & Oren R. (2001). Intra- and inter-annual variation in transpiration of a pine forest. Ecol. Appl., 11(2): 385-396.

Pregitzer K.S., Burton A.J., King J.S. & Zak D.R. (2008). Soil respiration, root biomass, and root turnover following long-term exposure of northern forests to elevated atmospheric Co-2 and tropospheric O-3. New Phytologist, 180(1): 153-161.

Pritchard S.G., Strand A.E., McCormack M.L., Davis M.A., Finzi A.C., Jackson R.B., Matamala R., Rogers H.H. & Oren R. (2008). Fine root dynamics in a loblolly pine forest are influenced by free-air-CO2-enrichment: a six-year-minirhizotron study. *Global Change Biology*, 14, 588-602.

Pritchard S.G., Taylor B.N., Cooper E.R., Beidler K.V., Strand A.E., Mccormack M.L. & Zhang S.Y. (2014). Long-term dynamics of mycorrhizal root tips in a loblolly pine forest grown with free-air CO2 enrichment and soil N fertilization for 6 years. *Global Change Biology*, 20, 1313-1326.

Qian S.S., Craig J.K., Baustian M.M. & Rabalais N.N. (2009). A Bayesian hierarchical modeling approach for analyzing observational data from marine ecological studies. Marine Pollution Bulletin, 58, 1916-1921.

Reich P.B., Sendall K.M., Stefanski A., Wei X.R., Rich R.L. & Montgomery R.A. (2016). Boreal and temperate trees show strong acclimation of respiration to warming. *Nature*, 531.

Roberts J. (1983). Forest transpiration - a conservative hydrological process. J. Hydrol., 66(1-4): 133-141.

Royo A.A. & Carson W.P. (2006). On the formation of dense understory layers in forests worldwide: consequences and implications for forest dynamics, biodiversity, and succession. Canadian Journal of Forest Research-Revue Canadienne De Recherche Forestiere, 36, 1345-1362.

Runkle J.R. & Yetter T.C. (1987). Treefalls Revisited - Gap Dynamics in the Southern Appalachians. Ecology, 68, 417-424.

Running S.W. & Hunt E.R. (1993). Generalization of a forest ecosystem process model for other biomes, BIOME-BGC, and an application for global-scale models. Scaling physiological processes: leaf to globe. Academic Press, San Diego.

Sanders N.J., Belote R.T. & Weltzin J.F. (2004). Multitrophic effects of elevated atmospheric CO2 on understory plant and arthropod communities. Environmental Entomology, 33, 1609-1616.

Schäfer K.V.R., Oren R. & Tenhunen J.D. (2000). The effect of tree height on crown level stomatal conductance. Plant Cell Environ., 23(4): 365-375.

Schäfer K.V.R., Oren R., Lai C.T. & Katul G.G. (2002). Hydrologic balance in an intact temperate forest ecosystem under ambient and elevated atmospheric CO2 concentration. Global Change Biology, 8, 895-911.

Schäfer K.V.R., Oren R., Ellsworth D.S., Lai C., Herrick J.D., Finzi A.C., Richter D.D. & Katul G.G. (2003). Exposure to an enriched CO_2 atmosphere alters carbon assimilation and allocation in a pine forest ecosystem. Global Change Biol., 9(10): 1378-1400.

Schlesinger W.H. & Andrews J.A. (2000). Soil respiration and the global carbon cycle. *Biogeochemistry*, 48, 7-20.

Schnitzer S.A. & Bongers F. (2011). Increasing liana abundance and biomass in tropical forests: emerging patterns and putative mechanisms. Ecology Letters, 14, 397-406.

Schuepp P.H. (1993). Tansley Review No. 59 Leaf Boundary-Layers. New Phytol., 125(3): 477-507.

Sefcik L.T., Zak D.R. & Ellsworth D.S. (2006). Photosynthetic responses to understory shade and elevated carbon dioxide concentration in four northern hardwood tree species. Tree Physiology, 26, 1589-1599.

Simpson E.H. (1949). Measurement of Diversity. Nature, 163, 688-688.

Singsaas E.L., Ort D.R. & Delucia E.H. (2000). Diurnal regulation of photosynthesis in understory saplings. New Phytologist, 145, 39-49.

Souza L., Belote R.T., Kardol P., Weltzin J.F. & Norby R.J. (2010). CO_2 enrichment accelerates successional development of an understory plant community. Journal of Plant Ecology, 3, 33-39.

Springer C.J. & Thomas R.B. (2007). Photosynthetic responses of forest understory tree species to long-term exposure to elevated carbon dioxide concentration at the Duke Forest FACE experiment. Tree Physiology, 27, 25-32.

Stan Development Team (2014). RStan: the R interface to Stan.

Steidl R.J., Hayes J.P. & Schauber E. (1997). Statistical power analysis in wildlife research. Journal of Wildlife Management, 61, 270-279.

Stewart J.B. (1988). Modeling surface conductance of pine forest. Agric. For. Meteorol., 43(1): 19-35.

Stokes V.J., Morecroft M.D. & Morison J.I.L. (2006). Boundary layer conductance for contrasting leaf shapes in a deciduous broadleaved forest canopy. Agric. For. Meteorol., 139(1-2): 40-54.

Stoy P.C., Katul G.G., Siqueira M.B.S., Juang J.Y., McCarthy H.R., Kim H.S., Oishi A.C. & Oren R. (2005). Variability in net ecosystem exchange from hourly to inter-annual time scales at adjacent pine and hardwood forests: a wavelet analysis. Tree Physiol., 25(7): 887-902.

Stoy P.C., Katul G.G., Siqueira M.B.S., Juang J.Y., Novick K.A., McCarthy H.R., Oishi A.C., Uebelherr J.M., Kim H.S. & Oren R. (2006). Separating the effects of climate and vegetation on evapotranspiration along a successional chronosequence in the southeastern US. Global Change Biol., 12(11): 2115-2135.

Stoy P.C., Palmroth S., Oishi A.C., Siqueira M.B.S., Juang J.Y., Novick K.A., Ward E.J., Katul G.G. & Oren R. (2007). Are ecosystem carbon inputs and outputs coupled at short time scales? A case study from adjacent pine and hardwood forests using impulse-response analysis. *Plant Cell Environ*, 30, 700-710.

Subke J.A., Hahn V., Battipaglia G., Linder S., Buchmann N. & Cotrufo M.F. (2004). Feedback interactions between needle litter decomposition and rhizosphere activity. *Oecologia*, 139, 551-559.

Talhelm A.F., Pregitzer K.S., Kubiske M.E., Zak D.R., Campany C.E., Burton A.J., Dickson R.E., Hendrey G.R., Isebrands J.G., Lewin K.F., Nagy J. & Karnosky

D.F. (2014). Elevated carbon dioxide and ozone alter productivity and ecosystem carbon content in northern temperate forests. Global Change Biology, 20, 2492-2504.

Tatarinov F.A., Kucera J. & Cienciala E. (2005). The analysis of physical background of tree sap flow measurement based on thermal methods. Meas. Sci. Technol., 16(5): 1157-1169.

Taylor P.J., Nuberg I.K. & Hatton T.J. (2001). Enhanced transpiration in response to wind effects at the edge of a blue gum (*Eucalyptus globulus*) plantation. Tree Physiol., 21(6): 403-408.

Thornton P.E., Lamarque J.F., Rosenbloom N.A. & Mahowald N.M. (2007). Influence of carbon-nitrogen cycle coupling on land model response to CO2 fertilization and climate variability. Global Biogeochem Cy, 21.

Tor-ngern P., Oren R., Ward E.J., Palmroth S., McCarthy H.R. & Domec J.C. (2015). Increases in atmospheric CO_2 have little influence on transpiration of a temperate forest canopy. *New Phytol*, 205, 518-525.

Tricker P.J., Trewin H., Kull O., Clarkson G.J., Eensalu E., Tallis M.J., Colella A., Doncaster C.P., Sabatti M. & Taylor G. (2005). Stomatal conductance and not stomatal density determines the long-term reduction in leaf transpiration of poplar in elevated CO_2. Oecologia, 143(4): 652-660.

Uddling J., Teclaw R.M., Pregitzer K.S. & Ellsworth D.S. (2009). Leaf and canopy conductance in aspen and aspen-birch forests under free-air enrichment of carbon dioxide and ozone. Tree Physiology, 29(11): 1367-1380.

Valentini R., Matteucci G., Dolman A.J., Schulze E.D., Rebmann C., Moors E.J., Granier A., Gross P., Jensen N.O., Pilegaard K., Lindroth A., Grelle A., Bernhofer C., Grunwald T., Aubinet M., Ceulemans R., Kowalski A.S., Vesala T., Rannik U., Berbigier P., Loustau D., Guomundsson J., Thorgeirsson H., Ibrom A., Morgenstern K., Clement R., Moncrieff J., Montagnani L., Minerbi S. & Jarvis P.G. (2000). Respiration as the main determinant of carbon balance in European forests. *Nature*, 404, 861-865.

Walker A.P., Hanson P.J., De Kauwe M.G., Medlyn B.E., Zaehle S., Asao S., Dietze M., Hickler T., Huntingford C., Iversen C.M., Jain A., Lomas M., Luo Y.Q., McCarthy H., Parton W.J., Prentice I.C., Thornton P.E., Wang S.S., Wang Y.P., Warlind D., Weng E.S., Warren J.M., Woodward F.I., Oren R. & Norby R.J.

(2014). Comprehensive ecosystem model-data synthesis using multiple data sets at two temperate forest free-air CO2 enrichment experiments: Model performance at ambient CO2 concentration. J Geophys Res-Biogeo, 119, 937-964.

Wang K.Y., Kellomaki S., Zha T. S. & Peltola H. (2005). Annual and seasonal variation of sap flow and conductance of pine trees grown in elevated carbon dioxide and temperature. Journal of Experimental Botany, 56(409): 155-165.

Wang Y.P., Kowalczyk E., Leuning R., Abramowitz G., Raupach M.R., Pak B., van Gorsel E. & Luhar A. (2011). Diagnosing errors in a land surface model (CABLE) in the time and frequency domains. J Geophys Res-Biogeo, 116.

Ward E.J., Oren R., Sigurdsson B.D., Jarvis P.G. & Linder S. (2008). Fertilization effects on mean stomatal conductance are mediated through changes in the hydraulic attributes of mature Norway spruce trees. Tree Physiol., 28(4): 579-596.

Ward E.J., Oren R., Bell D.M., Clark J.S., McCarthy H.R., Kim H.S. & Domec J.C. (2013). The effects of elevated CO_2 and nitrogen fertilization on stomatal conductance estimated from 11 years of scaled sap flux measurements at Duke FACE. Tree Physiol., 33(2): 135-151

Waring R.H. (2007). Forest ecosystems : analysis at multiple scales. Elsevier/Academic Press, Amsterdam; Boston.

Warren J.M., Pötzelsberger E., Wullschleger S.D., Thornton P.E., Hasenauer H. & Norby R.J. (2011). Ecohydrologic impact of reduced stomatal conductance in forests exposed to elevated CO_2. Ecohydrology, 4(2): 196-210.

Wilson K.B., Baldocchi D.D., Aubinet M., Berbigier P., Bernhofer C., Dolman H., Falge E., Field C., Goldstein A., Granier A., Grelle A., Halldor T., Hollinger D., Katul G., Law B.E., Lindroth A., Meyers T., Moncrieff J., Monson R., Oechel W., Tenhunen J., Valentini R., Verma S., Vesala T. & Wofsy S. (2002). Energy partitioning between latent and sensible heat flux during the warm season at FLUXNET sites. Water Resour. Res., 38: 1294-1304.

Wullschleger S.D. & Norby R.J. (2001). Sap velocity and canopy transpiration in a sweetgum stand exposed to free-air CO_2 enrichment (FACE). New Phytologist, 150(2): 489-498.

Wullschleger S.D., Gunderson C.A., Hanson P.J., Wilson K.B. & Norby R.J. (2002). Sensitivity of stomatal and canopy conductance to elevated CO_2 concentration - interacting variables and perspectives of scale. New Phytologist, 153(3): 485-496.

Wullschleger S.D., Childs K.W., King A.W. & Hanson P.J. (2011). A model of heat transfer in sapwood and implications for sap flux density measurements using thermal dissipation probes. Tree Physiol., 31(6): 669-679.

Zaehle S. & Friend A.D. (2010). Carbon and nitrogen cycle dynamics in the O-CN land surface model: 1. Model description, site-scale evaluation, and sensitivity to parameter estimates. Global Biogeochem Cy, 24.

Zalesny R.S., Wiese A.H., Bauer E.O. & Riemenschneider D.E. (2006). Sapflow of hybrid poplar (*Populus nigra* L. x P-maximowiczii A. Henry 'NM6') during phytoremediation of landfill leachate. Biomass Bioenergy, 30(8-9): 784-793.

Zhang S.S. & Allen H.L. (1996). Foliar nutrient dynamics of 11-year-old loblolly pine (*Pinus taeda*) following nitrogen fertilization. Canadian Journal of Forest Research-Revue Canadienne De Recherche Forestiere, 26, 1426-1439.

Biography

Do Hyoung Kim was born on February 15, 1981 in Gyeongju, South Korea. He received his B.S. in Environmental Science and Ecological Engineering in 2007 and his M.S. in Bio-resource and Ecology in 2009 from Korea University. He began his Ph.D work with Dr. Ram Oren at the Nicholas School of the Environment, Duke University in 2009. He published "Sensitivity of stand transpiration to wind velocity in a mixed broadleaved deciduous forest" in the journal *Agricultural and Forest Meteorology* in 2014 and "Response to CO_2 enrichment of understory vegetation in the shade of forests" in the journal *Global Change Biology* in 2016.